BIO-AGING OF POLYETHYLENE AND ITS IMPACT ON SORPTION OF ORGANICS

A THESIS SUBMITTED TO
THE GRADUATE SCHOOL OF NATURAL AND APPLIED SCIENCES
OF
MIDDLE EAST TECHNICAL UNIVERSITY

BY

MAHA DASSOUKI DIT TAHAN

IN PARTIAL FULFILLMENT OF THE REQUIREMENTS
FOR
THE DEGREE OF MASTER OF SCIENCE
IN
ENVIRONMENTAL ENGINEERING

JULY 2024

Approval of the thesis:

BIO-AGING OF POLYETHYLENE AND ITS IMPACT ON SORPTION OF ORGANICS

submitted by **MAHA DASSOUKI DIT TAHAN** in partial fulfillment of the requirements for the degree of **Master of Science** i**n Environmental Engineering, Middle East Technical University** by,

Prof. Dr. Naci Emre Altun
Dean, **Graduate School of Natural and Applied Sciences** _____

Prof. Dr. Bülent İçgen
Head of the Department, **Environmental Engineering** _____

Prof. Dr. İpek İmamoğlu
Supervisor, **Environmental Engineering, METU** _____

Prof. Dr. F. Dilek Sanin
Co-Supervisor, **Environmental Engineering, METU** _____

Examining Committee Members:

Prof. Dr. Ayşegül Aksoy
Environmental Engineering, METU _____

Prof. Dr. İpek İmamoğlu
Environmental Engineering, METU _____

Prof. Dr. Faika Dilek Sanin
Environmental Engineering, METU _____

Prof. Dr. Çağdaş Devrim Son
Biological Sciences, METU _____

Assoc. Prof. Dr. Yusuf Çağatay Erşan
Environmental Engineering, Hacettepe University _____

Date: 26.07.2024

I hereby declare that all information in this document has been obtained and presented in accordance with academic rules and ethical conduct. I also declare that, as required by these rules and conduct, I have fully cited and referenced all material and results that are not original to this work.

Name Last name: Maha Dassouki Dit Tahan

Signature:

ABSTRACT

BIO-AGING OF POLYETHYLENE AND ITS IMPACT ON SORPTION OF ORGANICS

Dassouki Dit Tahan, Maha
Master of Science, Environmental Engineering
Supervisor: Prof. Dr. İpek İmamoğlu
Co-Supervisor: Prof. Dr. F. Dilek Sanin

July 2024, 171 pages

Microplastics (MPs) are a global threat due to their ubiquitous presence and potential risks to food chain through interactions with organic contaminants (OCs). Additionally, MPs undergo aging in the environment, affecting their interaction with OCs. While UV-aging has been extensively studied, bio-aging of MPs remains underexplored. This study aims to comparatively evaluate sorption of two OCs namely, triclosan (TCS) and trichlorophenol (TCP) on pristine and bio-aged high-density polyethylene (HDPE) and low-density polyethylene (LDPE). Anaerobic and aerobic reactors containing PE were operated under mesophilic conditions to induce bio-aging on MPs, sorption experiments were then conducted with selected OCs. Results indicate that, during bio-aging, high doses of HDPE inhibit methane production, whereas LDPE induces no inhibition. This was attributed to the presence of additives in HDPE. Characterization studies revealed no change in carbonyl index (CI) for bio-aged HDPE, while CI increased for aerobic and anaerobic aged LDPE, indicating structural changes. Surface alterations, including rougher textures and minor changes in crystallinity, were observed in bio-aged MPs. Sorption results varied among OCs: (i) TCS consistently had higher sorption affinity than TCP, (ii) TCP had no affinity for anaerobically aged HDPE or LDPE, whereas sorption was

favorable for aerobically aged LDPE (iii) TCS sorption capacities were similar for pristine and aerobically-aged, but lower for anaerobically-aged LDPE. Overall, there are complex interactions between MPs and microorganisms in digesters, where HDPE and LDPE do not affect and are not affected by them equally. Bio-aged PE in turn exhibits a variety of sorption affinities towards OCs tested.

Keywords: Polyethylene, Bio-aging, Anaerobic Digestion, Aerobic Digestion, Organic Contaminants

ÖZ

POLİETİLENİN BİYO-YAŞLANMASI VE ORGANİKLERİN SORPSİYONU ÜZERİNDEKİ ETKİSİ

Dassouki Dit Tahan, Maha
Yüksek Lisans, Çevre Mühendisliği
Tez Yöneticisi: Prof. Dr. İpek İmamoğlu
Ortak Tez Yöneticisi: Prof. Dr. F. Dilek Sanin

Temmuz 2024, 171 sayfa

Mikroplastikler (MP'ler), her yerde bulunmaları ve organik kirleticilerle (OC'ler) etkileşimleri nedeniyle gıda zincirine yönelik potansiyel riskleri nedeniyle küresel bir tehdittir. Ek olarak MP'ler çevrede yaşlanmaya maruz kalır ve bu da onların OC'lerle etkileşimlerini etkiler. UV yaşlanması kapsamlı bir şekilde araştırılmış olsa da, MP'lerin biyolojik yaşlanması yeterince araştırılmamıştır. Bu çalışma, iki OC'nin, yani triklosan (TCS) ve triklorofenolün (TCP), saf ve biyo-yaşlandırılmış yüksek yoğunluklu polietilen (HDPE) ve düşük yoğunluklu polietilen (LDPE) üzerindeki sorpsiyonunu karşılaştırmalı olarak değerlendirmeyi amaçlamaktadır. PE içeren anaerobik ve aerobik reaktörler, MP'lerde biyolojik yaşlanmayı tetiklemek için mezofilik koşullar altında çalıştırılmış, daha sonra seçilen OC'lerle sorpsiyon deneyleri gerçekleştirilmiştir. Sonuçlar, biyo-yaşlandırma sırasında yüksek dozda HDPE'nin metan üretimini olumsuz etkilediğini, oysa LDPE'nin herhangi bir değişikliğe neden olmadığını göstermektedir. Bu durum, HDPE'deki katkı maddelerinin varlığına bağlanmıştır. Karakterizasyon çalışmaları, biyolojik olarak yaşlandırılmış HDPE için karbonil indeksinde (CI) herhangi bir değişiklik olmadığını ortaya koyarken, CI, biyolojik olarak yaşlandırılmış LDPE için artmış ve

yapısal değişikliklere işaret etmiştir. Biyo-yaşlandırılmış MP'lerde daha pürüzlü yüzey yapısı ve kristallinitede küçük değişiklikler üzere yüzey değişiklikleri gözlemlenmiştir. Sorpsiyon sonuçları OC'ler arasında farklılık göstermiştir: (i) TCS tutarlı bir şekilde TCP'den daha yüksek sorpsiyon afinitesine sahiptir, (ii) TCP'nin anaerobik olarak yaşlandırılmış HDPE veya LDPE'ye afinitesi yokken, LDPE için olduğu gözlemlenmiştir, (iii) TCS sorpsiyon kapasiteleri yaşlanmamış ve aerobik olarak yaşlandırılmış LDPE için benzer, ancak anaerobik olarak yaşlandırılmış LDPE için daha düşük gözlenmiştir. Genel olarak, çürütücülerdeki MP'ler ve mikroorganizmalar arasında, HDPE ve LDPE'nin onları etkilemesinin ve MP'lerin onlardan etkilenmesinin eşit derecede olmadığı görülmüştür. Biyolojik olarak yaşlandırılmış PE, test edilen OC'lere karşı çeşitli sorpsiyon afiniteleri sergilemiştir.

Anahtar Kelimeler: Polietilen, Biyo-yaşlanma, Anaerobik Çürütme, Aerobik Çürütme, Organik Kirleticiler

Because “Aile Her Şeydir” <•••>

To my Family

ACKNOWLEDGMENTS

First and foremost, I would like to express my deepest gratitude to my family, without whom this thesis would have likely turned into a series of tear-stained pages. To my parents and siblings, thank you for your unwavering support, endless patience, and for putting up with my thesis-induced mood swings. Your love and encouragement have been the bedrock of my journey.

I must also extend my gratitude to my academic advisors and jury members. Prof. Dr. İpek İmamoğlu and Prof. Dr. F. Dilek Sanin, thank you for your insightful feedback, for pushing me to think deeper, and for all your valuable efforts in creating "several multiple different varying" versions of this thesis, making each version shine brighter. I also extend my gratitude to Dr. Melek Özdemir for her expertise. I am also grateful to the Scientific and Technological Research Council of Turkey (TÜBİTAK) (220N044) for granting me the opportunity to carry out my research and for their generous provision of resources and support.

To my close friends and rocking researchers, for your collaboration and sharing in the triumphs and the frustrations of our work, you all deserve honorary degrees in "Thesis Patience and Support." Special shout-out to İrem Şimşek, who turned my shaky lab skills from "hopeful hypothesis" to "solid science" with patience and laughs. Big thanks to Elif Yaren Özen, Ülkü Dide Türkeli, Oğuzhan Altuntaş, Gökçe Çiftçi, and Rumeysa Çalışkan for making my journey delightful and for the private Turkish lessons – you are the real academic heroes! My gratitude also extends to all those I met and worked with and those who accompanied me on my "Türkiye's East to West" conference trips.

Lastly, thanks to countless cups of coffee and sugar/chocolate doses that fueled this thesis. This thesis is as much a product of my efforts as it is a testament to the incredible support system I am blessed with. Here's to all of you – we did it!

TABLE OF CONTENTS

LIST OF TABLES

TABLES

LIST OF FIGURES

FIGURES

LIST OF ABBREVIATIONS

ABBREVIATIONS

AD	Anaerobic Digestion	**MP**	Microplastic
ADS	Anaerobically Digested Sludge	**MQL**	Method Quantitation Limit
ATBC	Acetyl Tri-N-Butyl Citrate	**OC**	Organic Contaminant
ATBC	Acetyl Tri-N-Butyl Citrate	**PE**	Polyethylene
ATR	Attenuated Total Reflectance	**pH_{PZC}**	Point of Zero Charge
BET	Brunauer-Emmett-Teller	**RMSE**	Root Mean Square Error
BMP	Biochemical Methane Potential	**ROS**	Reactive Oxygen Species
BOD	Biochemical Oxygen Demand	**SAUB**	Specific Area Under Band
BPA	Bisphenol A	**SEM**	Scanning Electron Microscope
CA	Contact Angle	**SSA**	Specific Surface Area
CI	Carbonyl Index	**SSR**	Residual Sum Of Squared Error
CPs	Chlorophenols	**TCD**	Thermal Conductivity Detector
DEHP	Diethylhexyl Phthalate	**tCOD**	Total Chemical Oxygen Demand
DI	Deionized	**TCP**	Trichlorophenol
DO	Dissolved Oxygen	**TCS**	Triclosan
DSC	Differential Scanning Calorimetry	**Tm**	Melting Temperature
DW	Distilled Water	**TS**	Total Solids
EDC	Endocrine-Disrupting Chemical	**TSS**	Total Suspended Solids
FTIR	Fourier Transform Infrared Spectroscopy	**UV**	Ultraviolet
GC	Gas Chromatography	**VFA**	Volatile Fatty Acids
HDPE	High Density Polyethylene	**VS**	Volatile Solids
HOCs	Hydrophobic Organic Contaminants	**VSS**	Volatile Suspended Solids
LDPE	Low-Density Polyethylene	**WAS**	Waste Activated Sludge
MDL	Method Detection Limit	**WWTP**	Wastewater Treatment Plant
MG	Malachite Green		

CHAPTER 1

INTRODUCTION

1.1 Background

Plastics, resilient and durable materials, are omnipresent in nature (He et al., 2023). Due to the rapid development of the petroleum-based plastics manufacturing industry (Lu et al., 2023), estimates suggest that over 322 million tons of plastic are produced worldwide, with projections indicating a doubling of this amount by the 2040s (Priyanka & Saravanakumar, 2022; Wei et al., 2019). Approximately 40% of plastics are released into the environment without adequate treatment (Priyanka & Saravanakumar, 2022). This widespread distribution of plastics has rendered them ubiquitous across the globe, posing a significant threat to ecosystems worldwide (Gao et al., 2022). The most widely available plastic in the world today is polyethylene (PE) (Patel, 2016). PE can come in variety of densities (*i.e.* high-density PE (HDPE) and low-density PE (LDPE)) based on their intended use.

Microplastics (MPs), defined as particles smaller than 5 mm, are environmentally pervasive and originate from the fragmentation of plastic waste or the direct release of micro- and nano-sized plastics from various sources. MPs can enter water bodies through primary discharge and can also form through secondary fragmentation caused by aging and environmental processes (Lu et al., 2023). As "emerging pollutants," MPs have become a significant environmental concern, attracting substantial attention and research focus in recent years (Ho et al., 2020; Zafar et al., 2022). The origins and fate of MPs are subject to intensive investigation (Liu et al., 2022b), and they have been recognized as a global environmental threat due to their pervasive presence and potential risks to the food chain through interactions with organic contaminants (OCs) (Wang et al., 2022b).

MPs can undergo aging and weathering through abiotic and biotic factors in the environment (Lu et al., 2023; Zafar et al., 2022). Biotic aging involves biofilm formation which alters the physicochemical properties of MP surfaces and structural characteristics (Zafar et al., 2022). These alterations consequently may affect their interaction with OCs. For instance, interaction of MPs with heavy metal ions and OCs can change due to the change in their physiochemical properties as they age, which has an adverse effect on the environment and the food chain (Lu et al., 2023). Thus, understanding the sorption behavior of different OCs with MPs is crucial for assessing their fate, transport, and environmental impact (Lončarsk et al., 2020; Tong et al., 2021). Although OCs typically co-exist with aged MPs in the environment, studies related to the adsorptive role of especially bio-aged MPs are quite limited.

MPs can enter wastewater treatment plants (WWTPs) from various sources. Small fractions of these MPs escape the treatment process and are directly released with the effluent, eventually entering the aquatic ecosystem. The rest of the MPs are accumulated in sewage sludge which in turn becomes a significant source of MPs in the environment through biosolids applications (Lu et al., 2023). Sludge is commonly treated through processes like composting, aerobic, or anaerobic digestion (AD) (He et al., 2023). MP buildup in sludge can impact and get impacted by these treatment processes. Recent studies indicate that exposure to MPs during aerobic sludge digestion, even at environmentally relevant concentrations, may elevate oxidative stress levels and alter microbial community structures (Zhang et al., 2021b). Similarly, MPs presence in AD can have an impact on methane production and microbial community (Akbay et al., 2022). On the other hand, sludge can have various impacts on MPs such as surface alterations, changes in functional groups, and crystallinity of MPs (Lu et al., 2023).

The accumulation of MPs in sludge coupled with the potential sorption of OCs on MPs raises specific concerns regarding the land application of biosolids. As MPs undergo bio-aging under AD and aerobic conditions, their interaction with OCs can be altered. While UV-induced aging of MPs has been extensively studied, biological

aging, particularly during sludge digestion, has not been investigated as thoroughly (Campanaro et al., 2023; Zafar et al., 2022).

Despite extensive research on the sorption behavior and mechanisms of contaminants on MPs, many studies use pristine MPs that may not accurately represent conditions in nature and WWTPs (Ho et al., 2020). The interaction of PE with sludge in WWTPs can have several outcomes on the sorption of OCs. For instance, MPs can interact with sludge microorganisms and get exposed to biofilm formation which can likely influence the fate of chemicals by altering sorption dynamics (Cui et al., 2023). However, due to the lack of sufficient research in this area, the mechanism or effects of biofilm on the sorption of OCs on PE remain unclear.

The pervasive presence of MPs and their potential interactions with various OCs across different ecosystems necessitates a comprehensive examination of these interactions. Moreover, numerous recent studies (Costigan et al., 2022; Fu et al., 2021; Wang et al., 2020) have scrutinized the interactions between OCs and MPs, especially PE (Adan et al., 2022; Çiftçi et al., 2023). The sorption behavior of OCs on MPs depends on the structure and properties of both the OCs and the MPs (Çiftçi et al., 2023). Furthermore, a number of factors, including the type of MPs, the pH of the solution, the ionic strength, and the presence of coexisting dissolved organic matter, influence sorption of organic contaminants on MPs (Li et al., 2019b). Since MPs can be impacted by these factors during wastewater treatment, sorption mechanisms of OCs with bio-aged MPs can vary. Such mechanisms of sorption of OCs with bio-aged MPs, however, are not thoroughly investigated.

The presence of HDPE and LDPE in both AD and aerobic digestion processes may exert varying effects on WWTP systems, potentially influencing these processes in different ways. This variability has implications for stabilization efficiency and the beneficial utilization of biosolids. Notably, this dual impact has not been extensively examined in the existing literature. Additionally, the biodegradation or biofilm formation of MPs due to their predominance in biosolids treatments or in land,

represents weathering pathways that are not well represented in microplastic research (Alimi et al., 2022). Considering that nearly half of biosolids in many developed countries are applied to land (Wang et al., 2018), the potential global impact is high. Moreover, the influence of sludge on PE has not been thoroughly investigated, and the differential impacts of HDPE and LDPE under aerobic and anaerobic conditions remain unexplored. Furthermore, the impact of the sorption of OCs on anaerobic and aerobic bio-aged PE, as well as the related sorption mechanisms, have not been thoroughly investigated in the literature. Addressing these literature gaps is deemed crucial for a better understanding of the impact of environmentally relevant microplastics.

1.2 Objectives

Upon addressing identified gaps in the literature, this study aims to:

1) Examine the bio-aging potential of HDPE and LDPE in mesophilic anaerobic digesters operated as biochemical methane potential (BMP) reactors and in aerobic reactors
2) Assess the effects of HDPE and LDPE MPs on reactor performance to draw conclusions regarding the impact of PE on WWTPs, as well as the changing properties of MPs following bio-aging
3) Investigate the changing interaction of HDPE and LDPE before and after aerobic and anaerobic bio-aging with physiochemically diverse OCs namely: triclosan (TCS) 2,3,6-trichlorophenol (TCP), and malachite green (MG), via preliminary sorption tests.
4) Identify sorption capacities via isotherm studies and partitioning coefficients using the bio-aged PE depicting the greatest change in properties (*i.e.*, LDPE) for triclosan (TCS) and 2,3,6-trichlorophenol (TCP).
5) Scrutinize implications of changing interaction of bio-aged MPs with OCs for a better understanding of factors affecting management of MPs issue.

1.3 Organization of Thesis

This dissertation is organized as a compilation of two manuscripts, intended for future publication. The dissertation includes Introduction (Chapter 1), Literature Review (Chapter 2), and Materials and Methods (Chapter 3) sections, addressing issues related to bio-aging and sorption. The first manuscript (Chapter 4) and its supplementary information (Appendix A) investigate bio-aging studies on PE using aerobic and anaerobic reactors. The second manuscript (Chapter 5) and its corresponding supplementary information (Appendix B) investigate the sorption potential of two OCs on pristine and bio-aged PE. Some repetition may occur in the introduction and materials and methods sections of the relevant topics in the manuscripts. In addition, "Thesis Extra Information" (Appendix C) has been also included for further explanations of results that could not be included in the manuscripts. Lastly, the results of preliminary sorption tests with the third OC tested in this study, namely, Malachite Green are also included as part of Appendix C. Due to struggles with the impact of deionized water quality on the spectrophotometric determination of MG and sorption experiments, its inclusion in Chapter 5 was negated. Finally, Chapters 6 and 7 provide the Conclusions and Recommendations of this study, respectively.

CHAPTER 2

LITERATURE REVIEW

2.1 General Information on Microplastics

2.1.1 Types and Properties of Polyethylene

Made from ethylene gas, polyethylene (PE) is the most widely available plastic in the world today (Patel, 2016). In essence, PE is a thermoplastic polymer composed of a long-chain aliphatic hydrocarbon (Ronca, 2017). Figure 2.1 shows the molecular structure of PE with the molecular formula of $(C_2H_4)_n$.

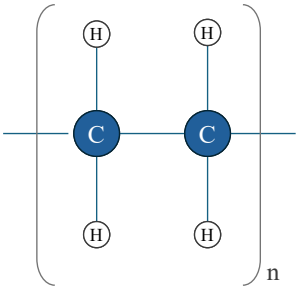

Figure 2.1 Molecular Structure of PE.

Nowadays, a wide variety of ethylene polymers can be produced using different utilizations. Because of PE variants, it can be customized for different uses such as packaging films, rigid containers, drums, pipes, and other applications. As PE can come in different forms and densities such as low, high, linear, or polar ethylene copolymer, PE is categorized and characterized according to the melt index and density. Density measures product crystallinity, which affects stiffness and performance of PE, whereas the melt index indicates PE's molecular weight and processability (Patel, 2016).

The choice of PE resin is typically determined by the physical characteristics needed for the intended end use of the product (Patel, 2016). PE can be prepared with altered structures at reduced pressures and temperatures to give it greater density, increased hardness, and increased softening points. These PE polymers are known as high-density PE (HDPE) (Patel, 2016; Ronca, 2017). To create low-density PE (LDPE), raw ethylene monomer is compressed to extremely high pressures, and free radical polymerization is started with a peroxide (Patel, 2016). Heavy-duty sacks, garbage sacks, food wrapping films, and general packaging are some of the major uses for LDPE films. Conversely, bags for groceries, trash, and deep freezers are commonly made of HDPE film. Pipes are another important application for HDPE due to its resistance to cracking and endurance of high pressure (Ronca, 2017). Changing properties of LDPE and HDPE are summarized in Table 2.1.

Table 2.1 Properties of LDPE and HDPE. Adapted from (Andrady, 2017; Sam et al., 2014).

MPs Properties	LDPE	HDPE
Glass Transition (°C)	-100	-80
Melting Point (°C)	~115	~135
Density (g/cm^3)	0.91-0.94	0.95-0.97
Crystallinity (%)	30-50	80-90
Flexibility	Flexible, highly malleable	Rigid
Transparency	Transparent	Opaque
UV/oxidation resistance	Low	Low
Strength (psi)	Low (600–2300)	High (5000-6000)
Surface energy (MJ/m^2)	32.4	32.4

2.1.2 Sources and Environmental Abundance

Once entering the environment, plastics undergo physical, chemical, mechanical, and biological reactions in nature, leading to their fragmentation into smaller pieces (He et al., 2023), influencing their transportation and bioavailability in different

environmental compartments (Gao et al., 2022). Based on their fragmentation size, plastic pollutants can be broadly categorized into various groups: nanoplastics (<100 μm) (Chae & An, 2017), microplastics (MPs) (100 μm - 5 mm), mesoplastics (5-25 mm), and macroplastics (>25 mm) (Lu et al., 2023).

Currently, categorized as primary and secondary, MPs warrant significant attention due to the potential adverse effects of MPs pollution on the environment and different ecosystems (Jemec Kokalj et al., 2019; Lu et al., 2023). MPs from primary sources are pollutants formed by plastic particles in raw or daily consumption materials and are directly discharged into aqueous environments through rivers and sewage treatment plants. MPs from secondary sources are macroplastic pollutants that break down and age due to physical, chemical, or biological processes, resulting in a reduction in volume and transformation into MP pollutants (Lu et al., 2023).

Out of the total plastic waste produced worldwide, only a minor portion is recycled or incinerated, and almost 79% is landfilled or left in the environment. The processes of incineration, landfilling, and environmental accumulation result in secondary pollution (Ma et al., 2023). The improper handling and inadequate management of plastics have resulted in the widespread presence of MP contaminants in rivers, lakes, groundwater, oceans, and sediments, raising significant concerns (Lu et al., 2023). Moreover, oceans, freshwater, soils, and polar zones have all been discovered to contain MPs (He et al., 2023).

Due to the challenges associated with degrading and recycling MPs such as their small size and persistence, they are omnipresent and uncontrollably accumulate in the environment for extended periods, posing a serious threat to ecological systems and human health (Liu et al., 2022b; Ma et al., 2023). It is expected that by 2050, 12 billion tons of plastic will be found and gathered if no control measures are employed. Thus far, investigations have revealed the presence and accumulation of MPs in deep-sea sediments, soil, organisms, and surface water (Liu et al., 2022b). For example, current research indicates that MP abundances in freshwater ecosystems can range in concentrations from 3×10^4 Particles/m^3 in estuaries to

1.87×10^5 Particles/m^3 in waters near large cities (Verdú et al., 2021). Moreover, MPs can be abundant in waste water treatment plants (WWTPs) where, in wastewater influent MPs accumulation can range from 2.6×10^5 to 3.2×10^5 Particles/m^3, and in sewage sludge, they can range from 1.5×10^3 to 2.4×10^4 Particles/kg dry solids (Akbay et al., 2022).

It has been demonstrated that WWTPs are primary recipients of MPs that are released into sewage as a result of everyday tasks such as residues from body wash, toothpaste, and detergents (Liu et al., 2022b). Although WWTPs discharge a significant amount of MPs through the effluent into the receiving water bodies, their potent hydrophobic qualities cause more than 90% of the MPs in WWTP influents to be eliminated during the treatment phases and accumulate in sewage sludge (Li et al., 2020; Wang et al., 2023; Wei et al., 2019).

Despite the very low MP content in the effluent, 2×10^6 MP particles/day were detected to enter the water body due to the large amount of sewage discharge. More MPs are building up in the environment as a result. Simultaneously, 70–98% of the MPs are accumulated in sludge, even with the high removal rate (He et al., 2023; Wei et al., 2021). Up to 170 MP particles/g-TS (total solids) have been found in sewage sludge thus far (Zhang et al., 2021b). Moreover, MP concentrations can vary from 1.0 to 56.4 particles/g of dry sludge (Wang et al., 2023; Wei et al., 2019). Other sources indicated that the abundance of MPs in the sewage sludge differs across nations from 50 particles/kg of sludge to 170,900 particles/kg of sludge (Li et al., 2020).

Sewage sludge can be treated and utilized as fertilizer, for example, by composting or anaerobic digestion (AD). Therefore, using treated sludge is thought to be a significant pathway for MPs to be transported to the environment (Lessa Belone et al., 2024). This shows that MPs may accumulate in soil, freshwater, and marine environments (Liu et al., 2022b). Furthermore, MPs have been shown to jeopardize soil safety and pose a major risk to the biota and nutrient cycle, making their deposition on the soil a cause for concern (Lessa Belone et al., 2024).

2.1.3 Environmental Impact

As MPs become ubiquitous in nature, they would pose an ecological threat to the environment, which has garnered significant attention and research interest over the past years (Ho et al., 2020; Zafar et al., 2022). MPs are now generally acknowledged as "emerging pollutants" in the environment, and researchers are paying close attention to the origins and eventual fate of MPs. As a result, MP pollution is a much bigger problem than we realize and should be taken seriously (Liu et al., 2022b). There have been reports that a broad range of aquatic biota, from large marine mammals to tiny zooplankton, can unintentionally consume MPs (Ho et al., 2020). MPs themselves can induce various detrimental effects on organisms, including oxidative stress, inflammatory responses, disruption of energy allocation functions, and a false sensation of satiation. The fragmentation of larger plastic particles into smaller fragments increases their bioavailability, potentially impacting microorganisms such as microalgae, which form the foundation of the trophic chain. Consequently, adverse effects on these foundational organisms may cascade through the food web, impacting higher organisms within a given ecosystem (Verdú et al., 2021).

According to literature, MPs can have various characteristics such as strong hydrophobicity, a large specific surface area, high porosity, and high mobility. These unique qualities enable MPs to have a strong sorption affinity and act both as carriers to prolong the migration of pollutants and adsorb them from the surrounding environment which causes them to have a detrimental impact on the biota that is both chemical and physical (He et al., 2023; Ho et al., 2020).

Furthermore, MPs not only directly harm the organisms that consume them, but they also transfer toxins into other organisms through the food chain (He et al., 2023). Because of this ability, MPs are thought to be a possible channel through which these pollutants could infiltrate aquatic food webs and ultimately endanger human health serving as anthropogenic pollutant vectors (Ho et al., 2020). Consequently, because of their complexity and potential for high ecological risk, MPs have drawn more

attention as common environmental pollutants found throughout the world (He et al., 2023).

In addition, MPs' presence in different environmental compartments can expose them to certain physicochemical weathering processes that can accelerate the release of additives contained within MPs. These additives, whose composition and concentrations are often undisclosed due to proprietary formulations, have the potential to adversely affect co-occurring organisms. Furthermore, MPs have been identified as a novel habitat for microorganisms, including pathogens and antibiotic-resistant bacteria, along with their corresponding antibiotic resistance genes (Verdú et al., 2021). Moreover, the adsorption efficacy of MPs for organic pollutants is continuously changing due to the ongoing release of monomers and additives caused by weathering, fragmentation, and aging. MPs modifications, release of additives, and their interactions with environmental pollutants during MP synthesis are concerning to the environment, especially their transformation and transportation mechanisms under different environmental conditions (Lu et al., 2023).

2.1.4 Aging in The Environment

Plastic aging and degradation are the primary processes in nature that produce MPs (Wu et al., 2020). Under the physical and mechanical influences of temperature, freezing and thawing, water, and wind, plastics break down into MPs also known as weathering. Weathering degree can be identified visually as MPs change color (yellowing). This process is an indication of how MPs alter as they age. Due to weathering, MPs surface characteristics, shape, particle size, and mechanical and thermal properties of plastics are affected. Moreover, MPs' oxygen-containing functional groups greatly expand, which may cause contaminants that have been adsorbed on the surface to be released and MPs polymer chains could break (Lu et al., 2023). Additives are used to prevent or reduce aging, and sometimes upon aging these additives in plastics can be released into the environment (Lu et al., 2023).

Conventional petroleum-based plastics are influenced by a variety of environmental factors and are slow to age and decay in nature. Up to 94% of plastic wastes in the environment are subjected to ultraviolet (UV) radiation, mechanical shock, hydrolysis, and bio-aging. Consequently, the formation of aged MPs is considered the ultimate fate of MPs in the environment (Wu et al., 2020).

Meanwhile, as MPs age, they are exposed to oxidation aging mechanism which influences the specific structures and compositions of MPs, including changes in size, crystallinity, and rubbery regions (Wu et al., 2020). Moreover, the hydrophilicity and hydrophobicity of plastics can change as MPs age (Lu et al., 2023). These alterations consequently, can impact the transport potential of MPs for pollutants due to the interactions of degraded MPs with heavy metal ions and organic contaminants (OCs), which has an adverse biological effect on organism uptake (Lu et al., 2023; Wu et al., 2020). Therefore, there is significant concern regarding the behavior and interactions of aged MPs in the environment, as their smaller size may enhance the transport of OCs and increase toxicity to the ecosystem (Wu et al., 2020).

Generally, there are two primary aging mechanisms for MPs: abiotic (e.g., photoirradiation, pH, and salinity variation) and biotic alterations (e.g., biological aging). Thermal breakdown and UV aging are the primary abiotic aging mechanisms. Meanwhile, microbial and enzymatic degradations are the primary biological aging mechanisms of MPs (Lu et al., 2023; Zafar et al., 2022). Figure 2.2 summarizes the types of MPs aging and the aging processes and mechanisms that could be found and applied to MPs in nature. Biological aging and photo-oxidation are the two most prevalent aging processes. MPs aged in these ways show notable changes in their physicochemical properties, which could further modify MPs' effects on the environment (Zafar et al., 2022).

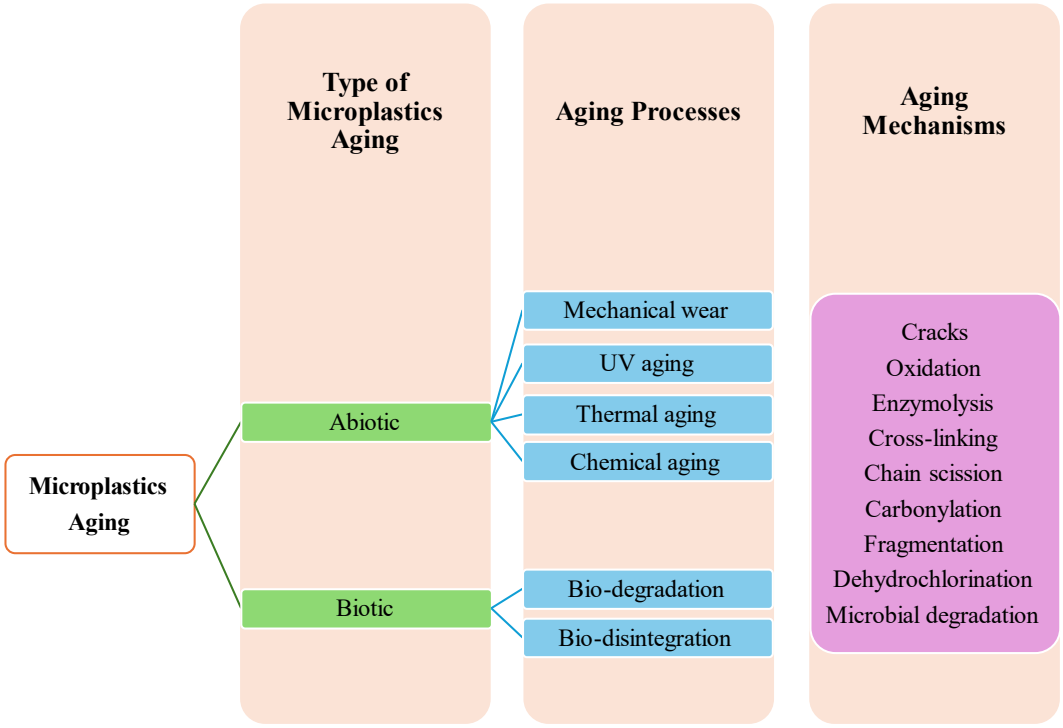

Figure 2.2 MPs Aging types, processes, and mechanisms in the environment. Adapted from (Lu et al., 2023).

Abiotic Aging

One form of abiotic degradation is photodegradation which is brought on by photon absorption from sunlight UV-A and UV-B photons (Lu et al., 2023). During photoaging, UV radiation breaks down polymers' molecules and initiates crosslinking reactions that result in the formation of new non-polymer structures, hydrocarbon and oxidized polymers, as well as a variety of low-molecular-weight compounds and oxidation products like gases (Liu et al., 2022a). Moreover, UV-aged MPs showed altered surface chemistry, increased surface roughness, and changed topography. Different binding affinities for additional organic pollutants may result from these surface modifications (Zafar et al., 2022). According to polymer characterization of functional groups, the vinyl, carbonyl, and hydroxyl concentrations can be observed for photo-aged MPs. As a result of PE photo-aging, hydroxyl can be produced as an intermediate product, while the amount of vinyl and carbonyl rises (Lu et al., 2023).

Biotic Aging

Similar to abiotic degradation, biological aging due to the microbial colonization of the MP surface can produce a biofilm that alters the surface's physicochemical and structural characteristics. One form of biotic aging can occur during WWTPs processes. Currently, there is no practical method to separate MPs from sewage sludge. However, it has been proposed that MPs in sewage sludge could be degraded through sewage sludge treatments, preventing their release into terrestrial systems. AD is a common treatment method for sewage sludge (Lessa Belone et al., 2024). AD can eliminate pathogens and odors, stabilize sludge, reduce sludge volume, and generate renewable energy (Li et al., 2020). In the absence of oxygen, microorganisms break down the organics in sludge through a biological process. Biogas is produced during this process, involving hydrolysis, acidogenesis, acetogenesis, and methanogenesis reactions. The typical operating temperature ranges for AD are 50-60°C (thermophilic process) or 30-40°C (mesophilic process) (Lessa Belone et al., 2024).

The AD process is depicted in Figure 2.3. The initial stage involves breaking down of organic matter, during which complex organic compounds like cellulose and starch are enzymatically converted into simpler soluble organic compounds. Polymers undergo enzymatic hydrolysis, transforming them into soluble monomers. Then, facultative and anaerobic bacteria metabolize sugars, amino acids, and fatty acids, converting them into hydrogen, acetate, carbon dioxide, and volatile fatty acids (VFAs). In acetogenesis, acetogenic bacteria, also referred to as acid formers, convert the products from the previous phases into simple organic acids, carbon dioxide (CO_2), and hydrogen (H_2). Hydrogen-producing acetogenic bacteria generate acetate, H_2, and CO_2 from volatile fatty acids and alcohols, whereas homoacetogenic bacteria produce acetate from CO_2 and H_2. However, the majority of acetate production is attributed to hydrogen-producing acetogenic bacteria. Finally, in the methanogenesis step, methanogenic archaea convert acetate and H_2/ CO_2 into methane (CH_4) and carbon dioxide (CO_2) (Rashed et al., 2015).

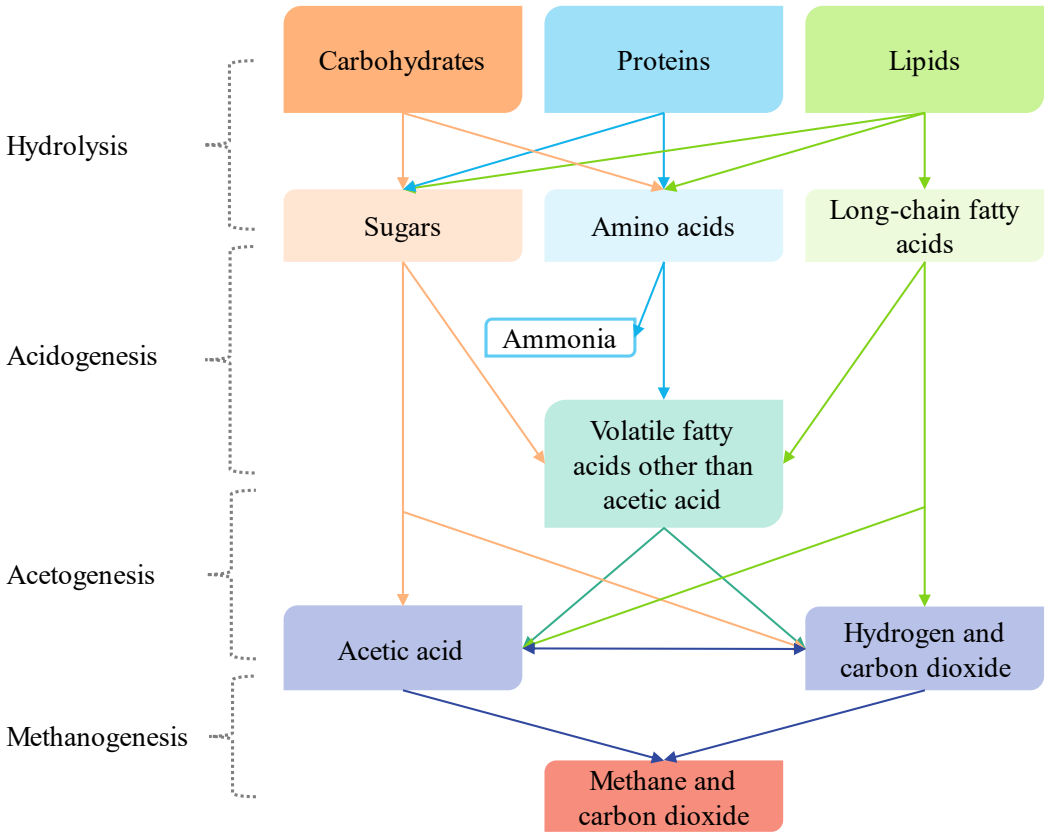

Figure 2.3 Anaerobic digestion process. Adapted from (Rashed et al., 2015).

Another common method for treating sludge is aerobic digestion, particularly in small-scale WWTPs. Because of its high nutrient content, aerobically digested sludge is frequently used to enhance soil quality and water retention. According to a recent study, during aerobic sludge digestion, exposure to environmentally relevant concentrations of MPs may increase oxidative stress and change the structure of the microbial community (Zhang et al., 2021b).

Aerobic digestion has two phases to produce digested sludge: the direct oxidation of biodegradable materials and endogenous respiration, which oxidizes cellular material (Roš & Zupančič, 2002). Typically, the aerobic process is conducted at room temperature, where the maximum rate of destruction of volatile solids occurs at 30°C, and the rate decreases at higher temperatures. Moreover, aerobic processes require constant aeration where, the difference between the actual oxygen concentration in the reactor and the solubility of dissolved oxygen (DO) must be at

least 6 mg/l, for aerobic biological degradation to occur effectively (Roš & Zupančič, 2002).

The research on how MPs age in aerobic processes is very limited. Literature mostly focus on aging of MPs in aerobic environments such as freshwater, lakes, and rivers and the effect of WAS biofilm on MPs (He et al., 2023; Jemec Kokalj et al., 2019; Priyanka & Saravanakumar, 2022; Verdú et al., 2023). However, no studies were found using aerobic mesophilic digestors to age MPs. Zafar et al., (2022) indicated that PE exposed to artificial freshwater and WAS were prone to surface modifications after the aging processes. Moreover, new functional groups (*i.e.* C=O) emerged indicating the oxidation of PE. Furthermore, biofilm formation was evident on the surface of PE after bio-aging as well as an increase in specific surface areas of PE with aging.

2.2 Microplastics and Sludge Treatment

2.2.1 Impact of MPs on Anaerobic and Aerobic Digestion

The most prevalent MPs in sludge are PE, polyvinyl chloride, polystyrene, polyethylene terephthalate, and polypropylene (Wei et al., 2019). PE, being widely used in packaging, is the most abundant and common polyolefin, making up the majority of MPs found in seawater and WWTPs, e.g., 4–51% of the MPs found in the WWTPs were PE (Tang et al., 2022; Wei et al., 2019). These MPs present a serious risk to WWTPs operations because they can act as conduits for the spread of pathogens and micropollutants. Moreover, the migration of MPs can cause the release of plastic additives and monomers, such as acetyl tri-n butyl citrate (ATBC), diethylhexyl phthalate (DEHP), and bisphenol-A (BPA), which can impair the physiological processes of microorganisms and worsen the efficacy of wastewater treatment (Tang et al., 2022). Because the plastics contain additives that enhance the MPs' characteristics and prolong their life by preventing microbial degradation, these MPs remain in the sludge. Nevertheless, these additives frequently leaching from

MPs, potentially have an effect on biota. ATBC is the highly prevalent additive leaching from PE MPs for example (Wei et al., 2019).

Additionally, the microorganisms involved in WWTPs can be affected in a variety of ways by the presence of PE MPs, sometimes in unexpected ways. According to a recent study, PE MPs caused the production of intracellular reactive oxygen species (ROS), which decreased bacterial viability during AD. However, after exposure to a range of PE MPs concentrations (50–10,000 particles/L), no discernible effects were found on the activity of ammonium and nitrite-oxidizing bacteria, denitrifies, and polyphosphate-accumulating organisms. When sedimentary microbial communities are exposed to PE MPs, a prior study even demonstrated increases in nitrification and denitrification rates through changes in microbial community composition and function (Tang et al., 2022).

AD is generally regarded as an affordable and environmentally friendly technique (Lessa Belone et al., 2024). However, the accumulation of MPs in sludge can negatively affect AD processes (Wang et al., 2023). Certain MPs have been shown to impede sludge hydrolysis, acidogenesis, and acetogenesis, thereby reducing hydrogen production during the alkaline anaerobic fermentation of sludge waste. Additionally, MPs can cause shifts in microbial structure towards hydrolysis and acidification. During the alkaline AD process, MPs have the potential to release harmful substances such as di-n-butyl phthalate (DBP) and ROS, which can adversely impact the process. For instance, PE are known for their detrimental impacts on AD due to the generation of ROS (Li et al., 2022).

Moreover, certain MPs have been found to leach toxic BPA, further hindering AD of WAS (Li et al., 2020, 2022). Additionally, the growth and metabolism of certain microbes can be inhibited by nanoparticles adhering to cell membrane surfaces. Consequently, the effects of various MP sizes, quantities, and compositions on AD can vary significantly. The AD conditions can influence both the leaching of harmful MP compounds and the digestion process itself (Li et al., 2020). Furthermore, it is still unknown what underlying mechanisms influence AD performance at varying

MP exposure levels. (Li et al., 2022). Therefore, it is crucial to conduct further research on the impact of MPs in sludge on AD (Li et al., 2020).

Previous research has shown that MPs can impact AD and methane production at every step. Possible mechanisms include (1) physical damage to sludge flocs and microbial cells by MPs' small sizes and sharp edges, lowering methane production (Akbay et al., 2022; Wang et al., 2023); (2) oxidative stress in cells induced by MP-generated ROS (Li et al., 2020; Tang et al., 2022; Wang et al., 2023); and (3) toxicity effects from MPs' toxic additives or toxic pollutants adsorbed on their surface (Wang et al., 2023). Some research has indicated that the additives included in MPs are primarily responsible for the inhibition of methane production during AD (Akbay et al., 2022; Wang et al., 2023) and the impact can extend to lowering biogas production at higher MPs abundance in WWTPs (Akbay et al., 2022).

As MPs age, their physical and chemical properties are modified. Moreover, the release of additives and intermediates from these MPs is accelerated. These alterations can influence the sludge's anaerobic microbial community. The impact of bio-aging of MPs on sludge's AD has not been extensively investigated. Some research has shown that the additives included in MPs are primarily responsible for the inhibition of MPs on methane production during AD. For instance, Wang et al., (2023) stated that DBP was the main cause of the lower methane yields and hydrogen production in their AD reactors. In contrast, inhibition of methane in AD can be attributed to other factors rather than additives leaching. For example, Wei et al., (2019) indicated that ATBC, the predominant additive that leaches from PE, did not inhibit AD and it was the formation of ROS that affected AD. These discrepancies suggest that the additives impeding AD might or might not be the main influence for AD inhibition. A full conclusion cannot be drawn due to that there is currently no published research on screening the essential elements of MP leachates that impede AD (Wang et al., 2023). Despite that, PE that are retained in WAS will eventually find their way into AD system, which will probably have a substantial negative impact on the system's efficiency. However, no information has been published

regarding the potential ways that PE MPs could influence the AD processes of WAS (Wei et al., 2019).

The impact of PE on the AD of WAS has been investigated by several studies (Table 2.2). These studies revealed a negative correlation between PE concentration and methane production, with higher PE concentrations associated with decreased methane generation. Additionally, elevated levels of PE were found to reduce both the hydrolysis (15%) and methane production (27.5%), particularly notable at concentrations ranging from 100 to 200 particles/g-TS (Wei et al., 2019). Similar trends were observed with electrochemical AD (Wang et al., 2022a). Furthermore, enhanced hydrolysis of proteins and soluble polysaccharides in the presence of PE were reported, leading to the accumulation of volatile fatty acids. Despite this, methane production exhibited reductions of 13.8% and 6.1% at PE sizes of 1000 μm and 180 μm, respectively (Shi et al., 2022a). Another study, indicated an improvement in methane production by 8.4% and 41.2% at thermophilic conditions due to PE presence (Zhang et al., 2021a). However, the majority of the studies did not specify the type or density of PE being used in the experiment which may have caused varying and unreliable results. One study indicated that HDPE reduced methane production by 7% (Lim et al., 2018). Identifying the density and type of PE used in studies as well as whether it contains additives or not is important as varying results can yield from changing the density of PE and the presence of additives on BMP reactors.

Table 2.2 Polyethylene effect on methane production.

Particle size	PE dose	Substrate	Mode (temperature)	Operation time	Major Findings	Reference
40±2 µm	10, 30, 60, 100, and 200 particles/ g-TS	WAS from secondary settler of a WWTP	BMP test, Batch (37± 1 °C)	44 days	- Low concentrations (10, 30, and 60 particles/g-TS) did not affect the methane production. - The hydrolysis rate coefficients were significantly lower (100 and 200 particles/g-TS) resulting in a 12.4–27.5% reduction in methane production. -ROS generation was determined to be the primary cause of inhibition rather than ATBC and DEHP additives.	(Wei et al., 2019)
40–48 µm	0.05, 1, and 10 mg/L sludge	Anaerobic granular sludge from a potato WWTP	Bio-electrochemical AD (BEAD) reactors, Batch (37 °C)	144 hrs.	- Methane production was inhibited by 10 mg/L PE by 30.71%. - PE decreased the abundance of hydrogenotrophic methanogens and acetogens. - PE inhibited important functional genes and enzymes.	(Wang et al., 2022a)
180 µm, 1000 µm	100 mg/g-TS	WAS from secondary sedimentation tank of a WWTP	Batch (37 °C)	40 days	- PE MPs suppressed methanation but increased acidification and hydrolysis. - PE MPs changed the microbial populations that are important in the functioning of anaerobic digestion. - When PE MPs-180µm and PE MPs-1mm were present, the production of methane dropped by 6.1% and 13.8%, respectively.	(Shi et al., 2022a)
0.7–450 µm	1000 mg/L sludge	Dairy wastes	Batch (55 °C, 65 °C)	35 days	PE increased COD removals to 52.8% and 52.4% at 55 °C and 65 °C, and improved methane production by 8.4% and 41.2%, respectively.	(Zhang et al., 2021a)
5-10 mm by 5-10 mm by 1 mm	N/A	Food waste	Batch (35 °C)	30 and 35 days	HDPE reduced methane yield by 7% suspected due to additives leaching from MPs.	(Lim et al., 2018)

2.2.2 Impact of Anaerobic and Aerobic Digestion on MPs

Microbial colonization of the MP surface during sludge processes can lead to increasing the number of binding sites and forming new functional groups (Zafar et al., 2022). The physical and chemical characteristics of MPs, such as their surface micro-morphology and roughness, surface charge, specific surface area, and density, may be impacted by biofilm formation. These characteristics may then have an impact on the pathogens and chemical pollutants' adsorption-desorption, vertical migration, and weathering on MPs in the environment (Tu et al., 2020).

MPs are known for being persistent in the environment and challenging to degrade through natural aging processes. However, certain microbes have the capability to break down these MP contaminants (Lu et al., 2023). MPs play a dual role in this process, serving as both carriers of carbon for microbial cycles and facilitating microbial growth and colonization (Lu et al., 2023). This microbial degradation technique offers a biodegradable and natural means of aging MPs, thereby mitigating the negative impacts of human activities on the environment. Enzymes secreted by microbes play a crucial role in breaking down MPs by splitting the catalytic chain into monomers. Consequently, microbial aging and enzymatic aging of MPs are closely linked.

Unlike photooxidation, which relies on photosensitive functional groups, microbial and enzymatic aging primarily depend on the interaction between functional groups and digestion. Lu et al., (2023) investigated the influence of various functional groups on the aging breakdown process of MPs. Findings reveal that functional groups such as vinyl, carboxy, and carbonyl have a significant impact on the breakdown process, while hydroxyl groups and crystallinity of MPs show negligible effects. They proposed that enzymes and microorganisms exhibit distinct aging and degradation mechanisms, influencing the hydrophilicity and hydrophobicity of degradation products. For instance, they emphasized that in the degradation of PE polymers through enzymatic activity, PE is initially converted into low polymers by

enzymes or external cells, followed by the production of CO_2, H_2O, and CH_4, serving as carbon sources for microbial metabolism.

2.3 Characterization of Microplastics

There is a dearth of research on the use of characterization techniques in the investigation and measurement of aging of MPs. The majority of research employed electron microscopy to scrutinize changes in MPs (Lu et al., 2023). Understanding the properties of MPs' surface structure is essential to investigate MPs' aging in the environment. However, since MPs' inherent toxicity and capacity to adsorb harmful compounds alter as they age, it is crucial to comprehend not only the structure of these materials but also how that structure changes over time. Consequently, characterizing the makeup of surface elements and functional groups through physical and chemical characterizations is needed (Lu et al., 2023). Fourier Transform Infrared Spectroscopy (FTIR), Differential Scanning Calorimetry (DSC), light microscope, Scanning Electron Microscope (SEM), and other techniques, are often used as characterization methods for MPs.

The advantages of these analytical techniques vary when it comes to characterizing MPs with various aging processes. More study on microbial aging supports optical approaches (Lu et al., 2023); for instance, light microscopy and SEM are useful tools for characterizing worn and weathered MPs and alterations on the surface of MPs. FTIR and Raman spectroscopy, on the other hand, can be used as methods to investigate the alterations in functional groups of MPs after aging. Generally, infrared methods are more effective in detecting oxidative end functional groups while Raman spectroscopy is more capable of characterizing backbone of polymers (Phan et al., 2022). Moreover, several techniques such as X-ray diffraction and DSC can be used to measure the crystallinity changes of MPs before and after bio-aging (Campanaro et al., 2023). Other MPs characterization techniques include but are not limited to, Brunauer-Emmett-Teller (BET), thermal gravimetric analysis (TGA), X-

ray photoelectron spectroscopy (XPS), and SEM equipped with energy dispersive X-ray analysis (SEM-EDS) (Lin et al., 2021).

Most of the current techniques for characterizing MPs still rely significantly on manual identification and are quantitative in nature as opposed to qualitative. Furthermore, while the characterization method can identify MP oxidation, it does not have a fingerprint or particular standards to identify the aging process (Lu et al., 2023).

2.4 Microplastics as Sorbents for Organic Contaminants

Plastic particles and fragments present in the environment have been identified to contain a variety of chemicals. Some of these chemicals are additives intentionally incorporated into the plastic during manufacturing, while others are environmental contaminants absorbed by the plastic from surrounding media, such as seawater. MPs have the capacity to sorb and concentrate hydrophobic organic contaminants (HOCs) from seawater which has garnered increasing attention in subsequent years (Karapanagioti & Werner, 2019). Recently, MPs have been recognized as a global environmental threat due to their pervasive presence and persistence and potential risks to the food chain through interactions with OCs across different ecosystems (Wang et al., 2022b) which necessitate a comprehensive examination of these interactions (Zhou et al., 2022). Therefore, an in-depth understanding of the processes influencing the fate of OCs in environmental systems is crucial across various fields, particularly ecotoxicology. The transport, bioavailability, and bioaccumulation of contaminants, as well as their toxic effects on organisms and transformation reactions, are all significantly dependent on sorption dynamics (Hummel et al., 2021).

Due to their physicochemical properties (*i.e.* fugacity capacity and hydrophobicity), MPs act as important vectors for the accumulation and transportation of hazardous chemicals (Lin et al., 2021; Lončarsk et al., 2020) and have a strong affinity for OCs

(Mo et al., 2021). These interactions open a new pathway for OCs to enter the food web (Verdú et al., 2021). OCs may be adsorbed or absorbed owing to the properties of MPs, especially regarding proportion of amorphous vs. crystalline regions. It is expected that both absorption and adsorption contribute to the sorption behavior of OCs on a soft polymer such as PE. The ability of MPs to sorb various contaminants, including antibiotics, persistent organic pollutants (Tong et al., 2021), heavy metals (Tong et al., 2021; Lončarsk et al., 2020), pharmaceuticals, polychlorinated biphenyls, polycyclic aromatic hydrocarbons, and perfluoroalkyl acids (Lončarsk et al., 2020), poses risks to aquatic organisms and ecosystems (Tong et al., 2021). These findings suggest that MPs serve as reservoirs for hazardous OCs in aquatic environments, raising concerns about potential adverse consequences for aquatic ecosystems due to the adsorption of organic pollutants onto MPs (Lončarsk et al., 2020). Thus, understanding the behavior of different OCs is crucial due to their significant impact on the fate and transport of pollutants (Lončarsk et al., 2020).

2.4.1 Mechanisms of interactions

Understanding the mechanisms of interaction between MPs and OCs is crucial for assessing the environmental impact of MPs (Tong et al., 2021) which may in turn affect their interaction with OCs. The hydrophilicity and hydrophobicity of plastics change as MPs age, which has an adverse biological effect on organism uptake (Lu et al., 2023). Due to aging, MPs surface characteristics are affected, surface shape and particle size vary, and mechanical and thermal properties of plastics are further reduced. Moreover, different binding affinities for additional OCs may result from these surface modifications (Zafar et al., 2022). Biological aging alters the surface's physicochemical and structural characteristics, increasing the number of binding sites and forming new functional groups (Zafar et al., 2022). The physical and chemical characteristics of MPs, such as their surface micro-morphology and roughness, surface charge, specific surface area, and density, may be impacted by biofilm formation. These characteristics may then have an impact on the pathogens

and chemical pollutants' adsorption-desorption, vertical migration, and weathering on MPs in the environment (Tu et al., 2020). Enzymes and microorganisms exhibit distinct aging and degradation mechanisms, influencing the hydrophilicity and hydrophobicity of degradation products. Although OCs typically co-exist with aged MPs in aquatic ecosystems, studies related to the adsorptive role of especially bio-aged MPs are quite limited.

The pervasive presence of aged MPs and their potential interactions with various OCs across different ecosystems necessitates a comprehensive examination of these interactions. Numerous recent studies (Costigan et al., 2022; Fu et al., 2021; Wang et al., 2020) have scrutinized the interactions between OCs and MPs, especially aged PE (Adan et al., 2022; Çiftçi et al., 2023). The primary mechanisms for sorption of organics to MPs identified include hydrophobic interactions, partitioning (absorption) into the amorphous regions of MPs, electrostatic interactions, and interactions on MP surfaces or crystalline regions (such as hydrogen bonding, π–π interactions, and halogen bonding), with multiple mechanisms generally acting concurrently (Li et al., 2019b). For instance, Hüffer & Hofmann (2016) indicated by linear isotherm models that partitioning into amorphous regions into MPs dominated the sorption of PE.

For OCs and non-aromatic MPs like PE, the primary mechanism can be van der Waals interactions. For instance, there is a significant relationship between log K_{ow} values and the sorption capacities of various antibiotic species on five different MPs tested (Costigan et al., 2022). Costigan et al., (2022) also emphasize the hydrophobicity of OCs (*i.e.*, log K_{ow}) as a good indicator of the sorption capacity of some polymer types and OCs, although they note that hydrophobicity alone may not be sufficient. Typically, MPs function as carriers for hydrophobic OCs owing to the hydrophobic nature and substantial surface area-to-volume ratio of MPs (Chen et al., 2022).

The sorption behavior of OCs on MPs depends on the structure and properties of both the OCs and the MPs in question (Çiftçi et al., 2023). For example, rubbery

polymers such as HDPE and LDPE are expected to demonstrate greater diffusion (e.g., permeability and greater free volume) than glassy polymers (Rochman et al., 2013). Moreover, less hydrophobic and lower molecular weight chemicals are expected to reach saturation with MPs faster than those with opposite characteristics (Rochman et al., 2013). Furthermore, the sorption capacity of MPs can be influenced by various factors such as MPs' particle size, specific surface area, degree of aging, changes in crystallinity, surface charge, and polarity. For instance, the number of adsorption sites and the capacity to adsorb OCs increase with smaller particle sizes and larger specific surface areas of MPs (Fu et al., 2021). In addition, Fu et al., (2021) indicated that the changes in functional groups (C-H and C-C oxidation) after aging resulted in an increase in MPs hydrophilicity and consequently improved their adsorption capacity for hydrophilic OCs. Similarly, increasing in crystallinity of MPs can result in less free volume for sorption and decrease in sorption affinity and capacity of OCs (Fu et al., 2021). Moreover, as MPs age, their polarity also changes leading to changes in the sorption capacity (Martín et al., 2022).

Furthermore, there are a number of factors, including the type of MPs, the pH of the solution and changes of the pH during sorption, temperature, the ionic strength, and the presence of coexisting dissolved organic matter that have been found to influence the sorption of organic contaminants on MPs (Li et al., 2019b). On the other hand, the properties of the OCs such as hydrophobicity and dissociated form can also influence sorption capacity (Fu et al., 2021). The adsorption capacity depends on whether the OC being sorbed is in its neutral or dissociated form. For example, if the solution pH of the OCs is higher than the point of zero charge (pHpzc) of MPs, their surface becomes negatively charged, attracting positively charged pollutants through electrostatic interactions. Conversely, when the environmental pH exceeds the pollutants' pKa, the pollutants become deprotonated and anionic, leading to electrostatic repulsion and reduced adsorption by MPs (Martín et al., 2022). In addition, high temperature and a high content of dissolved organic matter (DOM) such as biofilm leaching from bio-aged MPs decrease sorption to MPs by reducing

the availability of adsorption sites for OCs and thereby modifying the partitioning between the solid surface and water (Martín et al., 2022).

2.4.2 Effect of MP Bio-Aging on Interaction Mechanisms

The accumulation of MPs in WWTPs, coupled with the potential sorption of OCs, including endocrine-disrupting chemicals (EDCs), on MPs, raises specific concerns regarding the land application of biosolids. Even though a lot of research has been done to understand the sorption behavior and mechanism of contaminants on MPs, it's possible that the pristine MPs used in many of these studies don't accurately represent the situation in nature and in WWTPs (Ho et al., 2020). Longer exposure to natural weathering processes like bio-aging changes the physical makeup and morphology of plastic waste and significantly releases hazardous byproducts (Priyanka & Saravanakumar, 2022). These changes may influence the different interactions of OCs with bio-aged MPs, especially PE. Moreover, the presence of additives in PE might influence the interactions with OCs besides bio-aging (Lončarsk et al., 2020). Therefore, the study of the effect of OCs with MPs in WWTPs is significant.

AD and composting can lead to higher biodegradation of plastics. Therefore, the intensive mechanical abrasion and microbial activity during treatment processes in WWTPs may significantly alter the physicochemical properties of MPs compared to marine and freshwater environments. For instance, the physicochemical properties of MPs in sewage sludge are modified during treatment processes; for example, MPs are sheared into smaller sizes during lime stabilization, thermal drying causes surface melting and blistering, and the abundance of MPs decreases in AD (Li et al., 2019a).

The interaction of PE with sludge in WWTPs can bring several outcomes on sorption of OCs. For instance, plastic debris can interact with resident organisms, including microorganisms, as well as dissolved and particulate organic matter. For instance, biofilms likely influence the fate of chemicals by altering sorption dynamics (Cui et

al., 2023). However, due to lack of enough research on this area, there is no complete idea on the mechanism or effects of this hypothesis on the sorption of OCs on PE.

Furthermore, sludge obtained from WWTPs are applied to lands as biosolids, and one of the risks of this application is the presence of heavy metals and OCs in MPs. Due to their long-term accumulation in soil and desorption processes, these OCs and metals can enter the food chain, posing risks to human health. Moreover, it is hypothesized that the significant changes in the physicochemical properties of MPs during treatment processes may alter their adsorption potential for these pollutants. The formation of MP-contaminant combinations is potentially harmful to organisms, as pollutants absorbed on MPs can desorb in various organ sites and may have additional negative effects, such as altering enzyme biological activity. For example, it has been reported that the presence of MPs could increase metal exposure in earthworms and enhance the bioavailability of pollutants, indicating that MPs can act as vectors of pollutants and increase their risks in the terrestrial environment (Li et al., 2019a).

2.4.3 Organic Contaminants of Concern in This Study

2.4.4 Triclosan

Triclosan (TCS), an antimicrobial agent, common bactericide, and disinfectant, has been confirmed as a persistent endocrine disruptor and is bio-accumulative in aquatic and other organisms within the environment (Çiftçi et al., 2023). TCS is extensively utilized in toothpaste, skin care, dental, and disinfection products. Following routine use, TCS finds its way into the wastewater, resulting in a high residual level. TCS was found at concentrations of $>8.6\times10^{-2}$ and 5.4×10^{-3} mg/L in the wastewater influent and effluent, respectively (Shi et al., 2022b). Moreover, it is primarily introduced into agricultural soil through the application of biosolids, where TCS tends to concentrate during wastewater treatment. Concentrations of TCS as high as 949 ng/g were found in soil treated with biosolids (Chen et al., 2021c). Moreover,

TCS was found in sludges at concentrations ranging from 0.09 to 16.79 mg/kg due to its hydrophobic properties (Tong et al., 2021).

TCS has been reported to be toxic to aquatic organisms interfering with the biological receptors in vitro. Although not directly relevant to biosolids-amended soils, TCS may act as an EDC in rats by amplifying testosterone-induced androgen receptor-mediated transcriptional activity. With its confirmed presence in biosolids-amended soils, TCS has the potential to bioaccumulate in soil-dwelling organisms and exert toxic effects on higher organisms through trophic transfer. For instance, TCS has been shown to bioaccumulate in algae and snails exposed to WWTP effluent. Moreover, TCS can undergo transformation process creating other products which can also have varying impacts (Higgins et al., 2011).

TCS may have a significant negative impact on human health and the environment due to factors such as fish accumulation, inhibition of algal growth, and endocrine disruption (Higgins et al., 2011). According to literature, PE increases the concentration of TCS in the mussels' tissues when compared to exposure to TCS alone. Because MPs are so common in the aquatic environment, TCS was frequently found on their surface. Consequently, investigating the carrier effect of MPs on coexisting pollutants and potential ecological hazards will be aided by the TCS adsorption experiment on MPs (Shi et al., 2022b).

2.4.5 2,3,6 Trichlorophenol

Chlorophenols (CPs) are ubiquitous contaminants in the environment originating from various anthropogenic activities involving chemical, textile, and pharmaceutical sectors (Tubić et al., 2019). CPs can have significant environmental and human health hazards. CPs possess chemical structures that are readily oxidizable and serve as versatile intermediates in chemical synthesis. However, CPs exhibit low solubility in water due to their relatively high octanol-water partition coefficient (K_{ow}), resulting in a propensity to accumulate in sludge. Notably, CPs are

not only directly toxic but also possess carcinogenic, teratogenic, and mutagenic potential. Studies have indicated that CPs constitute the largest proportion of phenolic pollutants in sludge, accounting for 64.55% with a concentration of 170.90-6290.30 ng/g dry sludge (Chen et al., 2021c). Chlorophenols include widely applied pesticides and their degradation products (Tubić et al., 2019), and are widely used in the production of industrial commodities and, as a result, have been commonly detected in water bodies (Jiang et al., 2020).

2.4.6 Malachite Green

Malachite green (MG) is a water-soluble and commonly used cationic dye in textile dyes, food colorants, aquaculture fungicides, and insecticides (Tsai et al., 2022). Its toxic effects have garnered significant attention due to its detrimental impacts on aquatic life and humans because of inadequate disposal (Lin et al., 2021; Tsai et al., 2022). Because of its accessibility and affordability, MG is still used widely around the world despite being banned in some nations (Lin et al., 2021) especially as an effective fungicide and parasiticide in aquatic systems (Tsai et al., 2022).

It has been observed that the removal of dyes from water once polluted is particularly challenging through conventional wastewater treatment methods (Hameed & El-Khaiary, 2008). This difficulty arises due to the stability of many dyes in the presence of light and oxidizing agents, as well as their resistance to aerobic bio-oxidation. Moreover, dyes are detectable even at low concentrations and can adversely impact aquatic life and the food web (Ling & Mohd Suah, 2017). Furthermore, the presence of MG in water results in severe health effects, including mutagenesis, teratogenicity, chromosomal abnormalities, respiratory toxicity, fractures, and carcinogenesis (Ling & Mohd Suah, 2017). For instance, MG is highly cytotoxic to mammalian cells and promotes liver and kidney disease. Furthermore, MG persists in the aquatic environment and once absorbed by fish, is metabolized into other forms that can also have other impacts and different accumulation schemes. Consequently, MG not only harms the environment but also poses serious

public health risks through the food chain (Tsai et al., 2022). These adverse effects are significantly influenced by the exposure duration, temperature, and concentration of the dye (Ling & Mohd Suah, 2017).

CHAPTER 3

MATERIALS AND METHODS

3.1 Materials

3.1.1 Microplastics Used

Pristine HDPE MPs were obtained from a water tank supplier in Ankara, Türkiye. According to the company, shredding took place in OSTİM facility, and the raw material was imported from Iran. A Masterbatch company in Ankara kindly provided pristine LDPE-type pure MPs with the batch name PETILEN I22-19T. According to the information from the manufacturers, LDPE was pure and did not contain any additives, yet HDPE contained an additive (chemical unknown) to protect against UV-oxidation. Both MPs types were provided in powder form. The density of HDPE and LDPE was given by the manufacturer as 0.935 and 0.919 g/cm^3, respectively. These values fall within the usual densities found in the literature, which are 0.94 and 0.92 g/cm^3 for HDPE and LDPE, respectively (Puckowski et al., 2021). Using Attenuated Total Reflection-Fourier Transform Infrared Spectroscopy (ATR-FTIR) analysis as performed at METU Central Laboratory (MERLAB), polymer structure was confirmed as polyethylene (PE). The density and the PE backbone data from FTIR verify that the plastics are of the HDPE and LDPE variety.

Table 3.1 summarizes the characteristics of both PE types used in this study. FTIR spectra were compared with the library, resulting in HDPE and LDPE matching by 99% to PE. Perkin Elmer Diamond Differential Scanning Calorimetry (DSC) (Heating rate: 10 °C/min, Temperature range: 30°C to 300°C, Under N_2 atmosphere) at MERLAB was used to determine the crystallinity (X_c) and melting temperature (T_m) of PE by utilizing the data obtained from the 1st heating peaks. The PE's Brunauer-Emmett-Teller (BET) surface area was measured with a Micromeritics

ASAP-2020 Surface Area Analyzer using Krypton at University of Maine Laboratory as 0.0500 ± 0.0056 m^2/g and 0.0400 ± 0.0025 m^2/g for HDPE and LDPE respectively.

Table 3.1 Characteristics of HDPE and LDPE MPs used throughout the study.

MPs Type	Density (g/cm^3)	Melting Temperature (T_m, °C)	Crystallinity (%)	BET Surface Area (m^2/g)	MPs Structure (adapted from Kumar Sen & Raut, (2015))
HDPE	0.935	126.78	52%	0.0500 ± 0.0056	
LDPE	0.919	102.62	36 %	0.0400 ± 0.0025	

Pristine MPs' zeta potential and point of zero charge (pH_{PZC}) were measured by MERLAB. HDPE surface charge was verified to be negative, at any pH higher than roughly pH=2. Since two of the OCs (TCS and TCP) used in this study are ionizable, pH becomes a crucial factor in sorption. Understanding the surface charge at solution pH is crucial for this goal since it will help clarify sorption mechanisms like electrostatic attraction, repulsion, and hydrophobic interaction.

Finally, the water contact angle (CA) of pristine LDPE samples was measured using an Attension Theta goniometer at MERLAB. To determine the CA of the samples, thin films (2×2 cm) were prepared by placing 0.25 g of each sample between two glass slides and heating them at their melting points for 12 hours in an oven. After cooling to room temperature for approximately 2 hours, the thin films were removed from the glass slides. Measurements were repeated five times for each sample, and the average CA values were calculated. The contact angle measurement is a technique used to assess the surface hydrophobicity of MPs, with increasing contact angles indicating higher hydrophobicity (Sheng et al., 2021; Zhong et al., 2022). The average CA data for the LDPE pristine sample was 91.4±3.6 degrees, which suggests a hydrophobic nature. However, this value is associated with high uncertainty, due both to the high standard deviation of measurement and preparation of material prior

to measurement, hence CA measurements are deemed inconclusive. The water CA value is a reliable indicator of a material's hydrophobicity, with values less than 90° indicating hydrophilic nature and values greater than 90° indicating hydrophobic nature (Siddiqa et al., 2014).

3.1.2 Sludge Samples Used in Bio-aging

The study's waste activated sludge (WAS) and anaerobically digested sludge (ADS) samples were obtained from the Central WWTP of Ankara. With a daily capacity of 765,000 m^3 (4 million design population equivalent). It is an urban WWTP that treats municipal wastewater using a conventional activated sludge technology. WAS sample was taken from the secondary clarifier's sludge return line. The plant's mesophilic anaerobic digesters, which operate at 35°C, mix and digest the primary and WAS and provided the ADS that was used to seed the reactors. Before analysis, samples that were transferred to the lab were kept at 4°C. Table 3.2 lists the various uses for which WAS and ADS samples were used throughout this investigation. For each set-up, a new batch of WAS and ADS was collected from the WWTP.

To simulate inhibited seed in the Abiotic reactors of the BMP test, ADS samples were sterilized by adding mercury chloride ($HgCl_2$) at a concentration of 200 mg/g total suspended solids (TSS) and autoclaved for an hour at 121°C for 4 times on consecutive days.

Table 3.2 Sludge samples used in this study and their usage areas.

Sludge type	Area of use
WAS	Aerobic reactors BMP test (as substrate)
ADS	BMP test (as seed control reactors) BMP test (as seed for biotic reactors) BMP test (as inhibited seed for abiotic reactors)

3.1.3 Organic Contaminants Used in This Study

Neat standards of 2,3,6-Trichlorophenol (TCP) used in sorption experiments was supplied from Chemservice INC., Pennsylvania, USA, triclosan (TCS) was from TRC, Canada, and malachite green (MG) in oxalate form was obtained from ISOLAB, Türkiye. Table 3.3 and Table 3.4 summarize the physical and chemical properties of the three OCs in this study.

Table 3.3 Physical and chemical properties of TCP and TCS.

Common Name	2,3,6-Trichlorophenol (TCP)	Triclosan (TCS)
CAS	933-75-5	3380-34-5
IUPAC Name	2,3,6-trichlorophenol	5-Chloro-2-(2,4-Dichlorophenoxy)Phenol
Molecular Structure	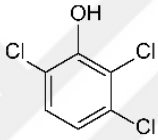	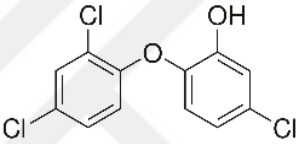
Molecular Formula	$C_6H_3Cl_3O$	$C_{12}H_7Cl_3O_2$
Molecular Weight (g/mol)	197.4	289.54
Solubility	Soluble in ethanol, ether, benzene, acetic acid, petroleum ether; slightly soluble in water	Soluble in ethanol, methanol, diethyl ether, and strongly basic solutions (such as 1M NaOH); slightly soluble in water
Solubility in water (g/L)	< 1 (at 20 °C)	0.010 (at 20 °C)
pKa	5.8	7.9
Log K_{ow}	3.77	4.76
Density (g/cm^3)	1.5 (at 20 °C)	1.49
Melting Point (°C)	58	55-58
Boiling Point (°C)	272	120
Vapor Pressure	0.00246 mmHg, 0.2 Pa (at 25 °C)	0.0000046 mmHg, 5.2×10^{-6} Pa
Physical Description	Colorless solid needles	White to off-white crystalline solid powder
Colors in aqueous solution	Colorless	Colorless
Odor	Phenolic odor	Slight aromatic odor
Nature	Hydrophobic	Hydrophobic
References	(National Center for Biotechnology Information, 2024a)	(National Center for Biotechnology Information, 2024c), (Singh & Kaur, 2023)

Table 3.4 Physical and chemical properties of MG.

Common Name	Malachite Green Oxalate (MG)
CAS	2437-29-8
IUPAC Name	[4-[[4-(dimethylamino)phenyl]-phenylmethylidene]cyclohexa-2,5-dien-1-ylidene]-dimethylazanium;2-hydroxy-2-oxoacetate;oxalic acid
Molecular Structure	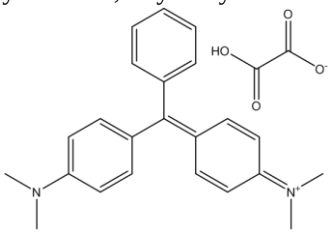
Molecular Formula	$C_{52}H_{54}N_4O_{12}$
Molecular Weight (g/mol)	927.01
Solubility	Soluble in water and alcohol
Solubility in water (g/L)	60 (at 25 °C)
pKa	pKa_1=2, pKa_2=8
Log K_{ow}	0.65
Density (g/cm^3)	N/A
Melting Point (°C)	164
Boiling Point (°C)	N/A
Vapor Pressure	N/A
Physical Description	Dark green solid powder crystals
Colors in aqueous solution	Yellow (pH 0.0-2.0), Green (pH 2.0-11.6), Colorless (pH 11.6-14)
Odor	Odorless
Nature	Hydrophilic
References	(National Center for Biotechnology Information, 2024b), (Road & Lincolnshire, 2014), (Oxalate, 2012)

3.2 Methods

3.2.1 Handling of Sludge Samples

WAS and ADS obtained from the WWTP were kept at 4°C to settle for one day. The sludges' clear supernatant was then siphoned, and the settled sludge was gently centrifuged for four minutes at 4000 rpm to thicken. The total solids (TS) values of the sludges were adjusted to 2% for reactor preparation.

3.2.2 Preparation of Microplastic Samples

HDPE and LDPE in powdered form were manually sieved to a size range of 425-500 μm using metal sieves. They were then washed using Deionized (DI) water, ultrasonicated for 30 min, and left to dry in an incubator at 25°C.

3.2.3 Anaerobic Bio-aging of Microplastics

Biochemical Methane Potential (BMP) Tests

Test reactor setups for mesophilic BMP were run at 35°C. The centrifuged ADS with TS value of 2% served as the inoculum for mesophilic reactors. The goal of TS adjustment is to standardize the conditions in the operated reactors at a typical solids content. The German standard (VD1 4630) mandates that the substrate's volatile solids (VS) concentration be greater than 10 g/L (Raposo et al., 2012). Values above 10 g/L (about 11–14 g/L) of VS content were also ensured with a 2% TS adjustment for WAS. Once the TS value was adjusted, the sludges were characterized. The following parameters were assessed after sampling: TS, VS, total suspended solids (TSS), volatile suspended solids (VSS), total chemical oxygen demand (tCOD), and pH. Table 3.5 indicates the sludge characteristics used in BMP tests. Each parameter was measured either in duplicate or triplicate. N/A indicates that a test was not performed.

Table 3.5 Initial characteristics of WAS and ADS used in the anaerobic BMP reactors.

	HDPE Set-up		LDPE Set-up 1		LDPE Set-up 2	
Parameter	WAS	ADS	WAS	ADS	WAS	ADS
TS (g/L)	19.4±0.8	20.2±0.3	19.8±0.9	20.4±0.1	19.7±0.4	18.3±0.8
VS (g/L)	12.6±1.4	10.5±0.2	13.9±1.3	13.4±0.1	14.3±0.4	9.8±0.5
VS/TS	0.6±0.05	0.5±0.003	0.7±0.03	0.7±0.007	0.7±0.006	0.5±0.003
TSS (g/L)	18.2±0.5	18.7±0.04	19.5	17.9	18.5±0.7	18.2±0.1
VSS (g/L)	15.8±0.04	11.1±0.5	18.0	13.1	14.8±0.2	11.3±0.05
tCOD (g/L)	N/A	N/A	24.5±0.1	17.1±0.04	25.1±0.04	21.2±0.1
pH	N/A	N/A	6.54	7.52	6.54	7.42

BMP Reactors Design

BMP reactors were run in 250 mL total capacity amber serum bottles with 200 mL active volume and 50 mL headspace. The WAS and ADS ratios in the reactors were modified to a TS value of 2% and an F/M ratio (g VS of WAS/g VSS/VS of ADS) of 1. The F/M ratio of 1 was chosen based on the literature (Owen et al., 1979; Raposo et al., 2012). Table 3.6 and Figure 3.1 summarize the design details of HDPE and LDPE reactor sets including the reactor labels, number of replicates, and PE doses used in each set-up. All reactors were labeled such that HDPE-containing ones start with "H", LDPE-containing ones start with "L", abiotic reactors are indicated by "A", seed control reactors "S", and biotic sets "B". Sludge control reactors were identified by zero beside the letter indicating that no dose of MPs was added. Even though control reactors did not have HDPE and LDPE, the letters (*i.e.* H and L) refer to the controls corresponding to each set-up. Control reactors were prepared with each set, and they had slightly different characteristics because sludge was obtained at different times from the WWTP. The contents of each reactor type are summarized in Table 3.6. LDPE bio-aging BMPs did not include abiotic reactors, only biotic and seed control (Table 3.6). A higher dose of 300 mg LDPE/g TS (1.2 g LDPE/reactor) was used in reactors containing MPs to recover higher amounts of MPs for further experimentation with OCs. Abiotic reactors, utilized only for HDPE, contained WAS along with sterilized and inhibited ADS to ensure that no microbial activity occurs, whereas biotic reactors had both ADS and WAS. Seed control reactors were configured to monitor the performance of the seed only. Two batches of LDPE reactors were run, indicated as "Set-up 1" or "Set-up 2". There was no difference between these two sets other than ADS and WAS, obtained from the WWTP almost seven months apart.

Table 3.6 Summary information on BMP reactor set-ups.

Label	Reactor Type	Reactor Label	Reactor Replicates	MPs (mg PE/gTS)	Reactors Sludge Contents
HDPE Set-up	Abiotic	HA0	2	0	Inhibited ADS + WAS
		HA	3	200	
	Biotic	HB0	2	0	ADS + WAS
		HB	10	200	
	Seed	HS0	2	0	ADS + Water
LDPE Set-up 1	Biotic	LB0-1	2	0	ADS + WAS
		LB-1	36	300	
	Seed	LS0-1	2	0	ADS + Water
LDPE Set-up 2	Biotic	LB0-2	2	0	ADS + WAS
		LB-2	56	300	
	Seed	LS0-2	2	0	ADS + Water

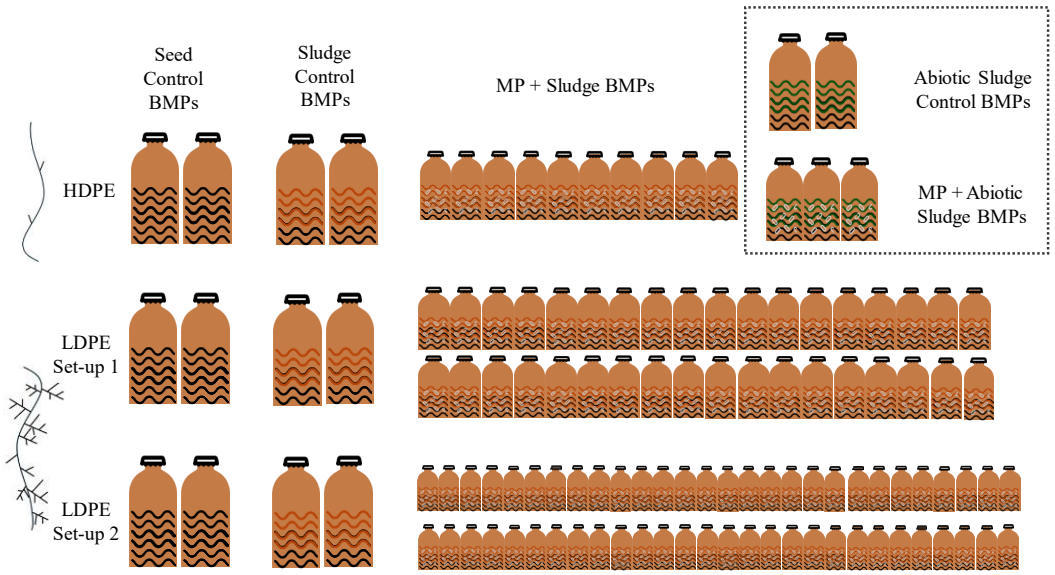

Figure 3.1 Bottles arrangement of HDPE and LDPE BMPs set-ups.

BMP Reactors Operations

By setting the reactor's TS value to 2% and the F/M ratio to 1, appropriate volumes of WAS and ADS were mixed for each set of BMPs. Complete sludge analysis including TS, VS, TSS, VSS, tCOD, BOD_5, and pH were performed both prior to and following BMP test. The recommended PE doses were added to each reactor.

The reactor bottles were sparged and purged with 99.9% pure nitrogen gas (N_2) and sealed with a rubber septum to ensure anaerobic conditions. Using a syringe needle, the reactor pressures were brought to atmospheric pressure following the purging. Reactors were incubated at 35^{o}C and manually shaken every day.

To observe the fate and effect of PE during the bio-aging process, HDPE reactors were operated for 50 days while LDPE reactors were operated for 60 days. In a typical BMP test, it is advised to terminate the BMPs once the daily production or cumulative CH_4 increase drops to 1% (Holliger et al., 2017). Consequently, it was determined that in the current study, biogas measurements would be taken every other day after a drop to 2% of daily CH_4 produced/cumulative CH_4 produced which occurred after 27, 15, and 20 days for HDPE set-up, LDPE set-up 1, and set-up 2 respectively. Additionally, methane content for HDPE set-up was measured daily for the first 27 days then each other day, while for LDPE set-ups it was measured twice per week.

3.2.4 Aerobic Bio-aging of Microplastics

Aerobic Digestion Reactors

Aerobic test reactor setups were run at 35°C. The working medium consisted of centrifuged WAS with TS value of 2% to provide a thickened sludge to ensure aging of PE. Once the TS value was adjusted, the sludges were characterized. The following parameters were assessed: TS, VS, TSS, VSS, tCOD, and pH. Table 3.7 indicates the WAS characteristics used in aerobic set-ups. Each parameter was measured either in duplicate or triplicate.

Table 3.7 Initial characteristics of WAS used in the aerobic reactors.

Parameter	HDPE Set-up	LDPE Set-up 1	LDPE Set-up 2
TS (g/L)	19.9±0.4	18.3±1.0	18.5±0.2
VS (g/L)	14.9±0.2	13.3±0.7	14.1±0.2
VS/TS	0.7±0.015	0.7±0.008	0.8±0.009
TSS (g/L)	19.2±0.2	17.2±3.4	18.9±0.4
VSS (g/L)	16.3±0.4	13.5±2.9	15.2±0.4
tCOD (g/L)	22.3±0.1	28.4±0.02	25.4±1.1
pH	N/A	6.6±0.1	6.6±0.05

Aerobic Reactors Design

Aerobic reactors in this study were run in flat-bottom glass flasks with a capacity of 6L. All reactors' sets were filled with WAS only adjusted at TS of 2%. Table 3.8 and Figure 3.2 summarize the design details of HDPE and LDPE reactor sets including the reactor labels, number of replicates, and doses used in each set-up. Higher doses of PE in LDPE set-ups were to produce bio-aged PE for upcoming sorption experiments. Out of the total 6 L volume, 5 L was filled for HDPE while 4 L were filled for LDPE-containing reactors.

Table 3.8 Summary information on aerobic reactor set-ups.

	HDPE Set-up	LDPE Set-up 1	LDPE Set-up 2
Reactor Label	HO	LO-1	LO-2
Replicate	1	3	4
Total Working Volume (L)	5	4	4
MPs Dose (PE g/ L WAS)	4	5	5

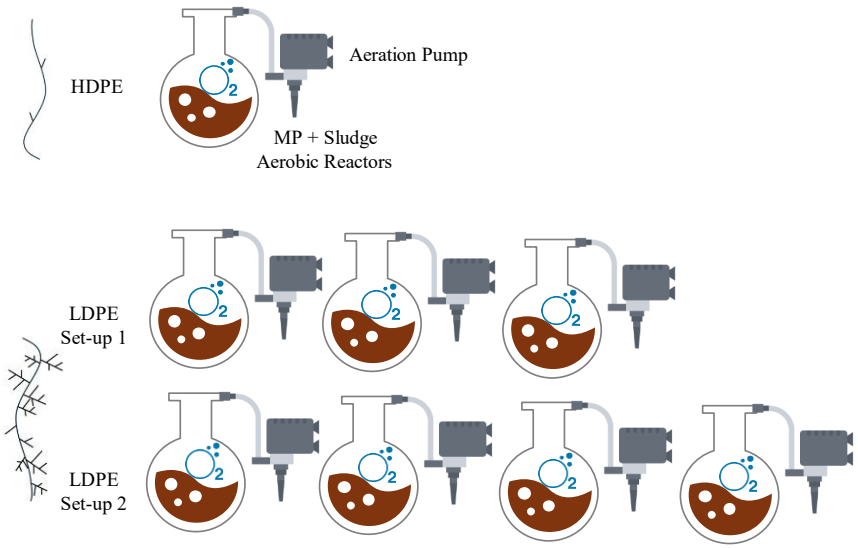

Figure 3.2 Set-up of HDPE and LDPE aerobic reactors.

Aerobic Reactors Operation

Upon filling the reactors with WAS, aerobic set-ups were operated in mesophilic conditions at 35°C. The reactors were aerated constantly using glass pipettes and aquarium pumps to continuously oxygenate the sludge. Each time water evaporated from the reactors, it was replaced with tap water to keep the volume of the sludge stable and to be able to measure the actual difference of sludge parameters after termination. To enable ample time for bio-aging, HDPE set-up was operated for 27 days. For LDPE set-ups, the same duration as BMP set-ups were aimed so they were operated for 60 days.

Initially and upon termination, TS, VS, TSS, VSS, tCOD, BOD_5, and pH were measured in each reactor. BOD_5 was also monitored almost weekly and upon termination for HDPE reactors.

3.2.5 Methods Used to Recover Microplastics After Digestion

Upon termination, MPs were extracted from each reactor according to the steps illustrated in Figure 3.3. Sludge containing MPs from the reactors was manually sieved using a 350 µm sieve to recover MPs. Subsequently, the sieves were backwashed into a beaker with tap water and vacuum-filtered. MPs from each reactor were gathered on paper filters before manually being picked into glass vials. Table 3.9 indicates the approximate percent recovery that could be obtained from each set-up. A portion of the gathered MPs particles were cleaned, namely, "washed" by soaking in approximately 17.5% hydrogen peroxide (H_2O_2) solution overnight at 25°C in a shaking incubator (200 rpm), to remove sludge residuals and biofilm (Şimşek, 2023). After that, distilled water (DW) was used to rinse the MPs, prior to drying at 25°C in an incubator.

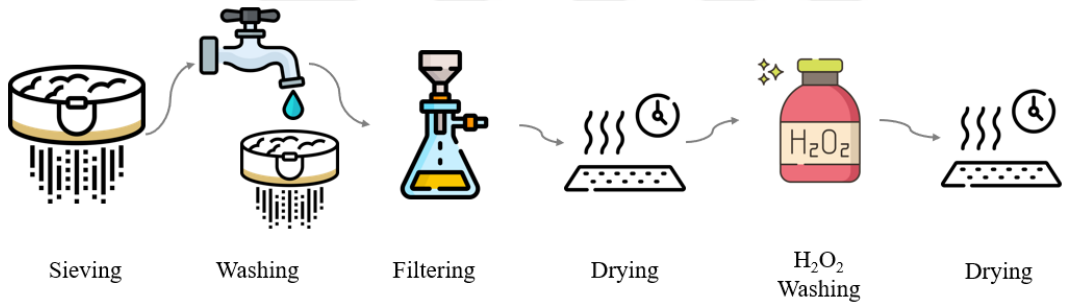

Figure 3.3 Schematic illustration of the MPs recovery procedure.

Table 3.9 Percent recovery of PE upon reactor termination.

	Aerobic	Anaerobic
HDPE Set-up	72 %	72 %
LDPE Set-up 1	93 %	89 %
LDPE Set-up 2	91 %	89 %

Recovered and washed MPs were labeled as depicted in Table 3.10 based on which reactors where they were obtained from.

Table 3.10 Summary description of MPs of this study.

Label	Type of PE	Type of Bio-Aging	Description
HP	HDPE	None	Pristine HDPE
HPW	HDPE	None	Pristine HDPE - H_2O_2 Washed
HBW	HDPE	Anaerobic Digestion	Bio-aged HDPE - H_2O_2 Washed
HAW	HDPE	Anaerobic Digestion	Bio-aged HDPE - H_2O_2 Washed
HOW	HDPE	Aerobic Digestion	Bio-aged HDPE - H_2O_2 Washed
LP	LDPE	None	Pristine LDPE
LPW	LDPE	None	Pristine LDPE - H_2O_2 Washed
LBW	LDPE	Anaerobic Digestion	Bio-aged LDPE - H_2O_2 Washed
LOW	LDPE	Aerobic Digestion	Bio-aged LDPE - H_2O_2 Washed

3.2.6 Sorption Experiments

Preliminary sorption experiments of OCs were carried out using pristine (HP and LP), H_2O_2 washed (HPW and LPW) and bio-aged-H_2O_2 washed (HBW, HOW, LBW-1, and LOW-1) HDPE and LDPE MPs. Sorption isotherms could only be conducted using the second bio-aged batch of LDPE (*i.e.*, LBW-2 and LOW-2) using 7 different concentrations for TCP and TCS.

Triplicate test reactors with singular solutions of each OC and MPs were used during sorption experiments. Two sets of controls, containing only OC of concern and only MPs were used during all tests. Sorption was conducted in 40 mL amber glass vials with a working volume of 36 mL. Solid to liquid ratio (S/L) was 25 g/L for TCP and MG and 10 g/L for TCS, in accordance with earlier experiments conducted as part of TUBITAK 220N044 project. Similarly, kinetic studies had previously established that it would take 24 hours for HDPE and 6 hours for LDPE, for TCP and TCS, while 2 days for MG using LDPE to reach sorption equilibrium. All preliminary sorption tests were conducted at 9 ppm, except for TCP (8 ppm for HDPE). Additionally, 15 ppm was also conducted for MG using the second LDPE bio-aging batch. pH of

water was adjusted to 6 for TCS and MG, and pH 4 for TCP. This made sure TCS and TCP were in their unionized form (pKa=5.8 for TCP, pKa=7.9 for TCS) and MG was in its cationic form (pKa=2 and 8 for MG). To keep TCP and MG within the predetermined pH range of 4.5, an acetate buffer was used on some tests during measurement via spectrophotometer. Isotherms for TCS and TCP were conducted using seven different concentrations, as follows: TCS (1, 2, 4, 5, 7, 8, 9 ppm) and TCP (0.5, 1, 4, 9, 20, 40, 60 ppm). Vials were shaken horizontally at 200 rpm, 25±2°C in a shaking incubator. Results of MG preliminary experiments and isotherms are available in Appendix C (section C.5).

Sorption Isotherm Models

Adsorption isotherm models were used to elucidate potential sorption mechanisms (Chen et al., 2021b). A total of five different linear and nonlinear isotherm models (*i.e.*, Henry, Freundlich, Temkin, Dubinin-Radushkevich, and Langmuir) were fitted to sorption data for TCS and TCP for relevant pristine washed (LPW) and bio-aged (anaerobic (LBW) and aerobic (LOW)) MPs (Table 3.11).

Table 3.11 Isotherm models used in this study (El-Azazy et al., 2021).

Model	Equation	Parameters (Unit)
Henry	L: $q_e = K_d C_e$	K_d (L/g)
Freundlich	L: $\ln(q_e) = \ln(K_F) + \frac{1}{n}\ln(C_e)$ NL: $q_e = K_F C_e^{\frac{1}{n}}$	n, K_F (L/g)
Temkin	L: $q_e = \frac{RT}{b_T}\ln(K_T) + \frac{RT}{b_T}\ln(C_e)$ NL: $q_e = \frac{RT}{b_T}\ln(K_T C_e)$	b_T (J/mol), K_T (L/g)
Dubinin-Radushkevich (D-R)	L: $\ln(q_e) = \ln(q_0) - K[\mathrm{RT}\ln(1+\frac{1}{C_e})]^2$ NL: $q_e = q_m \exp(-K(RTln\left(1+\frac{1}{C_e}\right))^2)$	q_m (µg adsorbate/ g adsorbent), K (mol²/KJ)
Langmuir	L: $\frac{C_e}{q_e} = \frac{1}{q_m K_L} + \frac{C_e}{q_m}$ NL: $q_e = \frac{q_m K_L C_e}{1+K_L C_e}$	q_m (µg adsorbate/ g adsorbent), K_L (µg/g)

*L: Linear model, NL: Non-linear model

3.3 Analytical Methods

Two main sets of analyses were carried out: one set involved reactors and sludge samples characterization before and after reactor operation to observe the effect of PE on the digestion processes. The other involved polymer analysis of PE before and after reactor operation to comprehend the impact of different digestion processes on PE.

3.3.1 Performance of Aerobic and Anaerobic Reactors

Table 3.12 lists the sludge sample analysis and the techniques used both before and after the test reactors were in operation.

Table 3.12 Measured sludge analysis parameters and their corresponding analytical methods* (APHA et al., 2017).

Analysis Parameter	Measurement method
TS, VS	Standard Method 2540 G APHA, AWWA, and WEF (2017)*
TSS, VSS	Standard Method 2540 D and 2540 E APHA, AWWA, and WEF (2017)*
Total COD	US EPA-approved digestion method (Jirka & Carter, 1975)
BOD_5	Standard Method 5210 B APHA, AWWA, and WEF (2017)*
pH	Standard Method 4500 H APHA, AWWA, and WEF (2017)*

Analysis of Solids

The Standard Methods (APHA, AWWA, and WEF 2017) were used to measure TS, VS, TSS, and VSS. While 2540G; which pertains to solid and semisolid samples, was followed for TS and VS measurements, TSS and VSS measurements were carried out in accordance with 2540D and 2540E (APHA et al., 2017).

Total Chemical Oxygen Demand (tCOD)

To determine the digestion efficiency, measurements of tCOD were made both before reactor setup and after termination. tCOD was measured according to a

digestion method recognized by the US EPA (Jirka & Carter, 1975). COD test vials were heated using a HACH COD heating thermo-reactor hotplate for two hours at 150°C.

Biochemical Oxygen Demand (BOD_5)

BOD_5 of aerobic and anaerobic reactors was measured according to the Standard Methods 5210B (APHA et al., 2017). Unseeded BOD test was applied since aerobic and anaerobic reactors contained adequate microbial consortia. For initial BOD_5 measurements, sludge samples were diluted based on tCOD results using a dilution ratio of 1:3700 – 1:4000 for aerobic reactors and 1:3000-1:3125 for BMPs. For termination, BOD_5 measurements dilution ratio was based on expected percent reduction from initial BOD_5 depending on whether it is an aerobic or anaerobic reactor. HDPE aerobic sludge was diluted to ratio of 1:2956 because the test was pursued for 27 days only. For LDPE aerobic reactors, sludge was diluted in a range of 1:35-1:45 while BMPs were diluted in range of 1:40-1:65. Winkler iodometric titration procedure was used for measurement of DO.

pH

An Oakton pH/mV/°C (pH 300 series) meter was used in conjunction with Standard Procedures, Method 4500 H, to measure pH (APHA et al., 2017).

Biogas Volume

Utilizing a water displacement apparatus, a manometric approach was employed to measure the biogas produced by the BMP reactors throughout their operation. To stop CO_2 diffusion, the displacement liquid was acidified by using 0.5% HCl to bring the pH down to 2. To adjust the solution pH, NaOH was also used (Zaman, 2010).

Biogas Composition

Gas chromatograph (GC) with a thermal conductivity detector (TCD) (Agilent 6890 N, Agilent Technologies, California, USA) was used to analyze the biogas composition of BMP reactors. An HP-Plot Q capillary column, measuring 30.0 m x

530 μm x 40.0 μm, was installed on the apparatus. Helium was used as the device's carrier gas, moving at a speed of 29 cm/s. The column temperature was raised to 65°C at a rate of 10°C/min after the first minute of measurements was completed at 45°C. For calibration, two distinct calibration gasses with 55:25:20 and 25:65:10 percent ratios of CO_2:CH_4:N_2 were utilized. A calibration curve between the certified and measured composition produced an equation. The measured values from the device match the calibration equation and a correction was made based on the calibration curve. A 100 μL gas-tight syringe (Hamilton #1710) was used for all gas measurements.

Cumulative CH_4 Production and CH_4 Yield Calculation

The primary performance metric of BMPs digestion process is CH_4 yield. The cumulative CH_4 must first be estimated to compute it. Equation 3-1 was used to compute the cumulative CH_4 volume. Then, Equation 3-2 was applied to determine the CH_4 yield (Trzcinski & Stuckey, 2012).

$$V_{CH4,t} = V_{biogas,t} \times \frac{\%_{CH4,t}}{100} \qquad \text{Equation 3-1}$$

$$M_t = \frac{V_{CH4,t-1} + V_{CH4,t} - B_t}{mass\ VS\ added} \qquad \text{Equation 3-2}$$

$V_{CH4,t}$: CH_4 volume measured at time t (mL),

$V_{biogas,t}$: Biogas volume measured at time t (mL),

$\%_{CH4,t}$: CH_4 percentage at time t,

M_t: Experimental cumulative CH_4 yield at time t (mL CH_4/ g VS),

B_t: Average of the cumulative CH_4 production in the seed controls (mL CH_4),

VS added: Amount of VS fed from WAS to the BMPs (g VS).

CH_4 Kinetics and Potential From WAS

The kinetics and potential of CH_4 production from WAS were assessed and compared using the hydrolysis rate (k) and biochemical CH_4 potential (B_0). Equation 3-3 was utilized to compute the degree of WAS degradation (Y_0) (Li et al., 2020; Wei et al., 2019).

$$Y_0 = \frac{B_0}{380} \times RSS$$ Equation 3-3

Y_0: Apparent VS destruction

B_0: Biochemical CH_4 potential (L CH_4/kg VS added)

380: The maximum theoretical methane potential of sludge at standard temperature and pressure (STP, 25 °C, 1 atm) is represented by 380 (L CH_4/kg tCOD) (L. Metcalf, H.P. Eddy, 2004)

RSS: VS/tCOD ratio of the WAS

To determine k and B_0, a one-substrate model is used in conjunction with the first-order kinetic model (Equation 3-4) (Li et al., 2020; Wei et al., 2019).

$$B_t = B_0(1 - e^{-kt})$$ Equation 3-4

B_t: Cumulative CH_4 yield (L CH4/kg VS added) at time t

t: Time (day)

3.3.2 Characterization of Bio-aging in Microplastics

Fourier-Transform Infrared Spectroscopy (FTIR)

Spectra from Fourier Transform Infrared (FTIR) spectroscopy fitted with attenuated total reflectance (ATR) of both pristine and bio-aged samples were examined to track the structural alterations that resulted from bio-aging. PE MPs' FTIR spectra were captured between 4000 and 400 cm^{-1} using a Perkin Elmer 400 FTIR Spectrometer

at the MERLAB. Using the Bruker Alpha-P FTIR Spectrometry and its software, OPUS v6.5, FTIR-ATR analysis was carried out on the MPs. OMNIC and commercial libraries were used in the software to align the polymer spectrum with the literature. The specific area under band method (SAUB) method, is used to calculate the carbonyl index (CI), which is an indicator of aging and a measure of the degree of PE degradation. From the FTIR spectra of the corresponding HDPE and LDPE MPs, the areas under the band between 1850-1650 cm^{-1} and 1500-1420 cm^{-1} were identified, and CI values were computed using Equation 3-5 (Almond et al., 2020) :

$$\text{Carbonyl index (CI)} = \frac{\text{Area under band } 1850 - 1650\ \text{cm}^{-1}}{\text{Area under band } 1500 - 1420\ \text{cm}^{-1}} \quad \text{Equation 3-5}$$

In addition, Keto CI, Ester CI, Vinyl bond index, and Internal double bond index were also calculated (Artham et al., 2009; Sudhakar et al., 2008), as given below:

$$Keto\ CI = \frac{I_{1715}}{I_{1465}} \quad \text{Equation 3-6}$$

$$\text{Ester } CI = \frac{I_{1740}}{I_{1465}} \quad \text{Equation 3-7}$$

$$Vinyl\ bond\ index = \frac{I_{1640}}{I_{1465}} \quad \text{Equation 3-8}$$

$$Internal\ double\ bond\ index = \frac{I_{908}}{I_{1465}} \quad \text{Equation 3-9}$$

Triplicate measurements were taken with FTIR, and from these triplicate spectra, average CI and other indices were calculated, with associated standard deviations.

Light Microscope and Scanning Electron Microscopy (SEM)

A manual Bushman brand light microscope with 10x magnification was used to obtain colored magnified photos of the pristine and bio-aged MPs. Samples were placed on a grid paper and photos were taken using a camera. The QUANTA 400F Field Emission SEM at MERLAB, a high-resolution scanning electron microscope

with a resolution of 1.2 nm, was used to capture SEM images of the pristine and bio-aged HDPE and LDPE samples. The MPs specimens were affixed to a sample holder using conductive and adhesive carbon tape. Subsequently, the non-conductive MPs were coated with a thin layer of gold to render them conductive. SEM images were then taken at magnifications ranging from 500x to 80,000x.

Differential Scanning Calorimetry (DSC) Analysis

Perkin Elmer Diamond Differential Scanning Calorimetry (DSC) and TA DSC250 at MERLAB were used to conduct DSC analyses. A nitrogen atmosphere was used for the analysis, and the temperature range was 30 to 300 °C for Perkin Elmer DSC and 25 to 300 °C for TA DSC, with heating and cooling rates of 10 °C per minute. Based on DSC analysis, Equation 3-10 was used to determine the percent crystallinity (X_c) for pristine and bio-aged samples using the first heating cycle (Sertchook et al., 2007) (Sertchook et al., 2007; Wunderlich, 1990).

$$Xc = \left(\frac{\Delta H_f}{\Delta H_f^c}\right) \times 100$$ Equation 3-10

ΔH_f: Heat of fusion of the PE samples as determined by DSC analysis,

ΔH_f^c: Heat of fusion of the extrapolated 100% crystalline PE (ΔH_f^c = 293 J/g).

3.3.3 Sorption

Preparation of Stock Solution and Initial Concentrations

TCP and TCS stock solutions (1000 ppm) were prepared from their neat standards using pure (99%) ethanol and then diluting for various concentrations of the OCs for sorption experiments using DW. MG stock solution (1000 ppm) and various diluted concentration solutions were prepared using Millipore DI (conductivity: 0.0549 µS/cm @ 25°C). MG stock was mixed for at least 24 hours before use.

pH Adjustments

TCP and TCS solutions at a concentration of 9 ppm were tested under varying water pH conditions, and their absorbance spectra were recorded, as shown in Figure 3.4. The scans revealed a shift in peaks and increased absorbance values when the pH exceeded the acidity constant (pKa) of each OC. This is due to the transition of OCs into their dissociated forms. To conduct sorption experiments with the unionized form of the compounds, the pH of water was adjusted to levels well below their respective pKa values—specifically, pH 6 for TCS, and pH 4 for TCP. Additionally, in order to measure TCP and MG at a pH lower than their pKa and at the pH of their maximum absorbance, an acetate buffer (Lee et al., 2013) at approximately pH 4.4 was employed in some tests during the spectrophotometric measurement phase.

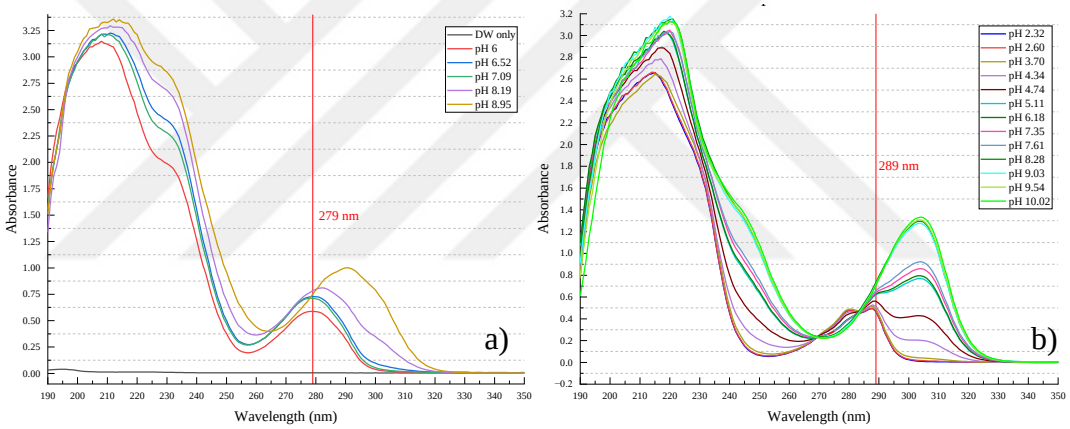

Figure 3.4 Absorbance scans of 9 ppm solutions of (a) TCS and (b) TCP at varying water pHs.

Cuvette Selection

For OCs measurements, quartz macro-cuvettes were used to obtain a higher resolution reading. For TCP and TCS measurements a cuvette (17.5 mL total volume) that had a path length of 50 mm was used. For MG measurements a cuvette (3.5 mL total volume) that had a path length of 10 mm was used.

Spectrophotometric Analysis

All OCs were measured directly using HACH DR 6000 UV/Vis Spectrophotometer. For reliable and consistent readings, the selected wavelength needs to correspond to

the maximum absorbance. At this peak absorbance, the absorbance of light is at its highest and the rate of change in absorbance with wavelength is at its lowest, minimizing measurement error. Spectrophotometric wavelength scans were conducted on each OC sample with a concentration of 5 ppm, within the wavelength range of 190-700 nm, and at the appropriate pH for each OC. The scans identified maximum absorbance wavelengths of 289 nm for TCP, 279 nm for TCS, and 617 nm for MG. Consequently, these wavelengths were chosen as the optimal measurement wavelengths for their respective OCs. Figure 3.5 illustrates the absorbance scans for each OC. The initial peak wavelengths for TCP and TCS, despite producing much higher absorbance compared to the later peaks at 279 nm and 289 nm, do not yield reproducible results, therefore the second maximum peak was chosen, as per literature (Hatinoglu et al., 2023; Lin et al., 2021).

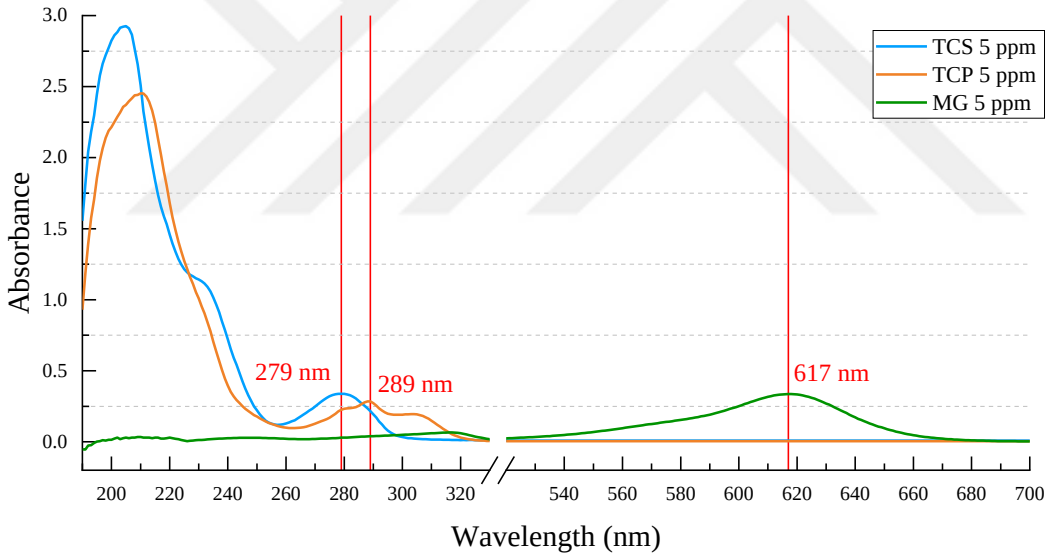

Figure 3.5 Wavelength scan for 5 ppm solutions of TCP, TCS, and MG for determining optimum wavelength to be used in sorption experiments.

Calibration Curves

Upon the adjustments of the analysis parameters and preparation of stock solutions, calibration curves were performed and R^2 >0.999 was obtained for all OCs as depicted in Figure 3.6 (a, c, and f) for TCS, TCP, and MG respectively. Additionally, the absorbance scans were also obtained for each OC concentration prepared for the

calibration curves of TCS (Figure 3.6b), TCP (Figure 3.6d and e), and MG (Figure 3.6g).

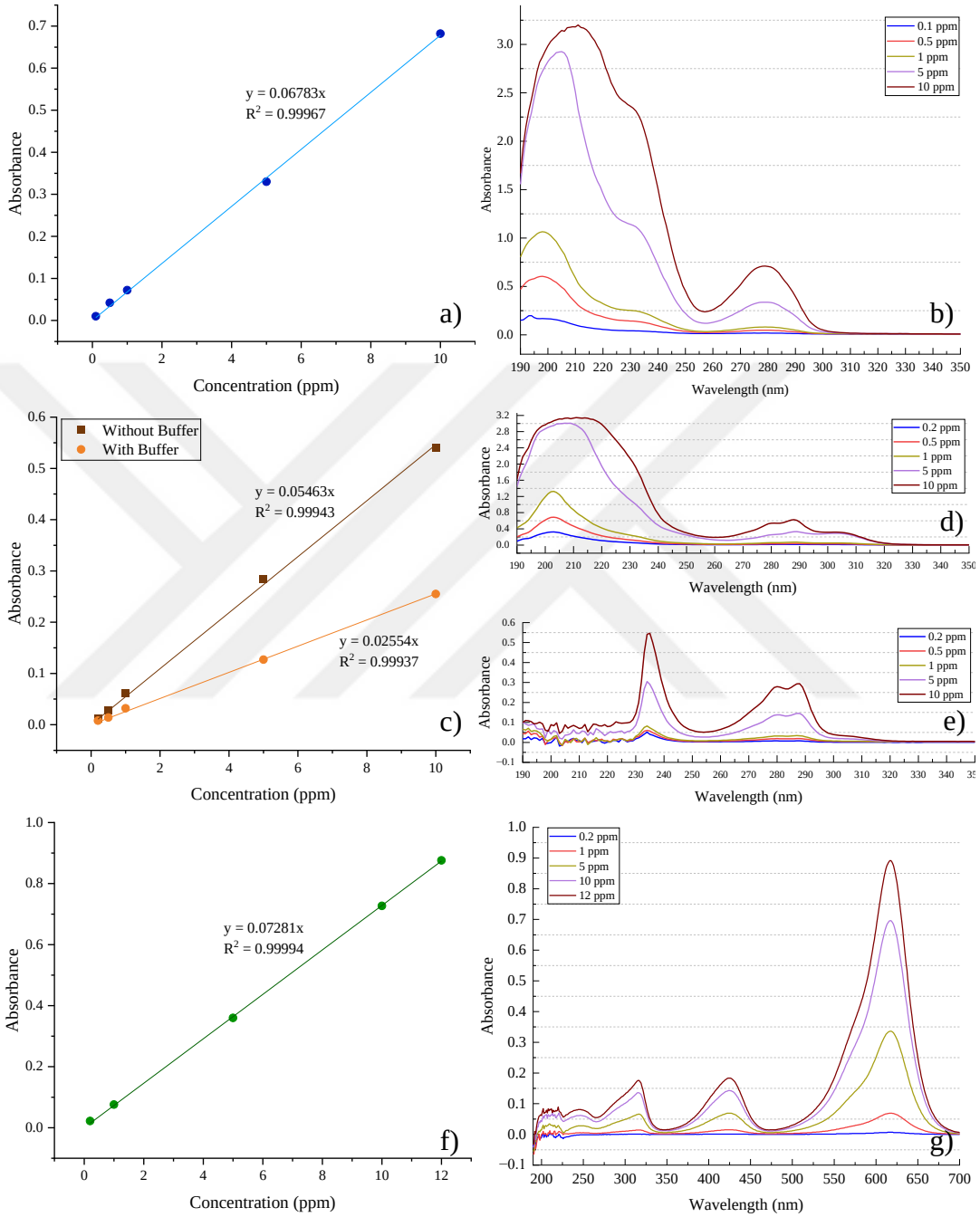

Figure 3.6 Calibration curves and absorbance scans of TCS (a & b), TCP (c, d (without buffer), & e (with buffer)), and MG (f & g) (with buffer).

Method Detection Limit (MDL) and Method Quantification Limit (MQL)

The USEPA (2016) method was used to determine the method detection limit (MDL) and method quantitation limit (MQL). Replicate samples of the OCs with low concentrations were prepared and analyzed, and using statistical analysis the smallest reliably detectable and quantifiable concentrations were established. MDL and MQL were determined to be 0.029 ppm and 0.088 ppm for TCS, 0.031 ppm and 0.092 ppm for TCP without buffer, 0.045 ppm and 0.134 ppm for TCP with buffer, and 0.0095 ppm and 0.0285 ppm for MG without buffer and 0.012 ppm and 0.036 ppm for MG with buffer, respectively. Table 3.13 summarizes the MDL and MQL for TCP with and without buffer.

Table 3.13 MDL and MQL for TCP with and without buffer.

	TCP-Without Buffer		TCP-With Buffer	
Trials	Abs	Concentration (ppm)	Abs	Concentration (ppm)
1	0.009	0.15	0.004	0.15
2	0.009	0.15	0.004	0.15
3	0.008	0.13	0.004	0.15
4	0.009	0.15	0.004	0.15
5	0.009	0.15	0.005	0.19
6	0.008	0.13	0.004	0.15
7	0.008	0.13	0.004	0.15
8	0.01	0.16	0.004	0.15
9	0.009	0.15	0.004	0.15
10	0.008	0.13	0.005	0.19
Avg	0.0087	0.143	0.0042	0.158
std	0.00068	0.01	0.00042	0.02
MDL		0.031		0.045
MQL		0.092		0.134

Control Correction of Sorption Data

To obtain the true sorption values attributable to the sorption on bio-aged MPs, all sorption test results were control corrected in order to eliminate interferences observed in MP-only control reactors. Correction was applied by subtracting the

absorbance that corresponds to the concentration that is observed for MP-only reactors from the test reactors to obtain the actual removal percent.

3.3.4 ANOVA and TUKEY

To determine the statistical significance among different sets (methane yield, carbonyl index, crystallinity, and sorption data) one-way ANOVA was applied using MS Excel, and TUKEY test (online website: Astatsa) was used to check for pairwise significance among groups. A p-value less than 0.01 (99% confidence level) was accepted as statistically significant for methane yield data, CI, crystallinity, and sorption data.

CHAPTER 4

BIO-AGING OF POLYETHYLENE DURING ANAEROBIC AND AEROBIC DIGESTION

Abstract

Wastewater treatment plants (WWTPs) can serve as accumulation sites for microplastics (MPs) from various sources. MPs are then concentrated in sludge and spread back into the environment during disposal or beneficial use of sludge. Polyethylene (PE) type MPs are known for their resistance to biodegradation, yet they may influence microbial communities in WWTP processes and may in turn be affected by these processes through aging. This study aims to investigate bio-aging of high-density PE (HDPE) and low-density PE (LDPE) MPs during biological sludge treatment processes with the motivation of understanding transformation of PE via in-depth structural and chemical characterization studies. Controlled experiments were conducted in mesophilic aerobic reactors and anaerobic digesters operated as biochemical methane potential (BMP) reactors. Findings revealed that high doses of HDPE inhibit methane production in BMPs by 26.2%, while LDPE shows no inhibition effect. Sludge characterization in aerobic reactors indicates no observed impact on biochemical oxygen demand (BOD_5) reduction. Fourier Transform Infrared Spectroscopy (FTIR) analysis shows no change in carbonyl index (CI) for bio-aged HDPE, whereas bio-aged LDPE exhibits increased CI, indicating changes in functional groups. Scanning electron microscope (SEM) characterization revealed surface alterations with rougher textures on bio-aged HDPE and LDPE. Differential Scanning Calorimetry (DSC) results indicated decreased crystallinity in bio-aged HDPE, while LDPE shows varying crystallinity changes, suggesting differing degrees of bio-aging. These dynamic changes serve as crucial indicators of PE degradation within environmental contexts and WWTPs

highlighting the effects of the persistence and transformation of PE due to biofilm formation, altering surface characteristics, and forming new functional groups.

Graphical Abstract

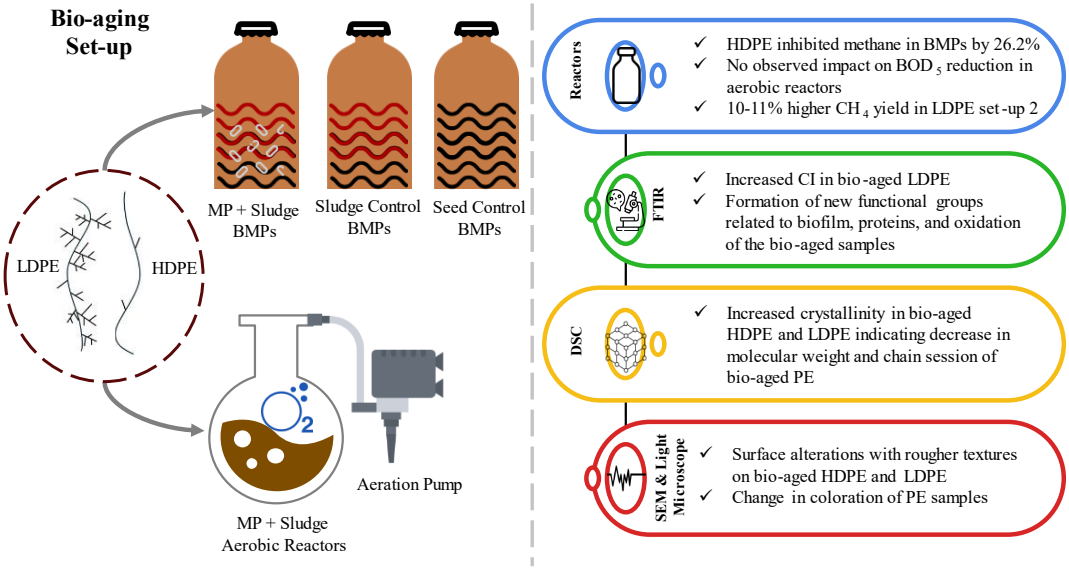

4.1 Introduction

Microplastics (MPs), (particles <5 mm) in water courses, are a product of both primary discharge into water bodies and secondary fragmentation due to aging and environmental processes. This fragmentation generally occurs through physical, chemical, or biological means (Lu et al., 2023). MPs, now acknowledged as "emerging pollutants," are a significant environmental concern, attracting substantial attention and research focus (Zafar et al., 2022), with their origin and fate scrutinized. PE constitutes a thermoplastic polymer composed of a long-chain aliphatic hydrocarbon (Ronca, 2017). PE variants, such as high-density PE (HDPE) and low-density PE (LDPE), are distinguished based on their density among other properties, contributing to their widespread applicability and environmental implications (Ronca, 2017).

Aging and degradation of MPs can be due to abiotic factors (e.g. photoirradiation), and biotic degradation (e.g. biological aging) (Lu et al., 2023; Zafar et al., 2022). Bio-aging involves microbial colonization leading to biofilm formation, altering the physicochemical properties of MP surfaces and structural characteristics, affecting the number of binding sites, and forming new functional groups (Zafar et al., 2022). The physical and chemical characteristics of MPs, such as their surface morphology and roughness, surface charge, specific surface area, and density may also be impacted by biofilm formation (Tu et al., 2020). UV-aging has been widely investigated in literature however, bio-aging of MPs have not been equally investigated, especially the effect of MPs on wastewater treatment plants (WWTPs) and the effect of biofilm on MPs.

One source of MPs release into aquatic environments is municipal WWTPs (Wei et al., 2019). As a direct result of efficient removal of over 90% of MPs during treatment phases (Li et al., 2020; Wang et al., 2023; Wei et al., 2019), the captured MPs accumulate in sludge. Sludge is commonly treated through biological stabilization processes like anaerobic digestion (AD) or aerobic digestion and the presence of MPs poses concerns for the efficient operation of these processes. Furthermore, MPs in sludge disposal introduces environmental distress, as they may persist and migrate to a variety of environmental compartments (He et al., 2023). MP concentrations can reach up to 170 particles/g-TS in sludge (Zhang et al., 2021b), highlighting their significance in WWTP systems. MPs in WWTPs are predominantly composed of polyethylene (PE) (4–51%), arguably the most widely available plastic in the world today (Tang et al., 2022).

MPs present a serious risk to WWTP operations through their interactions with sludge. Sludge digestion, a fundamental process in WWTPs, is primarily employed to stabilize biological sludge. MP buildup in sludge can impact AD, one of the sludge's post-treatment processes (Wang et al., 2023). AD and methane production can be impacted by MPs through the following possible mechanisms: (1) MPs' size and texture can physically harm sludge flocs and microbial cells and lower methane production (Wang et al., 2023), (2) MP (*i.e.*, PE) cause production of intracellular

reactive oxygen species (ROS) and induce oxidative stress in cells (Li et al., 2020; Tang et al., 2022; Wang et al., 2023), and (3) MPs' additives or toxic pollutants adsorbed on their surface can cause toxicity effects and act as conduits for the spread of pathogens and micropollutants (Wang et al., 2023).

Research has shown that the additives included in MPs are primarily responsible for the inhibition of methane production during AD (Wang et al., 2023). For instance, PE can contain additives (*i.e.*, UV stabilizers) that enhance its characteristics and durability, leading to prolonged persistence in sludge by preventing microbial degradation (Wei et al., 2019). When microbial communities are exposed to PE MPs, a study even demonstrated changes in microbial community composition and function (Tang et al., 2022). The impact of PE MPs on the AD of waste-activated sludge (WAS) has been investigated by several studies (Lim et al., 2018a; Shi et al., 2022aa; Wang et al., 2022a; Wei et al., 2019). These studies revealed a negative correlation between PE concentration and methane production, with higher PE concentrations resulting in lower methane production. It was reported that PE MPs changed the microbial populations that are important in the functioning of AD.

Aerobic digestion methods are found to be efficient, especially in smaller-scale WWTPs. Aerobically digested sludge is commonly utilized to enhance soil quality and water retention when applied to land. However, recent studies indicate that exposure to MPs during aerobic sludge digestion, even at environmentally relevant concentrations, may elevate oxidative stress levels and alter microbial community structures (Zhang et al., 2021b).

Conversely, MPs can be influenced by sludge digestion in multiple ways. MPs subjected to bio-aging show notable changes in their physicochemical properties (Zafar et al., 2022), where they can undergo changes in morphology, structure, color, size, and bio-toxicity (Lu et al., 2023). Moreover, biofilms on polymer surfaces not only alter their surface characteristics but can also lead to significant degradation due to surface attack by bacteria present in the biofilm (Artham et al., 2009). These alterations can influence how MPs interact with the environment and consequently

have an impact on the pathogens and chemical pollutants' adsorption-desorption mechanisms (Tu et al., 2020), which in turn would pose an ecological threat to the environment.

As ubiquitous components of WWTP sludge, investigation of the impact of HDPE and LDPE on aerobic and anaerobic digestion, as well as the impact of digestion on PE is of immediate concern. Disposal or beneficial use of biosolids requires a better understanding of bio-aging of MPs and its potential implications. To the best of our knowledge, this double-sided effect was not studied concurrently for aerobic and anaerobic digestion in the literature. The outcome of the interaction of PE with sludge may have a drastic global effect knowing that almost half of the biosolids in many developed countries are land-applied. Hence, the main aim of this study was to (1) investigate the bio-aging potential of HDPE and LDPE in mesophilic anaerobic digestors operated as BMP reactors and aerobic reactors, and (2) study the effects of HDPE and LDPE MPs on reactors' performance, so that conclusions can be drawn on the effect of PE on WWTPs and the environment as well as the changing properties of MPs after bio-aging.

4.2 Materials And Methods

4.2.1 Preparation of Microplastics and Sludge Used

HDPE MPs were obtained from a water tank supplier and pure LDPE was purchased from a Masterbatch company. The density of the HDPE and LDPE MPs was given by the manufacturers as 0.935 and 0.919 g/cm^3, respectively, and the polymer structure was confirmed via Fourier Transform Infrared Spectroscopy (FTIR) at METU Central Laboratory (MERLAB). Differential Scanning Calorimetry (DSC) at MERLAB was employed to assess the crystallinity and melting temperature (T_m) of each type of PE by utilizing data obtained from the first heating peaks. The crystallinity values were identified as 51.61% and 35.49%, with corresponding T_m of 126.8°C and 102.6°C for HDPE and LDPE, respectively. The PE's Brunauer-

Emmett-Teller (BET) surface area was measured with a Micromeritics ASAP-2020 Surface Area Analyzer using Krypton at University of Maine Laboratory as 0.0500 ± 0.0056 m^2/g and 0.0400 ± 0.0025 m^2/g for HDPE and LDPE respectively. Obtained HDPE and LDPE MPs were manually sieved to a size range of 425-500 μm. The MPs were then washed, sonicated, and left to dry in an incubator at 25°C.

The study's WAS and mesophilic (35°C) anaerobically digested sludge (ADS) samples were obtained from an urban WWTP, with a daily capacity of 765,000 m^3. To simulate inhibited seed in the abiotic reactors of the BMP test, ADS samples were sterilized by autoclaving and adding mercury chloride ($HgCl_2$) at a concentration of 200 mg/g total suspended solids (TSS). Sludge was centrifuged to achieve 2% total solids (TS) before use.

4.2.2 Design and Operation of BMP Reactors

The description of reactors and MPs of this study are summarized in Table A.1 in Appendix A. For HDPE anaerobic bio-aging process, three sets of reactors were designed: biotic (HB), abiotic (HA), and seed control (HS). There were two sets of biotic and abiotic reactors: one set without MPs (HB0 and HA0) and the other set (HB and HA) with a dose of 200 mg HDPE/g TS. LDPE bio-aging set-ups followed similar organization however they did not include abiotic reactors. A higher dose of 300 mg LDPE/g TS was used in reactors containing MPs employed in a total of 2 set-ups (LB-1 and LB-2). Similar to HDPE bio-aging, sludge controls (LB0-1 and LB0-2) and seed controls (LS0-1 and LS0-2) were utilized with each set-up. HDPE set-up, LDPE set-up 1, and set-up 2 were utilized with multiple reactors replications (12, 36, and 56, respectively) to produce a high amount of bio-aged PE for further tests and analysis.

BMP reactors were run in 250 mL amber serum bottles with 200 mL active volume. WAS served as a substrate in BMP reactors. The ADS served as the inoculum for biotic mesophilic reactor while abiotic reactors contained inhibited ADS to ensure

that no microbial activity occurs. With a TS value of 2% and an F/M ratio of 1 (Raposo et al., 2012), the WAS and ADS ratios in the reactors were modified to provide an appropriate substrate for the BMP test.

Complete sludge analysis including TS, VS, total chemical oxygen demand (tCOD), and pH were performed both prior to and following BMP set-ups. The designated PE doses were added to each reactor. The reactor bottles were sparged and purged with 99.9% pure nitrogen gas (N_2) and sealed to ensure anaerobic conditions. The reactors were then incubated in mesophilic conditions (35°C).

To enable ample contact time for PE bio-aging, HDPE reactors were operated for 50 days while LDPE reactors were operated for 60 days. In a typical BMP test, it is advised to terminate the BMPs once the daily or cumulative CH_4 produced drops to 1% (Holliger et al., 2017). Consequently, in the current study, biogas measurements were taken daily, then taken every other day after a drop to 2% of daily CH_4 produced/cumulative CH_4 produced. Before starting and after terminating the anaerobic test, TS, VS, tCOD, and pH were measured from each reactor set.

4.2.3 Design and Operation of Aerobic Reactors

Aerobic reactors in this study were run in flat-bottom glass flasks with a capacity of 6L and a working medium of WAS only. A single HDPE set-up (HO) was utilized with a working volume of 5 L and HDPE MPs dosage of 4 g/L WAS. LDPE set-up 1 (LO-1) and LDPE set-up 2 (LO-2) were run in triplicate and quadruplicate, respectively, with each running with a working volume of 4 L and LDPE MPs dose of 5 g/LWAS. TS in all reactors was adjusted to 2%. Upon filling with WAS, the reactors were aerated constantly using aquarium pumps to continuously oxygenate the sludge, and the reactors were incubated in mesophilic conditions (35°C). To enable maximum bio-aging potential, HDPE bio-aging set-up was pursued for 27 days while LDPE bio-aging set-ups were pursued for 60 days. Before starting and after terminating the aerobic LDPE tests, TS, VS, tCOD, biological oxygen demand

(BOD_5), and pH were measured from each reactor set, while only BOD_5 was tested before and after the HDPE set.

4.2.4 Analytical Methods

The Standard Methods (APHA, AWWA, and WEF 2017) were used to measure sludge and reactors' performance parameters. Method 2540G was followed for TS and VS measurements (APHA et al., 2017). tCOD was measured according to a digestion method recognized by the US EPA (Jirka & Carter, 1975). BOD_5 was measured according to 5210 B (APHA et al., 2017). All reactors' initial and final pH values were monitored in conjunction with Standard Methods, Method 4500H (APHA et al., 2017). Biogas volume produced by the BMPs was measured by a water displacement apparatus. Biogas composition in BMPs was analyzed using Gas chromatography (GC) with a thermal conductivity detector (TCD) (Agilent 6890 N).

To determine if the differences between reactor sets were statistically significant, one-way ANOVA was applied to the data using MS Excel; p-value less than 0.01 was accepted as statistically significant. The primary performance metric of BMPs digestion process was CH_4 yield. The kinetics and potential of CH_4 production from WAS were assessed and compared using the hydrolysis rate constant (k) and biochemical CH_4 potential (B_0) (Li et al., 2020; Wei et al., 2019).

4.2.5 Microplastics Recovery and Characterization of Bio-aging in Microplastics

Upon termination, reactor contents sieved and collected MPs were rinsed with water, and left to dry, then were "washed" by soaking them in 17.5% H_2O_2 overnight in a shaking incubator to remove any residual sludge or biofilm. MPs from anaerobic and aerobic test reactors were labeled as "bio-aged". Pristine MPs that were only washed overnight with H_2O_2 were also prepared for comparison purposes. To elucidate the physical and chemical alterations on HDPE and LDPE before and after bio-aging, a

thorough characterization of MPs was performed. Fourier transform infrared (FTIR) spectroscopy fitted with attenuated total reflectance (ATR) spectra at MERLAB was utilized to track any structural alterations. As a quantitative measure of aging, carbonyl index (CI) was calculated using the specific area under band method (SAUB) method (Equation A.3 in Appendix A) (Almond et al., 2020), as well as keto CI, ester CI, vinyl bond index, and internal double bond index (Equation A.4 - Equation A.7 in Appendix A) (Artham et al., 2009; Sudhakar et al., 2008). Bushman light microscope with 10x magnification was used to obtain magnified photos of MP samples. The QUANTA 400F Field Emission SEM at MERLAB was used to capture SEM images. Perkin Elmer Diamond DSC at MERLAB was used to determine the percent crystallinity (Equation A.8 in Appendix A) and T_m. One-way ANOVA using MS Excel and TUKEY was used to determine the statistical differences between CIs and crystallinities of all samples.

4.3 Results And Discussion

4.3.1 Performance of Anaerobic Reactors

Methane yield is a useful metric to compare AD performance, and the results of all BMP reactors are presented in Figure 4.1. Even though the HDPE reactors were not operated as long as LDPE reactors, the missing 10 days are completed by the 1st order model fit (Equation A.2) for comparison purposes as shown by dashed lines in Figure 4.1. Also, average cumulative volumes of biogas and CH_4, CH_4 yield, and sludge characterization results at reactor termination of all reactors are summarized in Table 4.1. Information on the methane content in the reactors can be found in Appendix C (Table C.4). Even though HDPE BMPs had lower MP doses than LDPE BMPs, reactors containing HDPE MPs exhibited the lowest performance in biogas volume, CH_4 volume, and CH_4 yield, revealing microbial inhibition. LDPE-containing reactors had no difference between them in terms of set-up parameters or MP doses, and they exhibited similar CH_4 and biogas volume, yet their CH_4 yields

differed from each other (Figure 4.1, LB Set-up 1 and LB Set-up 2). This is attributed to variations in the amount of substrate (WAS) added to each set. Owing to insufficient CH_4 production, abiotic reactors were excluded from calculations (Figure A.1a).

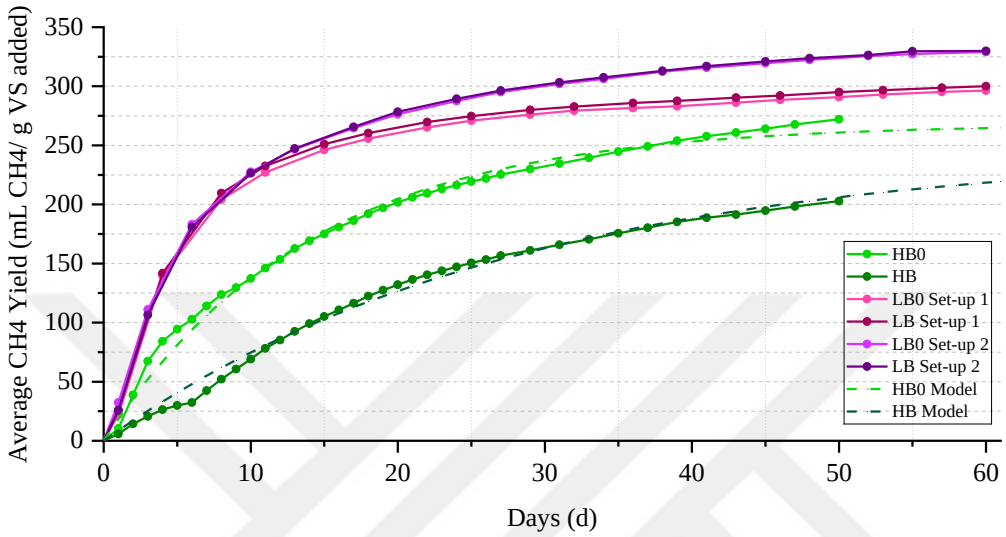

Figure 4.1 Methane yield of biotic reactors of HDPE set-up, LDPE set-up 1, and LDPE set-up 2.

Although cumulative biogas production was almost identical in both control sets of LDPE (*i.e.*, 772±26 mL for LB0-1 and 777±16 mL for LB0-2), CH_4 production was higher for Set-2 and the difference was more discernable (11% higher) when CH_4 yields were calculated (Table 4.1). A similar 10% higher CH_4 yield was also observed between the test reactors LB-1 and LB-2 containing LDPE. These can be attributed to the high concentrations of soluble organic content in WAS, as was also reported by Chen et al. (2021).

Table 4.1 Cumulative biogas, CH_4, CH_4 yield, and % removal of sludge parameters for BMPs*.

	Reactor Set	Cumulative Biogas Production (mL)	Cumulative CH_4 Production (mL)	CH_4 Yield (mL CH_4/ g VS added)	% TS Removal	% VS Removal	% COD Removal
	HB0	561.6±86.8	342.9±50.6	272.2	11.4±0.7	27.8±1.0	25.0±5.4
	HB	414.2±35.9	261.2±21.0	202.9	-2.6±1.8	-2.5±2.7	40.7±26.4
HDPE Set-up	HA0	43.8±60.6	20.8±29.5	N/A	8.7±9.2	14.4±12.7	1.9±9.9
	HA	17.7±4.8	0.8±0.3	N/A	-3.6±0.4	-7.5±3.6	25.3±6.1
	HS0	63.8±35.2	22±13.2	N/A	8.4±1.2	15.8±1.0	15.3±5.2
	LB0-1	772.4±26.0	477.9±0.0	296.4	29.1±0.3	37.6±6.6	26.3±5.4
LDPE Set-up 1	LB-1	762.8±62.9	482.8±13.8	300	2.9±5.2	-10.9±5.6	18.5±4.4
	LS0-1	174.3±2.1	78.1±0.0	N/A	28.9	33.5	-8.0±17.6
	LB0-2	777.2±15.9	492.7±0.0	329	20.0±4.5	25.0±4.1	31.7±2.9
LDE Set-up 2	LB-2	740.2±59.1	493.9±26.2	329.9	-5.8±1.0	-19.4±1.0	30.0±4.8
	LS0-2	185.4±3.4	78.6±0.0	N/A	13.1±0.7	17.9±2.2	1.2±9.0

*Presence of MPs created an interference during measurement of TS, VS, and COD, hence resulting in excessively low or negative results.

Our CH_4 yields observed for control reactors (*i.e.*, HB0 and LB0) (Table 4.1) surpassed some of the corresponding control reactor values reported in literature, e.g., 124 ± 6 mL CH_4/g VS added (Chen et al., 2021a), 146.3 ± 6.4 mL CH_4/g volatile suspended solids (VSS) (Wang et al., 2019), or 233.5 ± 1.0 mL CH_4/g VS added (Li et al., 2020). In a study by Hatinoğlu & Sanin (2022), under similar conditions (60 days of digestion with 2% TS value), the CH_4 yield for the control reactor without any MP addition was approximately 291.4 ± 1.4 mL CH_4/g VS added, which closely aligns with the values obtained in this study. As can be seen from the literature data, a variation of CH_4 yields can be observed due to the quantity and nature of VS added.

Biotic BMP reactors containing HDPE MPs demonstrated a decrease of 26.2% in biogas when compared to controls. This decline in biogas production which was also noticed in CH_4 production was attributed to microbial inhibition caused by the high dose of MPs and the potential release of additives (HDPE used in this study was confirmed to contain UV stabilizer by the manufacturer), consistent with prior studies (Li et al., 2020; Wei et al., 2019). Interestingly, in reactors containing MPs, although CH_4 volume, in parallel with biogas volume, was lower than those without MPs, the percentage of CH_4 in the biogas was not necessarily reduced (Table C.4 in Appendix C). This observation suggests that methanogens in the reactors remained present but might have experienced a decrease in population due to MP inhibition with their proportion in the overall population possibly remaining constant. Although these reactors exhibited inhibition relative to their controls, the CH_4 yield was higher than the sludge controls reported in literature conducted under similar conditions. Conversely, biogas and CH_4 production from abiotic reactors remained minimal throughout the observation period; for 23 days, no biogas was produced, with slight but negligible production observed in some replicates thereafter (Figure A.1a).

In contrast to the HDPE set-up, biotic BMP reactors with and without LDPE MPs exhibited similar biogas production in both set-ups, suggesting that LDPE presence did not impact the microbial community. Inhibition to methane production due to presence of PE at high doses was reported in literature such as 27.5 % and 12.4% (for 200 and 100 particles/g TS, respectively) (Wei et al., 2019), 30.71% (for 10

mg/L) (Wang et al., 2022a), 13.8% and 6.1% (for PE sizes of 1000 μm and 180 μm, respectively) (Shi et al., 2022a), and 7% reduction to methane yield by HDPE (Lim et al., 2018). However, most literature studies do not identify the density or type of PE and whether it was pure or contained additives, making comparison difficult with the current study. We believe the main factor causing inhibition in HDPE-containing reactors was the presence of antioxidants and UV stabilizers because higher doses of LDPE in similar reactors did not cause any inhibition in either set-up.

Total biogas and CH_4 production profiles in biotic reactors exhibited a pronounced trend closely aligning the CH_4 yield results, while minimal biogas and CH_4 production were observed in abiotic reactors. Figure C.1, Figure C.2, and Figure C.3 in Appendix C depict further information on the biogas and methane production profiles. Figure A.1 in Appendix A presents the average cumulative CH_4 production of HDPE set-up (Figure A.1a), LDPE set-up 1 (Figure A.1b), and LDPE set-up 2 (Figure A.1c) with error bars. High standard deviations were observed in the HDPE set-up during the initial days due to probable leakage, which was subsequently addressed (around day 6). Despite that, the difference between BMPs containing HDPE MPs and control reactors did not overlap, suggesting microbial inhibition as the probable cause. LDPE set-ups in general displayed low standard deviations, indicating homogeneity among replicates. The trend of biogas and CH_4 measurements is further explained in Appendix A.4. ANOVA results revealed a significant difference between HB0 and HB ($p<0.01$), pointing to inhibition. Conversely, significant differences were not found between LB0 and LB in neither set-up 1 nor 2, suggesting similar performance across these reactors. Additionally, no significant differences were observed among control reactors (HB0, LB0-1, and LB0-2) according to ANOVA ($p>0.01$). The visible differences in Figure 4.1 were not considered significant according to ANOVA because of the standard deviations associated with the set-ups (Figure A.1). However, significant differences were detected between HB, LB-1, and LB-2 ($p<0.01$), as illustrated in Figure 4.1. Additionally, seed controls also exhibited minimal biogas and CH_4 production

during the full operation period for both HDPE and LDPE set-ups (Figure A.1 in Appendix A).

The cumulative k and B_0 values for WAS across different setups were determined by employing a one-substrate model (Li et al., 2020; Wei et al., 2019). With an R^2 value exceeding 0.99, the relationship between CH_4 yield and B_t aligns closely. Table A.2 in Appendix A lists all calculated values. In considering the B_0 values, the trend in CH_4 yield remained consistent. In the HDPE set-up, the B_0 value exceeded the observed B_t value by 8%, indicative of inhibition of HDPE MPs on the microorganisms. Conversely, LDPE set-ups did not exhibit such inhibition, with LDPE-containing reactors showing slightly higher values of 1.3% (set-up 1) and 0.7% (set-up 2) when compared to controls, and the differences were not statistically significant. Overall, LDPE set-ups outperformed HDPE set-ups. These results suggest that, unlike HDPE, LDPE addition did not affect the capacity of WAS to produce CH_4 or its hydrolysis rate. Moreover, to complete the graphs for a better comparison of HDPE to LDPE set-ups, the first-order kinetic model (Equation A.2) was used on HDPE set-up data (Figure 4.1; dashed lines) as noted above. The model fits indicated that HDPE BMPs would be stabilized at 60 days as also observed by LDPE set-ups. When the fit was extended to 100 days for both HDPE and LDPE data (Figure C.4 in Appendix C; dashed lines), the model showed a perfect fit with data, and the same trend was observed indicating that BMPs were stable when they were terminated.

While Wei et al. (2019) reported that PE inhibits CH_4 potential at high doses, their study did not specify the type of PE used. Our results reveal that it may be the additives in HDPE inhibiting methane production, as our LDPE added at much higher doses repeatedly did not inhibit methanogenic activity. According to Wei et al. (2019), WAS hydrolysis was unaffected by low concentrations of PE MPs but was inhibited at higher concentrations. The reduced efficiency of AD at higher PE MPs levels was attributed to this inhibition (Wei et al., 2019). An additional factor contributing to HDPE inhibition was expected to be the leaching of additives. However, literature suggests that the influence of PE MPs on WAS AD is not solely

due to the released additives from PE MPs. Studies have shown that MPs induce the production of ROS, which decreases cell viability and restrains methanogenic activity. It is proposed that one of the primary impediments to the efficiency of WAS AD could be ROS generated by PE MPs (Wei et al., 2019). ROS was not measured in the current study. However, if the production of ROS had a dominant impact on digester operation, we would have expected to see inhibition in LDPE set-ups, which contained higher amounts of MPs when compared to the HDPE set-ups. Furthermore, studies from the literature report that, compared to HDPE, the production of ROS during the degradation of LDPE is generally higher due to the branched structure of the latter, which contains a greater number of tertiary carbons particularly susceptible to oxidative processes (Kumar Sen & Raut, 2015; Martínez-Romo et al., 2015). Consequently, due to its lower crystallinity, LDPE is prone to aging more, thereby indicating more extensive oxidative degradation relative to HDPE. Moreover, leaching of additives from HDPE MPs could have contributed to inhibition (Do et al., 2022), meanwhile their presence could have prevented bio-aging of HDPE. Since no measurements of additives were made, these comments are only speculative.

Comparison of initial and final characterization of test reactors became somewhat complicated for VS, TS, and tCOD parameters, due to interference of MPs during analysis. Laboratory control samples confirmed that MPs did not volatilize during TS measurement (105°C) but were completely oxidized during VS measurement (at 550°C) causing a major difference in weights of samples measurement. Moreover, tCOD control experiments with only water and MPs indicated that MPs melt during tCOD measurement (150°C) which causes a high tCOD reading despite having no organic matter. Consequently, a reliable final characterization could not be obtained because the exact quantity of MPs interfering with sludge analysis could not be practically measured. The lack of reported impact of MPs on VS or tCOD measurements in the literature may be attributed to the low doses of MPs present in those reactors. In our study, very high doses of HDPE and LDPE were utilized, which surpasses previously reported doses in the literature.

Methane yields of control reactors (HB0, LB0-1, and LB0-2) correlated with corresponding %tCOD removals yet did not correlate with VS removal. The control for LDPE Set-2 (LB0-2) exhibited the highest cumulative CH_4 production yet demonstrated the lowest VS removal efficiency (25%) and lower TS reduction (20%) than LB0-1. Control reactors do not contain MPs therefore are not expected to be affected by any interferences in TS, VS of COD measurement. One possible reason for this difference between controls could be the use of different WAS and ADS samples from the WWTP during setting up of reactors. HDPE biotic control reactors had the lowest methane production and TS removal (11.4%) but a VS removal of 27.8% (Table 4.1). In comparison to the results of this study of the control reactors, literature work with mesophilic BMPs reported similar TS removal of 23% (Bahçeci, 2019) in control reactors. However, higher VS removal of 43% (Jih-Gaw et al., 1999), 46% (Bahçeci, 2019), and 33.7% (Şimşek, 2023) using mesophilic controls of BMPs were also reported. COD removals observed in our study (25% up to 31.7%) were lower when compared to those reported in the literature for mesophilic BMPs, such as 36% (Bahçeci, 2019), 39% (Jih-Gaw et al., 1999), and 33.5% (Şimşek, 2023). pH values of the biotic sets consistently fell within the working range (7-8.1) for AD during both the setup and termination stages. Whereas, most methanogenic bacteria exhibit optimal activity between pH 6.5 to 8.2 (Speece, 1996). Across all reactors, pH remained stable while the pH values of seed controls were slightly elevated compared to samples due to digestion processes.

In abiotic reactors, there were less reductions in both TS (8.7%) and VS (14.4%) when compared to biotic reactors, aligning with the negligible CH_4 production and decreased activity of inhibited microorganisms. Similarly, there was no notable removal in tCOD (2%) as expected. Furthermore, the production of CO_2 and the conservation of N_2 by all abiotic reactors suggest the absence of methanogenic activity. Following the termination of the reactors, the pH increased in the control reactor from 6.0 to 6.3±0.6 and decreased in reactors containing HDPE from 6.0 to 5.8±0.1. These minor fluctuations observed in abiotic reactors are attributable to the presence of $HgCl_2$ and the inactivity of reactors. Likewise, seed controls displayed

varying TS, VS, and tCOD removals, corresponding with their minimal methane production throughout the operational period across all setups. Further information about the performance of Anaerobic reactors is available in Appendix C (section C.1). The complete sludge characterization for all reactors can be found in Table C.1, Table C.2, and Table C.3 in Appendix C.

4.3.2 Performance of Aerobic Reactors

Following the operational period, aerobic reactors' sludge was characterized. Full sludge characterization of aerobic reactors can be found in section C.2 in Appendix C (Table C.5, Table C.6, and Table C.7). Although final characterization for sludge parameters of the HDPE set-up was not conducted, BOD_5 measurements were performed to substitute for other parameters and elucidate the HDPE set-up's performance. A consistent decrease in BOD_5 levels was observed with increasing digestion time at various intervals throughout the operational period of the aerobic reactors. As reported, the end of the conventional aerobic digestion period is approximately 20-30 days (Tyagi et al., 2014). A stable reduction in BOD_5 content (almost 96%) was achieved at that time in all set-ups. Nevertheless, even after 60 days, a slightly more reduction in BOD_5 levels was noted in LDPE set-ups. Final BOD_5 analyses indicated comparable outcomes for HDPE and both LDPE setups. Notably, HDPE setup exhibited a BOD_5 removal of 96.4%, while LDPE setups demonstrated higher removals of 98.8% (set-up 1) and 98.3% (set-up 2). If the HDPE set-up digestion period was increased to 60 days a similar result to LDPE set-ups could have been observed.

LDPE set-up 1 and LDPE set-up 2 achieved TS removals of 29.7% and 22.2%, respectively, and VS removals of 38.5% and 39%, respectively. MPs posed a negligible interference with sludge analysis of aerobic reactors due to the high sludge volume to MP dosage ratio in each reactor, ensuring reliable final characterization of LDPE reactors. Although both LDPE set-ups had the same digestion parameters and MPs doses, tCOD measurements demonstrated differing removals, with LDPE

set-up 2 exhibiting higher removal (78.1%) than LDPE set-up 1 (52%), suggesting potentially greater bioactivity in LDPE set-up 2.

pH in LDPE reactors declined throughout the experimental duration, starting at pH 6.6 and decreasing to a range of 5.9-6.0 post-digestion. This decrease could be attributed to the rise in acidity of sludge over prolonged aeration periods because of elevated nitrate levels and the consequent reduction in buffer capacity (Moore, 1970), decreasing pH to a value of 6.0 or even lower as low as 5.0 (Bhargava & Datar, 1989). Another reason for the pH drop could be attributed to the nitrification reactions that produce both nitrite and (H^+) ions which decrease alkalinity (EPA, 2002). Further information about the performance of Aerobic reactors is available in Appendix C (section C.2).

4.3.3 Microplastics Characterization

Fourier Transform Infrared Spectroscopy

FTIR is used to identify any changes in the polymer structure, in terms of the formation of new functional groups. Recovered MPs obtained from the reactors exhibited indications of biological aging, as evidenced by the findings from the FTIR spectra (Figure 4.2). Alongside characteristic peaks of HDPE (Figure 4.2a) and LDPE (Figure 4.2b), new bands and an increase in the intensity of the carbonyl band were observed. The new bands observed in LDPE bio-aged samples at around 3600-3300 cm^{-1} are attributed to the stretching vibrations of O-H owing to microbial activity (Bonhomme et al., 2003). For both HDPE and LDPE, the broadband with increasing intensity at 1080-1086 cm^{-1} indicates polysaccharides, which are significant components of microbial biofilms due to metabolites production (Bonhomme et al., 2003). Moreover, the band around 1736-1740 cm^{-1}, seen only in washed and bio-aged LDPE samples, shows C=O ester stretching vibrations (Grause et al., 2020). These peaks may be due to H_2O_2 washing. The peak 1641 cm^{-1} shown only in the second batch of anaerobic bio-aged LDPE (LBW-2) indicates C=C

stretching due to oxidation (Grause et al., 2020). It was observed that between 1740-1641 cm^{-1} are the predominant wavelengths that are most commonly present in our bio-aged MPs samples. According to literature, peaks in that range represent stretching vibrations of ketone (C=O) which matches with the formation of biofilm and presence of proteins within PE structure (Gaston et al., 2016; Zafar et al., 2022). Peaks around 2000-2500 cm^{-1} were omitted from representation, as per MERLAB's recommendation. These peaks were attributed to CO_2 owing to the use of a new FTIR machine and were not correlated with PE backbone or aging.

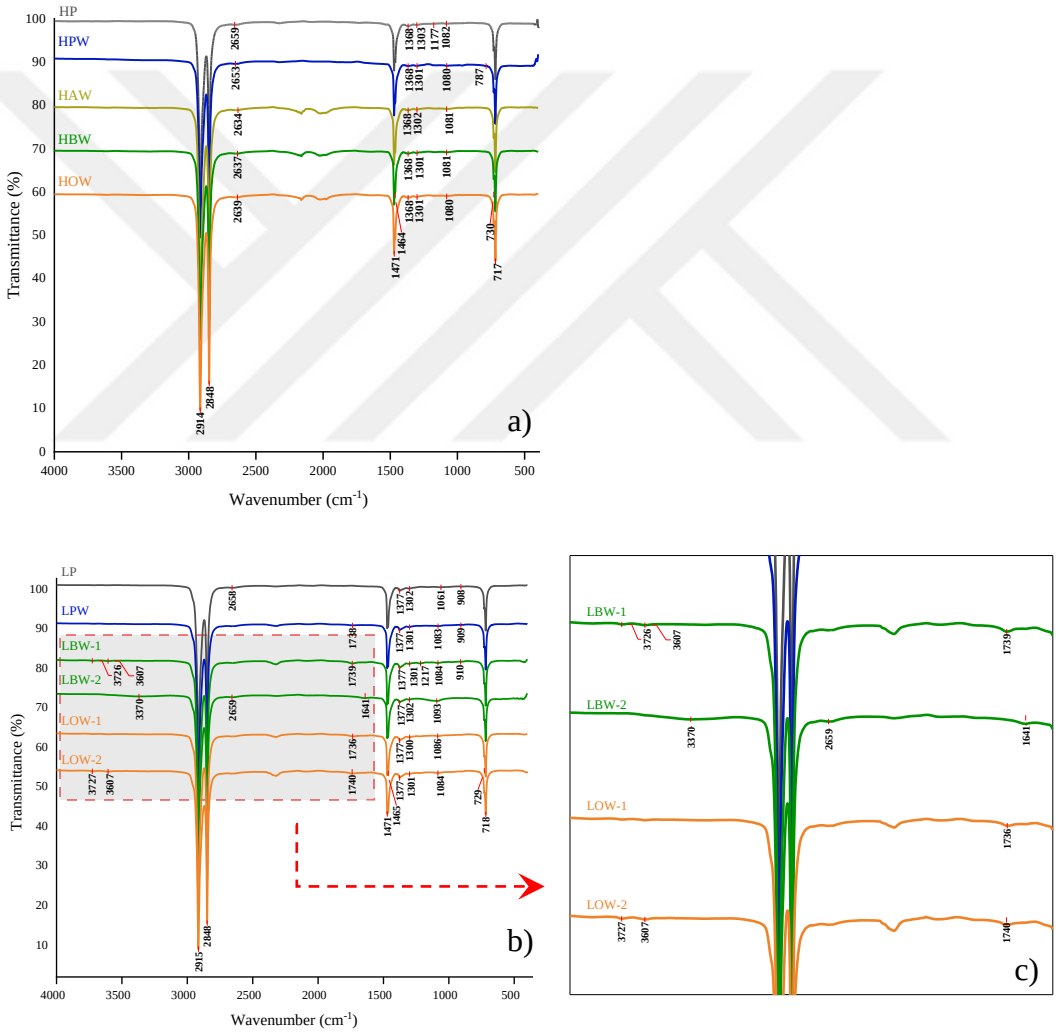

Figure 4.2 FTIR spectra of a) HDPE, b) LDPE before and after bio-aging, and c) zoomed-in representation of the extra peaks in LDPE spectra. Labels: Pristine (HP & LP), Pristine H_2O_2-washed (HPW& LPW), Abiotic (HAW), Anaerobically bio-aged (HBW & LBW), and Aerobically bio-aged (HOW & LOW).

Quantitative treatment of FTIR results is summarized in Table A.3 in Appendix A for pristine and bio-aged samples. Pristine and pristine washed samples are expected to have zero CI since pure PE does not contain carbonyl, but minor non-zero values could indicate unsaturation in PE structure. This is the case for HP, LP, HPW, and LPW, albeit having large standard deviations. On the other hand, bio-aging in biological reactors is expected to result in CI values that are higher with subsequent small standard deviations. This was the case for aerobic-washed LDPE (LOW-1 and LOW-2). In the literature, a reduction in CI due to microorganisms attaching to carbonyl groups on PE was also reported (Takada, 2019). Therefore, an increase in CI may not necessarily be an indication of better bio-aging of PE. Different CI values between anaerobic sets (LBW-1 and LBW-2) were calculated. While the former shows a distinctly increased CI of 0.100±0.007, the latter is inconclusive, with a CI of 0.019±0.018. On the other hand, the CI for both aerobic LDPE sets yields a distinct non-zero value (Table A.3 in appendix A), while the CI of all bio-aged HDPE samples are zero.

In-vitro biodegradation of HDPE with marine organisms was shown to be slower than that of LDPE (Sudhakar et al., 2008), which is parallel to our observations of LDPE showing bio-aging, but not so for HDPE. Studies on anaerobic and aerobic bio-aging of PE in general, are quite limited. In studies on the biodegradation of PE using different organic matter such as animal tissues, CI (SAUB method) ranged from 0.025-0.79 after bio-aging (Istomina et al., 2024). In another study using different microbial consortiums for bio-aging of LDPE, CI (SAUB method) did not exceed 0.2 after bio-aging (Pinto et al., 2022). Zafar et al. (2022) reported changes in the CI value (0.17-0.54), yet they used a different method of CI calculation which disables a direct comparison with our results. Sudhakar et al. (2008) and Artham et al. (2009) argue that an increase in CI is due to oxidation from dissolved oxygen (*i.e.*, abiotic factor), yet with extended exposure to organisms, CI decreases owing to microbial attachment, which indicates biodegradation (*i.e.*, biotic factor) through mechanisms such as ester formation (Sudhakar et al., 2008). In Artham et al.'s (2009) study, keto and ester CI did not exceed 0.5 for biodegraded HDPE and LDPE

(Artham et al., 2009). The vast difference of CI in our results between LBW-1 and LBW-2 may be associated with such phenomena (Table A.3 in Appendix A).

The results of ANOVA tests conducted on HP and LP compared to the bio-aged samples indicate significant differences between LDPE samples (*i.e.*, pristine vs. bio-aged) but not among HDPE. Pairwise comparisons (TUKEY) indicated that significant differences ($p<0.01$) occurred between different LDPE groups. However, no differences were observed between LP and LPW indicating no significant alterations to LP after H_2O_2 washing. Two batches of aerobic bio-aged LDPE have similar characteristics with each other; exhibiting an increase in carbonyl, keto indices, and vinyl and internal double bonds. Therefore, no statistical significance was present between LOW-1 and LOW-2 in terms of their CI. On the other hand, two batches of anaerobic bio-aged samples (LBW-1 and LBW-2) were significantly different from each other ($p<0.01$), in terms of their CI. Other indices calculated (*i.e.*, keto, ester, vinyl, and internal double bond) for the same samples did not exhibit such a difference. Further information on ANOVA parameters and pairwise comparison of CI groups is represented in Appendix C (Table C.8 and Figure C.5).

Differential Scanning Calorimetry

To interpret the physical changes on HDPE and LDPE, the crystallinity of the MPs before and after bio-aging was measured using DSC. A summary of DSC results is available in Table A.4. Although a minor increase can be observed in the crystallinity of HDPE and LDPE (as indicated by a higher delta H in Figure 4.3a and c, respectively), these changes are not significant ($p>0.01$) in either crystallinity or melting temperature (Figure 4.3b and d), upon aerobic or anaerobic bio-aging. Campanaro et al., (2023) studied crystallinity changes in PE films submerged in sewage sludge and could not detect a noticeable change in crystallinity. Even though our PE samples are MPs, as opposed to sheets, and exposed to live sludge in anaerobic/aerobic digesters, our results indicate minor changes in the crystalline structure of PE tested (Table A.4). ANOVA results of crystallinity are depicted in Table C.9 in Appendix C.

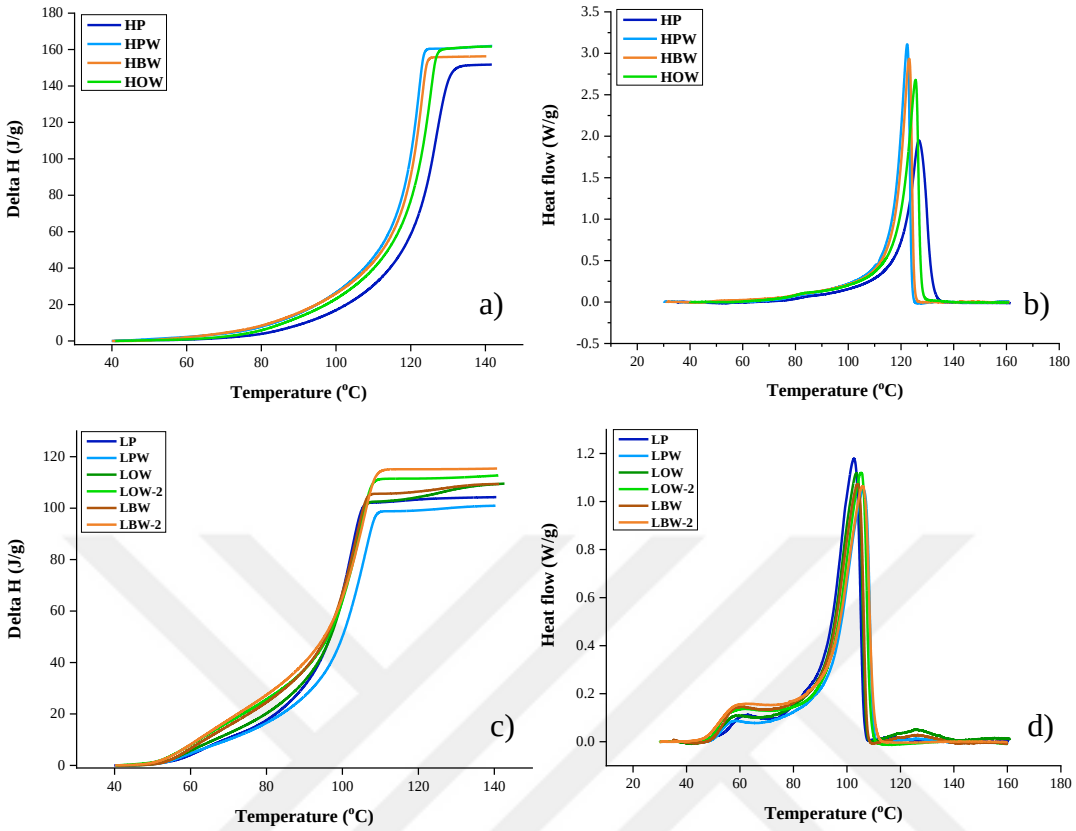

Figure 4.3 Temperature vs Heat of fusion and Heat flow for HDPE (a & b) and LDPE (c & d).

Light and Scanning Electron Microscopy

Light microscope and SEM images were captured to examine surface alterations of washed MPs before and after bio-aging (Figure 4.4). Anaerobically bio-aged MPs (*i.e.*, HBW, LBW) exhibited a more yellowish color compared to aerobically bio-aged ones (*i.e.*, HOW, LOW), which displayed a light grey-brownish appearance. SEM images of HPW & LPW appear rough in texture, yet some changes are evident upon bio-aging; such that HDPE had a more curdy appearance after aerobic bio-aging, while LDPE, wrinkles and curves seem to increase with anaerobic and aerobic aging. Alassali et al. (2018) observed smooth surfaces in SEM images of pristine HDPE particles, whereas aged particles exhibited increased surface roughness due to surface peeling-off effects. Additionally, Gao et al., (2022) reported that the initially smooth surface of pristine MPs became rougher after H_2O_2 digestion treatment, likely due to oxidative attack by H_2O_2, which may account for

the observed roughness in our pristine washed samples. Further information about the light microscopy and SEM images of all PE samples is available in Appendix C (section C.3, Figure C.6, Figure C.7, and Figure C.8).

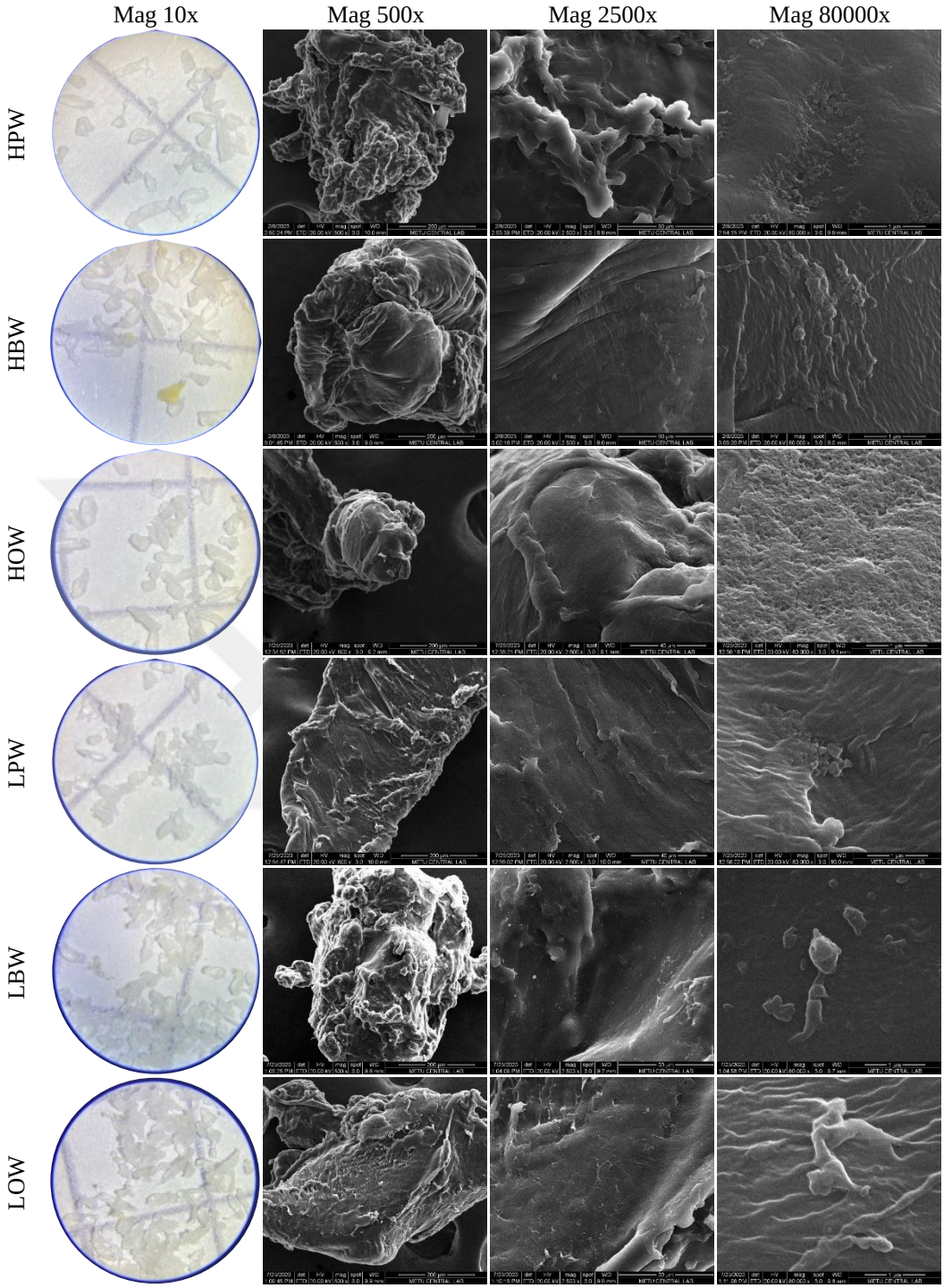

Figure 4.4 Light microscope and SEM images of HDPE and LDPE washed with H2O2 before (HPW and LPW) and after aerobic (HOW and LOW) and anaerobic bio-aging (HBW, LBW).

4.4 Conclusion

This study identified variations between aerobic and anaerobic bio-aging techniques in terms of the impact of PE on the reactors and the influence of different bio-aging conditions on PE. The results indicate that HDPE MPs exhibit a methane inhibition effect on anaerobic reactors; however, HDPE itself remains unaffected by the anaerobic process, as evidenced by stable CI and crystallinity results. Conversely, LDPE does not detrimentally impact AD but is significantly influenced by the process, as indicated by the differences in CI and crystallinity between pristine and bio-aged LDPE samples. Although LDPE were used at much higher doses in the BMPs than HDPE, the presence of additives (e.g., UV stabilizers) in HDPE may account for its methane inhibition effect and its resistance to the sludge influence, contrasting with the additive-free LDPE, which does not affect microorganisms but is altered by them. Either type of PE did not exhibit any impact on aerobic reactors, although they were influenced differently by aerobic digestion.

The bio-aging of PE under various conditions underscores the need to understand the fate and impacts of MPs in environmental systems. These alterations can affect WWTP efficiency and enable MPs to carry other pollutants. As PE undergoes bio-aging, it can fragment and accumulate in filtration systems, leading to clogging and reduced efficiency of mechanical filters and membranes. Additionally, the presence of MPs in sludge can interfere with biological treatment processes. MPs provide surfaces for microbial colonization, potentially altering the microbial community structure and impacting the degradation of organic matter. Furthermore, the ability of MPs to adsorb and carry other pollutants, such as heavy metals and OCs, can introduce additional challenges for WWTPs, complicating the treatment process and potentially leading to the release of these pollutants into the environment. Understanding these dynamics is crucial for improving WWTP operations and mitigating the environmental impacts of MPs.

This study reveals critical insights into the structural and chemical changes of HDPE and LDPE post bio-aging, highlighting their persistence and interaction mechanisms,

including biofilm formation and surface modifications. MPs can alter soil properties and microbial communities, impact soil biota and digestion processes, and potentially bioaccumulate and bio-magnify through food webs. MPs may transfer across trophic levels and serve as vectors for chemical contaminants, posing toxic risks. Further studies are essential to understand the effects of MPs' bio-aging on the environment and evaluate the sorption dynamics of organic contaminants onto MPs, particularly regarding land application of biosolids.

CHAPTER 5

THE EFFECT OF BIO-AGED POLYETHYLENE ON SORPTION POTENTIAL OF TRICHLOROPHENOL AND TRICLOSAN

Abstract

Microplastics (MPs), emerging environmental pollutants, are affected by various environmental factors which may in turn impact their interactions with organic contaminants (OCs). Bio-aging of polyethylene (PE) during anaerobic and aerobic digestion may alter its interactions with OCs. This presents substantial risks to ecosystems, underscoring the need to understand the sorption behavior of different OCs with environmentally relevant PE. This study investigates the changing interaction of anaerobically and aerobically aged PE with two different model compounds, namely, triclosan (TCS), and 2,3,6-trichlorophenol (TCP). Preliminary sorption tests were conducted with pristine, anaerobically, and aerobically bio-aged high-density PE (HDPE) and low-density PE (LDPE). In addition, sorption isotherms were conducted with aforementioned forms of LDPE. Preliminary sorption studies indicated generally favorable sorption of the OCs on pristine and aerobically aged HDPE. Aerobically bio-aged HDPE had removals of 89% for TCS and 48% for TCP, and LDPE had removals of 84% for TCS and 18% for TCP. On the other hand, anaerobically aged PE TCS sorption varied, with increased sorption on HDPE (92.5% removal) yet decreased sorption on LDPE (76% removal). However, neither HDPE nor LDPE showed any affinity towards TCP. This is mostly attributed to the sorbent's impact on solution pH, resulting in TCP phenolate formation. Having a negative charge, the phenolate form had no affinity for either sorbent. Isotherms were only conducted for bio-aged LDPE and a parallel finding was observed there, such that anaerobically aged had the lowest capacity of 626 μg/g for TCS and 295 μg/g for TCP when compared to pristine and aerobically-aged forms of LDPE. Other factors affecting the variations in sorption of the OCs to PE

involved differences in their solubility, hydrophobicity, interaction of OCs with biofilm residuals in MPs, and alterations of PE crystallinity and functional groups after bio-aging. The findings offer insights into the sorption mechanisms and environmental impact of aged MPs, enhancing our understanding of their role in pollutant transport and accumulation in the ecosystems.

Graphical abstract

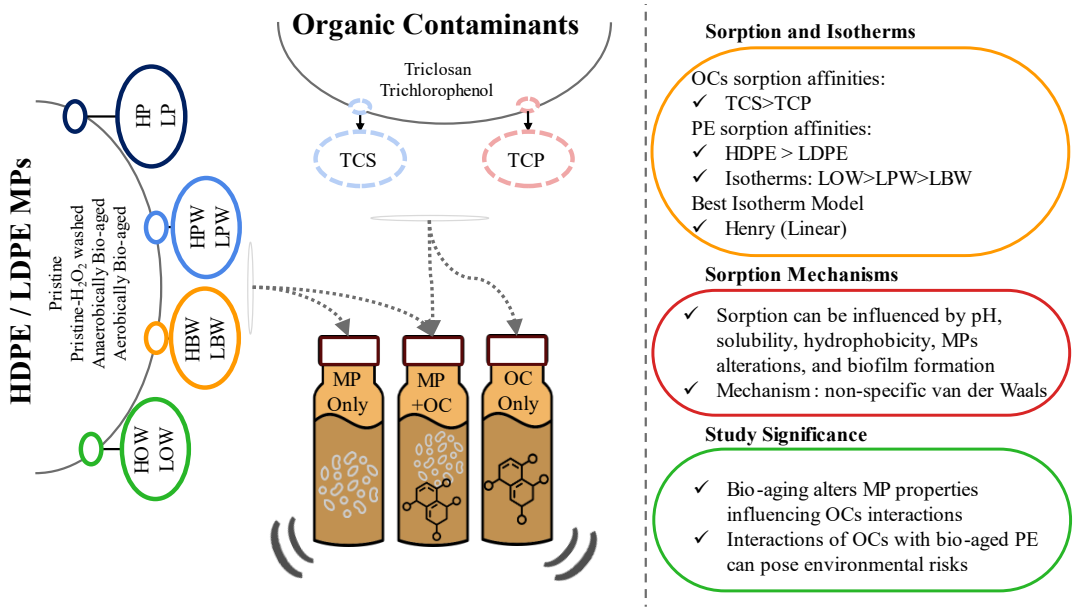

5.1 Introduction

Microplastics (MPs) (particles < 5 mm) have been recognized as a global environmental threat due to their pervasive presence and potential risks to the food chain through interactions with organic contaminants (OCs) (Wang et al., 2022b; Zhou et al., 2022). Due to their physicochemical properties, MPs may accumulate and help transportation of hazardous chemicals (Lin et al., 2021; Lončarsk et al., 2020aShi et al., 2022b). Studies report sorption affinity of MPs towards OCs; including persistent organic pollutants (Tong et al., 2021), heavy metals (Tong et al., 2021; Lončarsk et al., 2020), pharmaceuticals, or perfluoroalkyl acids (Lončarsk et al., 2020), indicating risks to ecosystems (Tong et al., 2021). Thus, understanding

sorption behavior of different OCs with environmentally relevant, *i.e*., aged MPs is relevant for understanding their fate and transport (Lončarsk et al., 2020) as well as assessing any environmental impact (Tong et al., 2021).

MPs can undergo physical, chemical, and biological aging in the environment (He et al., 2023), which may in turn affect their interaction with OCs and have adverse effects on the environment and the food chain (Lu et al., 2023). For instance, MPs interactions can be influenced by physiochemical properties changes due to aging. As MPs age, they undergo chemical alterations such as new functional groups, and physical alterations such as changes in shape, particle size, surface roughness as well as thermal properties which may result in different binding affinities for OCs (Zafar et al., 2022). Biological aging, due to microbial colonization and biofilm formation on the MP surface, can alter the surface's physicochemical and structural characteristics, increasing the number of binding sites and forming new functional groups (Zafar et al., 2022). Due to biofilm formation, MPs surface micro-morphology, roughness, surface charge, specific surface area, and density may be impacted (Tu et al., 2020). Although OCs typically co-exist with bio-aged MPs in the environment, studies related to the adsorptive role of especially bio-aged MPs are quite limited (He et al., 2023; Verdú et al., 2023; Zafar et al., 2022; Zhou et al., 2022).

Polyethylene (PE) is the most common polyolefin and makes up most MPs found in WWTPs (4-51%). PE is composed of a long-chain aliphatic hydrocarbon and can come in various forms and densities, two common ones are high-density PE (HDPE) and low-density PE (LDPE) (Ronca, 2017). Even though a lot of research has been done to understand the sorption behavior and mechanism of OCs on MPs, the study on bio-aged MPs has not been thoroughly investigated (Ho et al., 2020). Longer exposure of PE to bio-aging changes their physical makeup and morphology, releasing hazardous byproducts (*i.e.* additives) (Priyanka & Saravanakumar, 2022), which might influence the interactions with OCs besides bio-aging (Lončarsk et al., 2020). Therefore, the study of the effect of OCs with MPs in WWTPs is of interest. The interaction of PE with sludge in WWTPs can bring several outcomes on sorption

of OCs. For example, MPs can interact with microorganisms and organic matter. Biofilms, which are enriched with proteins, lipids, and polysaccharides, frequently form on surfaces which can influence the fate of chemicals by altering sorption dynamics (Cui et al., 2023). However, due to lack of enough research on this area, there is no complete idea on the mechanism or effects of biofilm on the sorption of OCs on PE.

Wastewater treatment plants (WWTPs) receive MPs from various sources, where MPs accumulate in sludge (Akbay et al., 2022). This accumulation, coupled with the potential sorption of OCs, including endocrine-disrupting chemicals (EDCs), on MPs, raises specific concerns regarding land application of biosolids. Anaerobic digestion (AD) is one of the common treatment methods for sewage sludge (Lessa Belone et al., 2024). Also, aerobic digestion is frequently adopted by small-scale WWTPs. Because of its high nutrient content, aerobically digested sludge is frequently used to enhance soil quality and water retention (Zhang et al., 2021b). Under these treatment methods and similarly in the environment, MPs undergo bio-aging which may alter their interaction with OCs. While UV-induced aging of MPs has been extensively studied, bio-aging, particularly during sludge digestion, has not been investigated as thoroughly (Zafar et al., 2022).

The pervasive presence of MPs, especially aged MPs, and their potential interactions with various OCs across different ecosystems necessitate a comprehensive examination of these interactions. Numerous recent studies (Costigan et al., 2022; Fu et al., 2021; Wang et al., 2020) have scrutinized the interactions between OCs and aged MPs, especially PE (Adan et al., 2022; Çiftçi et al., 2023). For OCs and non-aromatic MPs like PE the primary mechanism can be non-specific van der Waals interactions only. Moreover, there is a significant relationship between hydrophobicity of OCs (log K_{ow}), the sorption capacities of OCs (Costigan et al., 2022), and the crystallinity of MPs (Fu et al., 2021; Verdú et al., 2021). Furthermore, alterations on MPs after aging like changes in crystallinity, hydrophobicity of MPs, functional groups, surface characteristics, and the presence of biofilm can yield various outcomes with sorption of OCs (Fu et al., 2021; Wang et al., 2020).

Furthermore, a number of factors, including the type of MPs, the pH of the solution, the ionic strength, and the presence of coexisting dissolved organic matter, have been found to influence the sorption of OCs on MPs (Li et al., 2019b).

Two OCs, namely triclosan (TCS) and 2,3,6-trichlorophenol (TCP) are used as model compounds in this study to comparatively evaluate their sorption on pristine and bio-aged HDPE and LDPE. Triclosan (TCS) is an extensively utilized antimicrobial agent found at ppm levels in wastewater (Shi et al., 2022b), and can also be concentrated in sludge (Tong et al., 2021). Similarly, chlorophenols are frequently detected in water bodies, constituting the largest proportion of phenolic compounds in sludge (Chen et al., 2021c). The concentration of these OCs in WWTPs' sludge which also includes MPs, makes them prone to different interactions with these MPs owing to their hydrophobicity and substantial surface area-to-volume ratio (Chen et al., 2022). Even though a lot of research has been done to investigate the interaction mechanisms of these OCs on MPs, research on environmentally relevant, bio-aged MPs upon anaerobic and aerobic sludge digestion processes is extremely limited. In lieu of identified gaps in the literature, this study aims to explore sorption and interactions of TCP and TCS having diverse physicochemical properties on pristine, anaerobically, and aerobically bio-aged HDPE and LDPE type MPs. The outcomes of this study would summarize the implications of changing interaction of bio-aged MPs with OCs for a better understanding of factors affecting management of MPs.

5.2 Materials And Methods

5.2.1 Microplastics Used in the Study

Pristine HDPE obtained from a water tank manufacturer and LDPE from a masterbatch company were manually sieved to a size range of 425-500 μm. They were then washed with deionized water, ultrasonicated, and left to dry in an incubator at 25°C. The densities of the HDPE and LDPE MPs were given by the manufacturers

as 0.935 and 0.919 g/cm^3, respectively, and the polymer structure was confirmed via Attenuated Total Reflection-Fourier Transform Infrared Spectroscopy (FTIR) at METU Central Laboratory (MERLAB). Differential Scanning Calorimetry (DSC) at MERLAB was used to measure the crystallinity of PE. The Brunauer-Emmett-Teller (BET) specific surface areas (SSA, measured with Krypton at University of Maine) were 0.0500 ± 0.0056 and 0.0400 ± 0.0025 m^2/g for HDPE and LDPE, respectively. MPs in pristine form were exposed to anaerobic and aerobic bio-aging using lab-scale anaerobic and aerobic digesters at 35^{o}C for 60 days, as explained in detail elsewhere (Chapter 4). All MPs (*i.e.*, pristine, anaerobically, and aerobically bio-aged HDPE and LDPE) were washed using 17.5% H_2O_2 to remove any residual sludge prior to use in sorption experiments.

Bio-aged MPs were characterized via FTIR, DSC, and Scanning Electron Microscope (SEM), as provided in detail elsewhere (Chapter 4). A summary of characterization information is presented in Table B.1 in Appendix B. As indicated from characterization, HDPE had higher crystallinity than LDPE. Overall bio-aging lead to a slight increase in crystallinity which indicates chain scission of PE polymer. However, these changes were not significant ($p>0.01$). Moreover, an increase in carbonyl index (CI) was observed after LDPE bio-aging indicated weathering of PE. In addition to the backbone structure of LDPE, new bands and increased intensity in carbonyl band were observed (maximum CI of 0.118±0.029 for LOW and 0.100±0.007 for LBW as can be seen in Chapter 4). These alterations were attributed to microbial activities that took place over 60 days while aging LDPE in bio-reactors.

5.2.2 Sorption Experiments

Neat standards of 2,3,6-trichlorophenol (from Chem Service Inc., Pennsylvania, USA) and triclosan (TRC, Canada) were used in sorption experiments. Table B.2 in Appendix B summarizes properties of OCs. Triplicate test reactors with singular solutions of OCs and MPs were used during sorption experiments. Two sets of controls, containing only OCs and only MPs, were used during all tests. Sorption

was conducted in 40 mL amber glass vials with a working volume of 36 mL. Solid to liquid ratios (S/L) were 25 g/L for TCP and 10 g/L for TCS. All preliminary sorption tests were conducted at 9 ppm, except for TCP (8 ppm for HDPE). Isotherms including LDPE for TCS and TCP were conducted using seven different concentrations, as follows: TCS: 1, 2, 4, 5, 7, 8, 9 ppm, and TCP: 0.5, 1, 4, 9, 20, 40, 60 ppm. pH of water was adjusted to 6 for TCS, and pH 4 for TCP to make sure they are in their unionized forms (pKa=5.8 for TCP, pKa=7.9 for TCS). Kinetic studies had previously established that it would take 24 hours for HDPE and 6 hours for LDPE, for both TCP and TCS to reach sorption equilibrium. Vials were shaken horizontally at 200 rpm, 25±2°C in a shaking incubator. Sorption tests were carried out with pristine HDPE and LDPE washed with H_2O_2 (named HPW and LPW, respectively), anaerobically aged HDPE and LDPE (named HBW and LBW, respectively), and aerobically aged HDPE and LDPE (named HOW and LOW, respectively).

5.2.3 Analytical Methods

Stock solutions of TCS and TCP were prepared by dissolving them in ethanol in amber vials and then stored at 4 °C in the dark (Verdú et al., 2021). Working solutions were freshly prepared before experiments. All compounds were measured spectrophotometrically using quartz cuvettes, and absorbance readings were taken at initial and equilibrium time via HACH DR6000 UV-Vis spectrophotometer at their maximum absorbance wavelengths of 289 and 279 for TCP and TCS, respectively. The method detection limit (MDL) and method quantitation limit (MQL) were determined as 0.031 ppm and 0.092 ppm for TCP and 0.029 ppm and 0.088 ppm for TCS, according to USEPA (2016).

To keep TCP under the range of the pKa and hence at the wavelength of its maximum absorbance, an acetate buffer (Lee et al., 2013) was used during final spectrophotometric measurements of LDPE preliminary and isotherm setups. The acetate buffer during measurement was necessary to ensure all reactors remained

below the pKa at the time of measurement. Without the buffer, if the pH exceeded the pKa, a shift in the absorbance peak of TCP was observed, resulting in higher absorbance readings, which correspond to higher concentration values Figure C.16 . This was realized in LBW sorption trials when negative values were observed, therefore, buffer was used during measurement in setups involving LDPE. This, however, was not done in setups involving HDPE, as they had been done previously. Moreover, all sorption test results were control-corrected to normalize the values based on any absorbance read due to release of matter from the MPs. This ensures delineating sorption from any other impact of bio-aged MPs on solution chemistry.

5.2.4 Sorption Isotherm Models

A total of five different isotherm models, one linear (Henry) and four non-linear (Freundlich, Temkin, D-R, and Langmuir) were fitted to sorption data for OCs for relevant pristine washed and bio-aged (anaerobic and aerobic) MPs (Table B.3 in Appendix B). Moreover, ANOVA using MS Excel and TUKEY test was also performed on removal data from preliminary sorption and isotherms to check for statistically significant differences (at 99% confidence level) among LDPE groups.

5.3 Results

5.3.1 Triclosan Sorption on Bio-Aged Polyethylene

The outcomes of preliminary sorption experiments of TCS with HDPE and LDPE are depicted in Figure 5.1. The results of sorption on each bio-aged set-up are depicted in Figure C.9 (Appendix C). The results reveal a consistent affinity of TCS for sorption onto pristine (P) and pristine-washed (PW) PE ($p<0.01$). This finding is important as it suggests that washing with H_2O_2, which is a necessity for removing biofilm from PE after bio-aging, does not affect interaction of TCS with PE. Hence, LPW and HPW are considered as references for comparative evaluation of sorption

onto bio-aged PE. Among bio-aged materials, aerobic bio-aging does not seem to yield any different TCS sorption when compared to pristine or washed HDPE or LDPE. On the other hand, anaerobically aged (HBW) material was different from the rest. In terms of sorption between HDPE and LDPE, HDPE exhibited a greater affinity for TCS, with HBW demonstrating the highest TCS removal (92.5%) when compared to the rest. TCS has the lowest affinity towards anaerobically aged LDPE, despite having a high standard deviation.

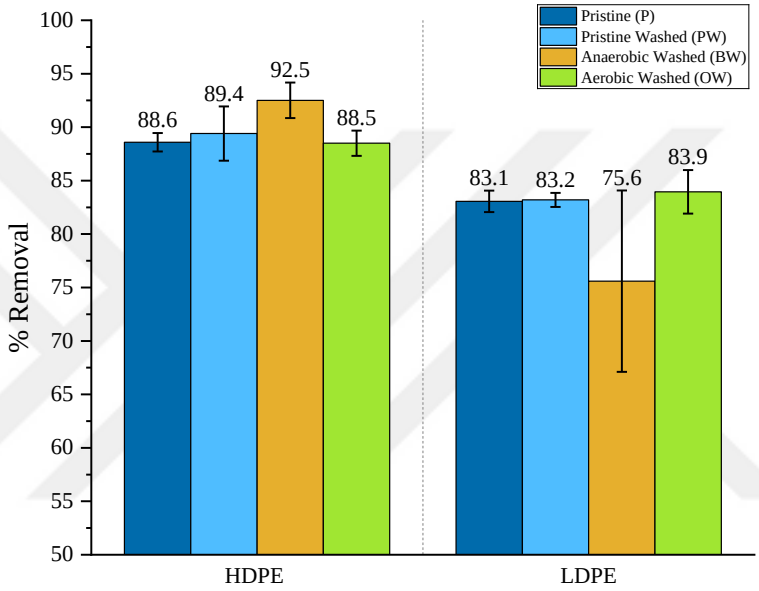

Figure 5.1 Results of preliminary sorption TCS on HDPE and LDPE before and after bio-aging.

Isotherm studies are conducted with LDPE that is washed and after both bio-aging conditions. Figure 5.2a shows isotherm data for all three sorbents, *i.e.*, LPW, LBW, and LOW. As can be seen from the figure, sorption affinity showed a decreasing order of LOW≥ LPW>LBW, even though the differences were not significant between LOW and LPW ($p>0.01$). The relatively low affinity of LBW as was observed in preliminary sorption tests is clearly visible in isotherm results (Figure 5.2a). Isotherm model fits (Figure 5.2 b, c, and d) indicate that the linear sorption model, namely, Henry, yields the best fit for TCS among the five chosen models (Table B.4 in Appendix B). The results of the other linear isotherm fits can be found in Table C.10 in Appendix C. The resulting sorption constants, *i.e.*, K_{pew}, for TCS in

decreasing order is 0.465 L/g for LOW, 0.399 L/g for LPW, and 0.158 L/g for LBW. The maximum sorption capacity was measured as 750.2±0.8, 742.9±8.1, and 626.6±35.2 µg/g for LPW, LOW, and LBW, respectively. Despite having low standard deviations (LPW and LOW), the last concentration didn't fit the linear trend closely due to approaching the solubility limit of TCS (10 g/L) leading to slightly lower sorption capacity. The removal percentages of each isotherm concentration are shown in Figure C.12 in Appendix C.

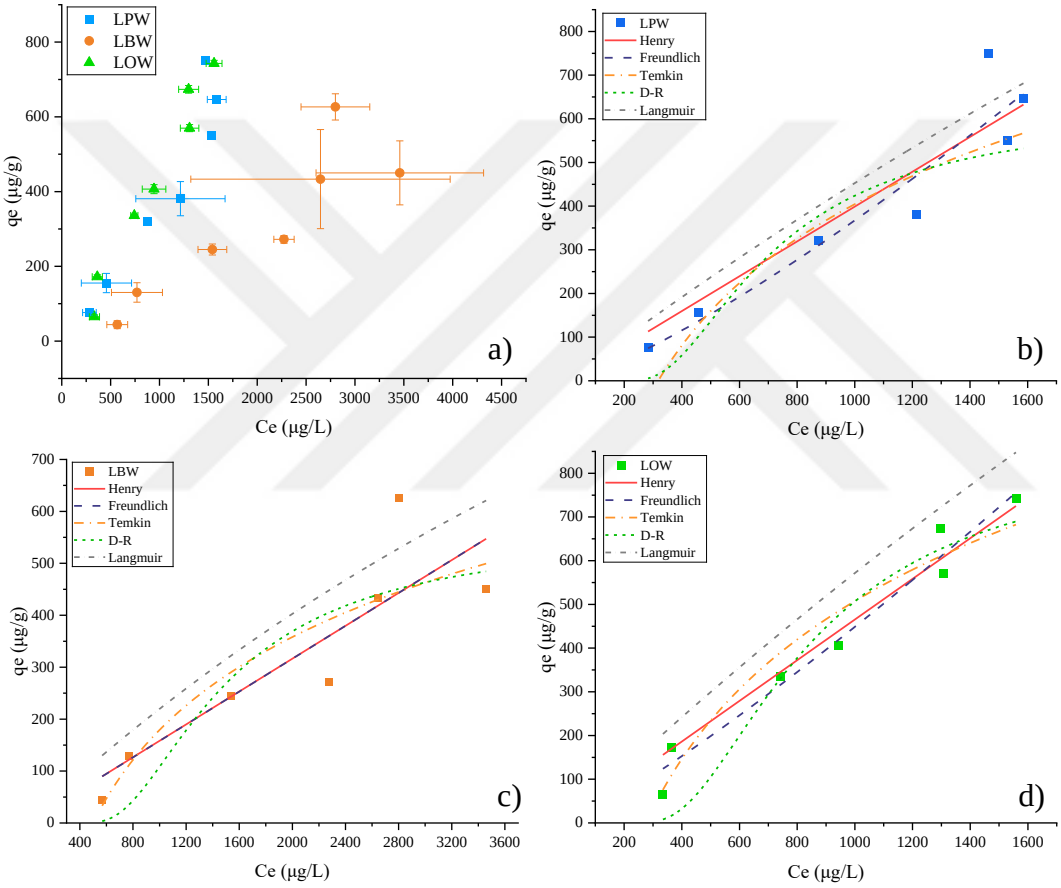

Figure 5.2 a) TCS Isotherm data of pristine-washed (LPW), aerobically aged (LOW), and anaerobically aged (LBW) LDPE and isotherm models fits for b) LPW, c) LBW, and d) LOW.

Figure B.1 (a-c) in Appendix B illustrates the pH measurements of control reactors and test reactors before and after sorption of TCS. Absorbance scans of the reactors at equilibrium concentrations are depicted in Figure C.15 in Appendix C. As depicted, all pH values fell below the pKa of TCS (7.9), indicating that sorption

occurred with the neutral form of TCS. Absorbance scans of the test reactors after reaching equilibrium were also taken. TCS-only control reactors (Figure B.2a), LPW, and LOW scans exhibited a maximum peak at the expected wavelength associated with TCS (279 nm). This indicated that LOW MPs do not result in a change in the pH of the solution or do not follow a different interaction as sorption proceeds. Conversely, despite pH being below pKa, LBW reactors indicated an interaction with water that resulted in a shift in the TCS peak (Figure B.2b) from 279nm to 290nm. As can be seen in the absorbance scans (SI) for all concentrations of LBW-containing reactors, TCS is modified, suggesting interactions other than sorption, e.g., degradation or complexation that results from contact of LBW with TCS. In the literature, there is one study that mentions TCS biodegradation into 2,4-dichlorophenol, under anaerobic environments (Gangadharan Puthiya Veetil et al., 2012). Interestingly, 2-4-dichlorophenol absorbs light at 290 nm (Sun et al., 2012). However, it is highly unlikely to have any anaerobic microbial activity in the LBW sorption vials, and also there is no experimental evidence to confirm the presence of 2,4-dichlorophenol in the vials.

5.3.2 Trichlorophenol Sorption on Bio-Aged Polyethylene

Figure 5.3 presents the results of preliminary sorption tests with TCP. The results of sorption on each bio-aged set-up are depicted in Figure C.10 (Appendix C). Equilibrium concentrations in the HDPE test were not measured using an acetate buffer; however, the initial solutions were maintained lower than the pKa (*i.e.*, pH of 4). The impact of using acetate buffer on measurements is further explained in Figure C.16 in Appendix C. As shown in the figure, considering the standard deviations, a significant difference ($p<0.01$) was not present in sorption affinity between pristine (P) and pristine H_2O_2-washed (PW) MPs for neither HDPE nor LDPE setups. Consequently, PW was used as a reference for TCP sorption experiments. Additionally, HDPE MPs exhibited a higher affinity for TCP sorption compared to LDPE. Generally, anaerobically bio-aged MPs (HBW and LBW)

displayed no sorption affinity for TCP. However, the incompatibility of LDPE with TCP was much higher, when compared to HDPE, in terms of changes in water chemistry. The negative removal values are attributed to leaching of substances from anaerobically bio-aged MPs, which interfered with spectrophotometric measurements. A greater release of substances into solution was observed in anaerobically aged LDPE samples when compared to its HDPE counterpart. All results are corrected with MP-only controls, still, higher absorbances were recorded at equilibrium when compared to the initial yielding in practically impossible negative removals. In contrast, aerobically aged MPs (HOW and LOW) exhibited some affinity towards TCP sorption albeit lower than that of PW. Among these, HOW showed robust removal (48%), whereas LOW yielded 18% removal on average. The high standard deviation associated with the latter indicates highly variable sorption, which is further scrutinized with isotherm tests.

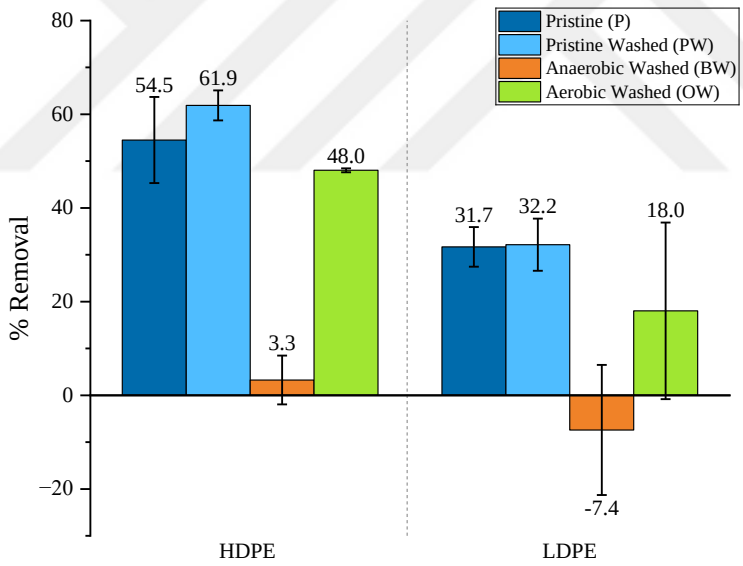

Figure 5.3 Preliminary sorption results of TCP with HDPE and LDPE.

Figure 5.4 summarizes the isotherms conducted on LPW, LBW, and LOW with TCP. The sorption affinity follows a decreasing order of LOW > LPW > LBW. Both LOW and LPW exhibit a gradual increase in the amount of sorbed TCP as the concentrations rise, resulting in lower equilibrium content in the aqueous phase. It should be noted that for LOW, the variation among triplicate sorption reactors in

isotherm studies was much lower, when compared to preliminary sorption reactors presented above, possibly due to homogeneous aged material in the vials. Aerobic bio-aged LDPE was deemed at an acceptable uniformity, also supported by a carbonyl index of 0.118±0.029 (Chapter 4).

Conversely, LBW shows no tendency for TCP sorption at any concentration below 60 ppm, with only a slight affinity for sorption at this maximum concentration. The isotherm model fits (Figure 5.4b, c, and d) indicate that the Henry linear model provides the best fit, with high R^2 values of 0.995 and 0.959 for LPW and LOW, respectively, yet no satisfactory model fit could be obtained for LBW, owing to lack of sorption (Table B.4 in Appendix B). The results of the other linear isotherm fits can be found in Table C.10 in Appendix C. In addition, the D-R non-linear model also exhibited satisfactory fit for LOW, with a higher R^2 of 0.984 than Henry, and lower RMSE. Comparing the K_{pew} values, LOW has the highest K_{pew} (0.018 L/g) compared to LPW (0.011 L/g). The maximum sorption capacities for LOW, LPW, and LBW with TCP are 694.6±71.2, 458.3±59.4, and 294.8±71.2 μg/g respectively. The removal percentages of each isotherm concentration are shown in Appendix C, Figure C.13 (measurements with buffer) and Figure C.14 (measurements without buffer).

Figure B.1 in Appendix B presents the pH of TCP and MPs at equilibrium without the use of an acetate buffer. The results indicate that for TCP with LPW and LOW (Figure B.1d and f), the pH after equilibrium did not exceed the pKa of TCP. However, for TCP with LBW (Figure B.1e), the pH was observed to be close to pKa. This suggests that the biofilm from LBW MPs may have interfered, raising the pH from 4 to near the pKa limit. These pH changes correspond with the absorbance scans, where a shift in peak was observed, indicating that TCP may be partially in its dissociated (phenolate) form. Absorbance scans of the reactors at equilibrium concentrations without buffer are depicted in Figure C.15 in Appendix C. Additionally, the leaching of substances from LBW MPs may react with the TCP solution, altering its pH. This interaction underscores the complexity of sorption

processes involving anaerobically bio-aged MPs, highlighting the influence of biofilm and leaching substances on the equilibrium conditions and the behavior of TCP in such systems.

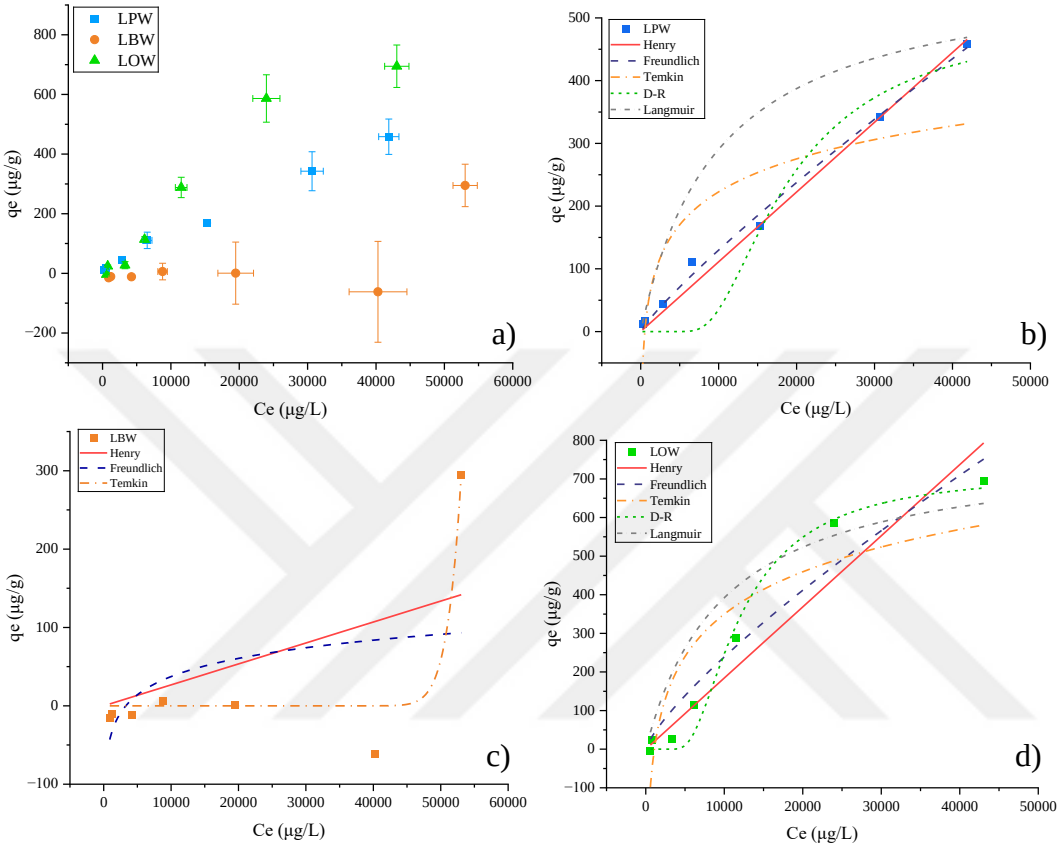

Figure 5.4 a) TCP Isotherm models LPW, LBW, and LOW, and Isotherm models fit for b) LPW, c) LBW, and d) LOW.

5.4 Discussion

Figure 5.5 gives an overview of all preliminary sorption tests in terms of ranges and means of percent removals for each OC, bio-aging, and PE type. The comparison of TCP, TCS, and MG removals is depicted in Figure C.11 in Appendix C. The first apparent finding from the results is the consistently high affinity of TCS for almost any type of PE (e.g., above 80% removal observed for all cases except for anaerobically aged LDPE which is around 75%), whereas a spectrum of removal

efficiencies from zero (or negative, due to interfering species, in the case of anaerobically aged LDPE) all the way to 60% removal for pristine HDPE is true for TCP. There may be a number of reasons for the results: (i) the log K_{ow} value of TCS (4.76) is one order of magnitude higher than that of TCP (3.77), therefore its higher hydrophobicity would enable a higher affinity onto PE when compared to TCP (Fu et al., 2021), (ii) the solution pH for sorption reactors were different for the two compounds. Sorption took place at an initial pH of 4 for TCP, whereas it was 6, much closer to neutral for TCS (owing to their different pKa values). An acidic solution may have promoted leaching of compounds from bio-aged PE into the solution phase when compared to a more neutral solution. Also, lower pH may have resulted in a higher interaction of H+ ions with bio-aged PE surface, negatively affecting sorption, (iii) The control reactors containing only MPs (*i.e.*, aerobically or anaerobically aged) in all sorption set-ups showed a slightly higher absorbance when compared to water only or pristine-washed control reactors. This absorbance read at the corresponding wavelengths of TCP and TCS indicated minor interference to measurement due to release of compounds from bio-aged PE. We attribute this leaching to biofilm formed in digesters, which may not have been completely removed with H_2O_2 washing. Spectrophotometric measurement in the UV range may be prone to such interferences. Nevertheless, to obtain the true sorption values attributable to sorption on bio-aged MPs, all sorption test results were corrected with relevant control reactors to eliminate any interference from such releases from MPs.

Furthermore, at high sorbate concentrations, LBW showed much greater variation in sorption capacity, when compared to the other two sorbents. This could be due to uneven aging of PE in anaerobic reactors, resulting in varying sorption levels, especially with LDPE. As LDPE contains a higher fraction of amorphous portion when compared to HDPE, the effect of bio-aging could be more diverse for LDPE when compared to the more crystalline HDPE. Many organic and inorganic constituents may partition into the amorphous regions of PE, and this could be expected to be more prominent in LDPE (crystallinity of 35.5%) when compared to HDPE (crystallinity of 51.6%) (Karapanagioti & Werner, 2019).

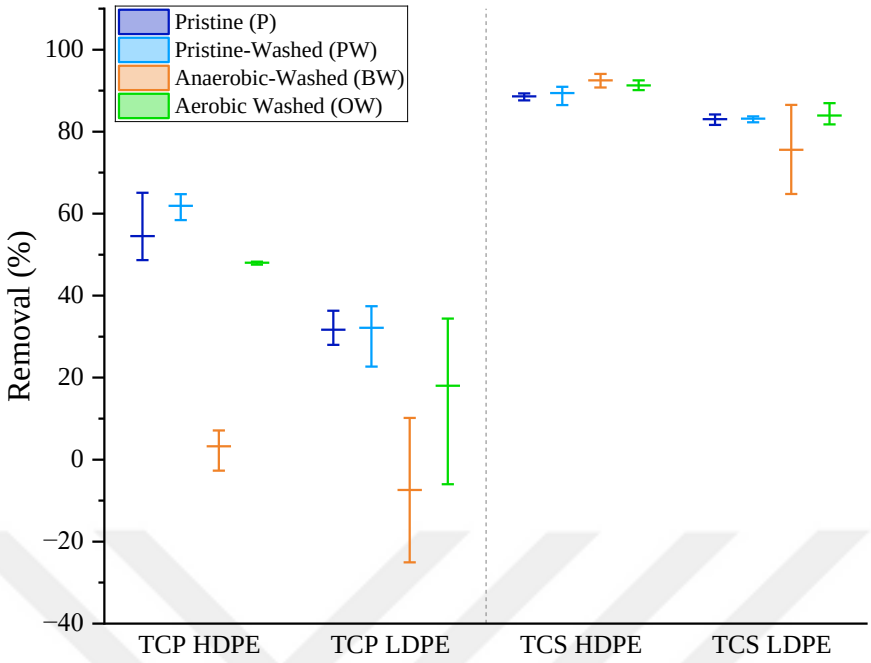

Figure 5.5 Summary of preliminary sorption results for TCP and TCS, before and after bio-aging of HDPE and LDPE.

The influence of crystallinity extends to predicting sorption affinities for environmental pollutants and impacts polymer chain mobility (Campanaro et al., 2023). A polymer typically comprises a well-ordered crystalline phase and an amorphous region (Verdú et al., 2021). There are two sorption conditions that can determine the differences in sorption between HDPE and LDPE: Diffusion rate and sorption capacity. The increased diffusion rate of non-polar compounds into less crystalline polymers is well-established in the literature (Verdú et al., 2021). In the present study, LDPE was observed to reach equilibrium (*i.e.*, 6 hours) faster than HDPE (*i.e.*, 24 hours). This aligns with literature where lower crystallinity of LDPE corresponds to a higher diffusion rate of hydrophobic molecules into MPs. On the other hand, in terms of sorption capacity, Verdú et al., (2021) indicated that the enhanced sorption capacity of LDPE aligns with its low crystallinity. Similarly, Fu et al., (2021) indicated that the higher crystallinity and SSA of HDPE results in a more tightly packed molecular structure with less free volume and therefore provides less sorption affinity for OCs. However, in this study, in both OCs sorption, both

pristine and bio-aged HDPE exhibited a higher sorption affinity than LDPE (51.6% for HDPE compared to 35.5% for LDPE) despite having higher crystallinity.

Another factor other than crystallinity could have played a role in increasing the sorption affinity of HDPE over LDPE which is the presence of additives (UV-stabilizers) in HDPE. Previous studies have indicated that the presence of additives in some MPs can enhance sorption by increasing the hydrophobicity and particle void volume of the sorbent (Cui et al., 2023). Hydrophobic and electrostatic interactions are dominant mechanisms for sorption of many contaminants onto MPs (Cui et al., 2023). Since, contrary to LDPE, HDPE contained UV-stabilizers, which may have had an additional effect on enhancing sorption of TCP and TCS, when compared to LDPE.

Surface interaction is another significant factor influencing sorption of chemicals on polymers. The surface physiochemistry can be altered by the degree of polymer weathering, which is often indicated by changes in crystallinity, formation of hydroxyl, carbonyl, carboxyl, or other polar moieties that may interact more readily with OCs, as well as an increase in external surface area due to cracking (Verdú et al., 2021). FTIR, DSC, and SEM of aged samples in this study indicate slight changes of chemical (oxidation) and physical (modifications in crystallinity) nature in MPs as a result of bio-aging (Chapter 4). Besides that, FTIR indicated changes in functional groups such as the presence of proteins as an influence of microorganisms during aging on PE. Moreover, an increase in CI was observed upon bio-aging which was more dominant in LDPE upon aerobic aging, rather than anaerobic aging. These changes, in turn, could have negatively impacted sorption of TCP; possibly owing to biofilm filling pore spaces, and oxidized polymer surface becoming more available for polar water molecules and/or hydrogen ions at the test pH of 4 for TCP. At a pH of 4 more hydrogen ions are available which causes a better interaction with the bio-aged PE's more polar surface which slightly prevents sorption of OCs. Overall, it was evident that various bio-aging processes and the degree of bio-aging yielded different results when compared to pristine PE, especially for anaerobic bio-aging.

According to literature, the presence of biofilm on MPs generally enhances sorption of heavy metals and OCs. Studies indicated that biofilm formation altered tetracycline and copper adsorption on PE MPs, which was attributed to the SSA increases after biofilm growth. Likewise, other studies showed that LDPE exposed to biofilm facilitated metals accumulation (Verdú et al., 2023). These results aligned with aerobically bio-aged LDPE (LOW) isotherm sorption results where LOW showed higher sorption affinity towards TCP and TCS, however, that was the opposite case for LBW where it showed decreased affinity for sorption with TCS and no affinity to sorb TCP. These findings imply that the sorption of TCS and TCP by bio-aged MPs, particularly those subjected to anaerobic bio-aging, may involve different interaction mechanisms compared to pristine or aerobically bio-aged MPs. Furthermore, TCS and TCP may interact with other OCs, potentially influencing the sorption capacity of bio-aged MPs in WWTPs or the environment.

Furthermore, if a prediction model (Hatinoglu et al., 2023) is applied to predict the sorption potential of OC to LPW, LOW, and LBW, a 10% higher prediction error (56% for TCS and 53% for TCP) is observed with LBW when compared to LOW (error of 46% for TCP and 43% for TCS). This also aligns with the varying sorption results that LBW shows in sorption due to the different interaction mechanisms. On the other hand, LPW showed a much lower error with sorption for TCS (5%) when compared to TCP (37%). This indicates that washing did not affect the sorption behavior of LPW when interacting with TCS. However, washing could have affected the sorption of LPW to TCP even though it was not evident by percent removals.

According to ANOVA and TUKEY tests, preliminary sorption assessments among LP, LPW, LBW, and LOW revealed significant statistical differences ($p < 0.01$) in TCP sorption between LP/LPW and LBW. In addition, for TCS, a significant difference ($p < 0.01$) was observed between LOW and LBW. Further analysis of isotherm data for both TCP and TCS showed significant statistical differences ($p < 0.01$) in sorption between “LPW and LBW” as well as “LOW and LBW.” These findings suggest that LBW exhibits distinct interactions with OCs compared to LOW or pristine PE. This divergence is likely due to variations in aging conditions and the

possibly different interaction mechanisms of anaerobic biofilms with OCs. Moreover, LBW was exposed to a complex sludge mixture indicating that the interaction mechanisms with OCs can also become increasingly complex. This complexity may be attributed to the evolving different physicochemical properties of PE as it ages anaerobically, potentially leading to changes in surface characteristics and biofilm formation dynamics. Details on ANOVA results for TCP and TCS are presented in Appendix C (Table C.11-Table C.14).

Isotherm results with TCS and TCP both showed Henry (linear) as the best-fitting isotherm model. It was reported that sorption of hydrophobic compounds such as TCS and TCP into PE tends to be linear due to the amorphous regions of PE (Çiftçi et al., 2023; Karapanagioti & Werner, 2019; Tong et al., 2021). A plausible explanation for this phenomenon is that the amorphous regions of PE (pristine or aged) enable partitioning of OCs into these cavities. Aging may or may not change the amorphous portion of PE – as crystallinity results of DSC do not yield a great difference with aging. However, new functional groups are observed indicating changes in PE structure. These changes, with the presence of a high proportion of amorphous regions, may result in a greater preferential accumulation of TCS and TCP. Shi et al. (2022) state that the enhanced free volume in the rubbery domains of aged PE contributes to their higher sorption capacity for TCS. Results also indicated that of the non-linear models Freundlich had the best fit to LPW (for TCS and TCP) and LOW (for TCS). Similarly, Temkin fits LBW (TCS), and D-R fits LOW (TCP), while no model fits LBW with TCP. Literature studies also reported Freundlich as a best-fit isotherm model of some nonpolar organic compounds (*i.e.* TCS) on PE (Chen et al., 2021b, 2022; Hüffer & Hofmann, 2016; Wu et al., 2020) which can also be attributed to the solubility of the compounds. However, isotherms for sorption by rubbery PE were generally highly linear, with Freundlich exponents (n) approximately equal to 1 (Hüffer & Hofmann, 2016). These results line up with n values obtained from Freundlich non-linear isotherms from this study. This phenomenon suggests that the sorption of TCS and TCP by MPs occurs through partitioning into bulk polymer rather than through molecular adsorption on a

uniform, limited surface (Mo et al., 2021). Shi et al. (2022) similarly report that linear models were more suitable than Freundlich for fitting the adsorption isotherms of TCS on both virgin and UV-aged PE. Furthermore, Tong et al., (2021) reported a K_{pew} value of 0.536 L/g with sorption of TCS on pristine PE which was higher than our obtained results. A good fit of the D-R non-linear model to LOW with TCP indicates a pore-filling mechanism. Conversely, an unsatisfactory fit to Langmuir model may indicate that adsorption energies are not distributed homogenously and the assumption of site limitation for monolayer sorption may not be valid (Chen et al., 2021baShi et al., 2022b).

An important parameter affecting sorption behavior of OCs is the pH. TCS is an ionizable compound and Shi et al., (2022) and Ma et al., (2019) demonstrated that as TCS deprotonates under alkaline conditions, its sorption capacity decreases. Furthermore, Adan et al. (2022) observed an effect of pH on the sorption of 2,3,6-trichlorophenol (TCP) where, at a pH of 4 the sorption removal by pristine PE MPs was observed to be as high as 72%, at a pH of 6 it decreased to 58%, and at pH of 8 removal decreased drastically to 25%. These findings suggest that the anionic phenolate form of TCP exhibits a markedly reduced affinity for PE MPs (Çiftçi, 2024). Bio-aged MPs may still contain biofilm residuals even after washing, so we observe a tendency for TCP and TCS solutions to reach a pH of 6 and higher, at equilibrium. This tendency did not influence the sorption capacity of TCS onto bio-aged PE since it did not exceed pKa, however, it explains the shift in peaks and the loss of affinity of TCP (pKa=5.8) for HBW and LBW. Moreover, the pH of sludge usually ranges between 6-8, and the availability of TCS and TCP in WWTPs and their interactions with MPs could be influenced in a variety of ways as they interact in their disassociated form.

It should be noted that the two types of bio-aged PE (*i.e.*, aerobic and anaerobic) did not have the same impact on the pH of the solution. As can be seen in Figure B.1 in Appendix B, the aerobic bio-aged LOW had a lower impact on the pH of the solution when compared to LBW in both TCS and TCP sorption reactors. Even though all the OCs used are ionizable, the value of the pKa and pH of the experiment has an impact.

TCS was tested at pH 6 and always favorably sorbed, yet TCP had to be tested at pH 4 yet this impacts sorbent and any release of compounds from PE causing varied results in sorption, especially with LBW.

Despite having pH below pKa, TCS absorbance scans showed a shift in peak with LBW tests. This shift suggests an interaction between LBW and TCS or the leaching of another substance from LBW. For instance, when TCS was subjected to LBW, a form of degradation to a deprotonated TCS product could have taken place such as 2,4-dichlorophenol (measurable by UV-Vis spectrophotometer at an absorbance of 290 nm) (Sun et al., 2012) which is also the maximum peak after shifting in our scans (Gangadharan Puthiya Veetil et al., 2012). Any other degradation product that absorbs at 290 nm is also possible. On the other hand, an unidentified compound leaching from LBW could have also formed a complex with TCS which resulted in an absorbance at 290 nm. Therefore, sorption may not be the only or the dominant mechanism affecting TCS removal during its interaction with LBW.

The extended chains of $–CH_2–CH_2–$ units in PE lack substantial electronegative atoms or functional groups, making PE non-polar (Hüffer & Hofmann, 2016). Hence the principal mechanism of interaction of PE with an organic is likely to be non-specific van der Waals interactions (Hüffer & Hofmann, 2016). In this study, the main mechanism of TCS and TCP sorption onto pristine HDPE and LDPE is hence expected to be van der Waals interactions. Any unsaturation in PE structure or formation of new functional groups would open the way for other electron acceptor-donor (*i.e.*, H-bonding) type interactions. The effect of biofilm on BW and OW is expected to have an effect on sorption mechanisms. For instance, the potential leaching of dissolved organic matter (DOM) from LOW and LBW could have reduced the extent of sorption of OCs if the interaction between the DOM and the OC was stronger than the interaction between the OC and the bio-aged PE (Xu & Ghossein, 2018) (Verdú et al., 2021). Since the sorption mechanism with LBW and TCS might not be dominant, this conclusion could have been also applicable to TCS besides TCP due to the higher hydrophobicity of TCS.

Moreover, bio-aging may affect sorption mechanisms of OCs favorably or unfavorably, depending on the type of changes that happen on PE (e.g., surface oxidation, peeling, pore filling, etc.). The presence of polar groups in biofilms enhances dipole interactions and hydrogen bonding on bio-fouled microplastics compared to pristine surfaces (Ma et al., 2019). Research on TCS sorption has demonstrated that the interactions between OCs and biofilms are predominantly influenced by polar and electrostatic forces (Verdú et al., 2023). Previous observations have indicated that the hydrophilicity of plastic surfaces increases upon biofilm colonization and aging (Fu et al., 2021). The reduced sorption of TCS on BW microplastics colonized by biofilm can be attributed to the relatively high hydrophilicity of the biofilm, which correlates with a diminished capacity to retain non-polar compounds (*i.e.* TCS and TCP) (Verdú et al., 2023). As visually observed from the reactor sets, *i.e.*, bio-aged MPs (BW and OW) exhibited better mixing in the solution rather than only staying at the surface as clumps (LP), so it is deduced that they tend to be less hydrophobic than pristine MPs. Therefore, even if pH remained below pKa, it is hypothesized that the interaction mechanism of TCS and TCP could have been also influenced by the leaching and the hydrophilicity of the biofilm rather than the bio-aging degree of MPs. Further information about the sorption results of TCS and TCP is available in Appendix C (section C.4)

5.5 Significance of The Sorption Study on The Environment

Given that OCs frequently coexist in the environment with MPs, particularly those that have undergone bio-aging during WWTP sludge treatment processes or otherwise, the findings of this study elucidate the conditions to which MPs may be subjected following their interactions with sludge. Biofilm formation occurs rapidly on most submerged surfaces and can significantly alter the physical and chemical properties of MPs. The sorption of OCs to MPs in natural environments is likely complicated by various additional factors. These include the development of biofilm, as well as the presence of algae, bacteria, and fungi on the surfaces of MPs. As seen

from the results of this study, the different bio-aging techniques had different outcomes on the PE physiochemical properties leading to various sorption affinities with the two model OCs. It has been hypothesized that numerous factors may interfere with sorption processes. Changes in surface micro-morphology and roughness, surface charge, SSA, and density may influence the vertical migration, weathering, and adsorption-desorption dynamics of chemical pollutants and pathogens on MPs in the environment (Cui et al., 2023). These changes result in a variety of interaction mechanisms between OCs as seen from TCS and TCP.

The alteration of sorption interactions due to bio-aging could have significant implications for the environmental impact of MPs and the management of sludge. Sludge, which can contain up to 56,000 MPs/kg, retains 72–99% of MPs during treatment (Frost et al., 2022). This material is commonly applied as a soil additive on agricultural land in many countries. The sorption of contaminants, such as the EDC TCS, onto MPs incorporated in wastewater sludge, may pose an additional environmental threat due to bioaccumulation (Higgins et al., 2011). Therefore, if MPs in the environment, particularly those associated with WWTPs, exhibit high sorption of TCS the application of biosolids to land could result in unintended toxicological impacts on terrestrial organisms. However, further research is needed to determine the potential bioaccumulation of these OCs in the organisms (Verdú et al., 2023).

5.6 Conclusion

Overall, physicochemical changes and alterations such as increasing CI and crystallinity due to aerobic and anaerobic bio-aging of HDPE and LDPE exhibited varying effects on sorption of TCS and TCP. Overall, TCS showed higher sorption affinity in general (on average >75% removals) when compared to TCP (maximum of 60% for HDPE pristine and no affinity for anaerobic LDPE). This can be attributed to higher hydrophobicity of TCS, differences in pH of solutions, and leaching of biofilm from bio-aged MPs, especially LBW. It was shown here that bio-

aging has an impact on MPs, in turn affecting how bio-aged MPs and OCs interact. For instance, a shift in peak was observed with TCS and LBW interactions. Moreover, changes in pH were observed with TCP tests upon its interaction with LBW MPs which could have affected its sorption affinity. This indicated that LBW could have leached chemicals or biofilm that led to the disassociation of TCS and TCP into other products and therefore diminishing sorption of these OCs into LBW. In addition, isotherm results showed decreasing sorption affinity for both OCs (LOW>LPW>LBW) with LOW and LPW showing comparable sorption capacities with TCS, and LOW having the highest sorption capacity (694.6±71.2 μg/g) for TCP. This indicates that bio-aging mechanism affects the way LDPE would interact with OCs. Implications of the study are that not only the presence of MPs but also potentially enhanced or unpredictable sorption of organics onto bio-aged MPs in media such as biosolids may be of concern. Our study shows that there is no clear trend of increasing or decreasing sorption of organics with bio-aging of MPs due to the different impacts of aerobic and anaerobic digestion on PE as well as to different working mechanisms of OCs.

CHAPTER 6

CONCLUSION

This study investigated the bio-aging of HDPE and LDPE MPs within mesophilic aerobic and anaerobic digesters to understand their transformation dynamics under different biological conditions. HDPE and LDPE were subjected to bio-aging processes in these reactors to observe changes in their structural and chemical properties, which are in-turn investigated for their effect on sorption of OCs.

The presence of HDPE and LDPE MPs exhibited distinct effects on reactor performance during the study. HDPE MPs inhibited methane production in anaerobic reactors (26.2%), likely due to the presence of additives such as UV stabilizers, which may interact adversely with microbial processes. In contrast, LDPE MPs did not inhibit anaerobic digestion but underwent significant changes in properties, as indicated by variations in CI and crystallinity. Neither type of PE significantly impacted aerobic reactors' performance, although both experienced structural modifications due to aerobic digestion. These findings suggest that while HDPE may pose challenges to anaerobic processes in WWTPs, LDPE may be more susceptible to environmental bio-aging during wastewater treatment.

Characterization of PE samples upon bio-aging revealed changes in PE functional groups indicating biofilm presence and oxidation (C=O) of PE. Moreover, significant alterations ($p<0.01$) in LDPE were observed. An increased carbonyl index (CI) (0.019-0.100 for anaerobically aged LDPE and 0.079-0.118 for aerobically aged LDPE) was evident for LDPE samples, while HDPE samples did not exhibit any change in CI. Moreover, a statistically insignificant increase in crystallinity was noted. Furthermore, both bio-aged HDPE and LDPE samples under both aging conditions showed changes in surface roughness evidenced by SEM, indicating noticeable bio-aging.

The study further explored how bio-aging under both sludge digester conditions altered the interaction of HDPE and LDPE MPs with all three OCs namely, TCS, TCP, and MG. Preliminary sorption tests revealed that TCS had a higher sorption affinity compared to TCP, with TCS removals exceeding an average of 75%, whereas TCP showed a maximum removal of 60% for pristine HDPE. The differences in sorption capacities were attributed to the hydrophobicity of TCS, solution pH, and biofilm leaching from bio-aged MPs. Moreover, anaerobically bio-aged HDPE showed the highest affinity for TCS but not for TCP. On the other hand, aerobically bio-aged HDPE displayed high, yet slightly reduced sorption affinity to TCP compared to pristine PE. However, aerobically bio-aged LDPE showed the highest sorption capacity with TCP and TCS, suggesting that aerobic aging significantly affects the interaction between LDPE and OCs whereas, anaerobically aged LDPE showed no affinity to TCP sorption. Anaerobically aging had a major impact on MPs and sorption of both OCs. For instance, a shift in peak was observed with TCS, and changes in pH were observed with TCP tests which could have affected the sorption affinity. This indicated that the leaching of chemicals or biofilm might have led to the disassociation of TCS and TCP into other products and therefore diminishing sorption of these OCs. Sorption results of MG, on the other hand, revealed similar sorption affinities for pristine, pristine-washed, and anaerobically aged HDPE and LDPE, in contrast to a diminished affinity for aerobically aged MPs. MG is expected to be present in its cationic form at the pH tested, however, complex and unidentified interactions with deionized water negated detailed mechanistic evaluations to be made.

Isotherm studies were conducted to quantify sorption capacities and partitioning coefficients of bio-aged LDPE, which showed the greatest change in properties. The results indicated decreasing sorption affinity for both OCs (LOW>LPW>LBW) with LOW and LPW showing comparable sorption capacities with TCS, and LOW having the highest sorption capacity (694.6±71.2 μg/g) for TCP. Results reveal that bio-aging affects the way LDPE interacts with OCs. These interactions underline the

complex relationship between MPs and OCs, which is influenced by the bio-aging process.

The implications of the study highlight the critical need for effective management strategies to address the ecological risks posed by bio-aged MPs in WWTPs and the broader environment. The altered sorption behavior of bio-aged MPs can influence the efficiency of WWTPs and the fate of OCs in treated wastewater and biosolids, especially for MG and TCS. Enhanced or unpredictable sorption of organics onto bio-aged MPs, particularly under aerobic conditions for the case of this study, suggests potential for increased TCS and TCP transfer across trophic levels and into food webs. On the other hand, the anaerobic bio-aged MPs showed an increased potential for the transfer of MG and TCS through the environment. Conversely, anaerobic bio-aging of PE doesn't seem to enhance the transfer of TCP. Moreover, as these OCs are present in sludge at different pH levels, the interaction of PE with these OCs can be influenced differently. These influences can yield different sorption outcomes such as the complexation of TCS with other compounds or the deprotonation of TCS and TCP to other degradation products as also hypothesized in this study.

Additionally, PE is not the only type of MP that can affect WWTPs and influence OCs. Sludge can contain various types and sizes of MPs, each potentially impacting the performance of WWTPs differently. Moreover, the presence of diverse OCs with varying characteristics can result in a variety of interactions between OCs and MPs. For instance, in this study, both TCS and TCP are hydrophobic OCs, yet their interactions with PE aged under different conditions varied, depending on factors (*i.e.,* log Kow, pH, molar volume). Furthermore, MPs can undergo a variety of aging processes, such as UV-aging, which can alter sorption and interaction mechanisms between different MPs and OCs. In this study, various factors such as PE type and OC characteristics yielded a wide range of outcomes. Therefore, understanding the interactions of other MPs aging under different conditions with various OCs is essential for developing strategies to mitigate the environmental impact of MPs and to ensure safe application of biosolids in land management practices.

CHAPTER 7

RECOMMENDATIONS

Based on the findings of this study, the following recommendations for further studies are proposed:

- Investigate the effect of different doses of pure and additives induced HDPE and LDPE on AD: Future research should explore the impact of varying concentrations of pure and additives-enhanced HDPE and LDPE on the efficiency and stability of AD processes, examining factors such as methane production, microbial community dynamics, and overall reactor performance.
- Investigate the effect of leaching additives from PE on AD and aerobic reactors: It is essential to assess how additives leaching from PE materials influence the functionality and efficiency of both anaerobic and aerobic reactors. This includes studying potential toxic effects, changes in microbial activity, and alterations in biochemical processes.
- Investigate the difference in sorption mechanisms between pure and additives-induced PE on OCs: Comparative studies should be conducted to understand how the presence of additives in PE materials affects the sorption mechanisms of various OCs. This can involve examining adsorption kinetics, isotherms, and the influence of different additives on sorption capacity.
- Effect of sorption of OCs on bio-aged MPs at different bio-aging degrees and different environmental contexts: Research should focus on how different degrees of bio-aging and environmental conditions (e.g., temperature, pH, presence of other contaminants) impact the sorption behavior of OCs on bio-aged microplastics. This will help in understanding the long-term environmental fate of OCs associated with aged MPs.

- Address the gaps in the mechanism of MG-oxalate interactions with different water media: Further studies are needed to elucidate the interaction mechanisms between malachite green (MG) and oxalates in various water media. This includes exploring the role of different ionic strengths, pH levels, and the presence of other dissolved substances on the interaction dynamics.

Furthermore, several recommendations can be made to address the environmental impacts of MPs, particularly PE MPs, in WWTPs and broader environmental contexts:

- Enhancement of WWTP Technologies: Implement advanced filtration and separation technologies within WWTPs to more effectively capture and remove MPs from influent streams. This can reduce the concentration of MPs in treated sludge and minimize their re-entry into the environment.
- Development of Biodegradable Alternatives: Promote the development and use of biodegradable plastics as alternatives to conventional HDPE and LDPE. Encouraging the adoption of such materials can mitigate the persistence and negative impacts of MPs on the environment.
- Optimization of Sludge Management Practices: Optimize sludge management practices, including the treatment and disposal processes, to limit the release of MPs into soil and water systems. Enhanced protocols for the safe application of biosolids in agriculture should be established to prevent MP contamination.
- Further Research on Sorption Mechanisms: Conduct in-depth studies on the sorption mechanisms of various OCs with both pristine and bio-aged MPs. Understanding these interactions can inform strategies to mitigate the transfer and accumulation of pollutants in ecosystems.
- Long-term Environmental Monitoring: Establish long-term monitoring programs to track the environmental fate and transport of MPs from WWTPs to natural ecosystems. Monitoring should focus on the effects of bio-aged MPs on soil and water quality, as well as on flora and fauna.

REFERENCES

Adan, A., Koçaş, B., Özdemir, M., & Sanin, F. D. (2022). A Comparative Sorption Study for Phenol & Tricholorophenol onto Polyethylene Type Microplastics. *6th Eurasia Wate Management Symposium*, 4–7.

Akbay, H. E. G., Akarsu, C., Isik, Z., Belibagli, P., & Dizge, N. (2022). Investigation of degradation potential of polyethylene microplastics in anaerobic digestion process using cosmetics industry wastewater. *Biochemical Engineering Journal*, *187*, 108619. https://doi.org/10.1016/j.bej.2022.108619

Alassali, A., Moon, H., Picuno, C., Meyer, R. S. A., & Kuchta, K. (2018). Assessment of polyethylene degradation after aging through anaerobic digestion and composting. *Polymer Degradation and Stability*, *158*, 14–25. https://doi.org/10.1016/j.polymdegradstab.2018.10.014

Alimi, O. S., Claveau-Mallet, D., Kurusu, R. S., Lapointe, M., Bayen, S., & Tufenkji, N. (2022). Weathering pathways and protocols for environmentally relevant microplastics and nanoplastics: What are we missing? *Journal of Hazardous Materials*, *423*. https://doi.org/10.1016/j.jhazmat.2021.126955

Almond, J., Sugumaar, P., Wenzel, M. N., Hill, G., & Wallis, C. (2020). Determination of the carbonyl index of polyethylene and polypropylene using specified area under band methodology with ATR-FTIR spectroscopy. *E-Polymers*, *20*(1), 369–381. https://doi.org/10.1515/epoly-2020-0041

Andrady, A. L. (2017). The plastic in microplastics: A review. *Marine Pollution Bulletin*, *119*(1), 12–22. https://doi.org/10.1016/j.marpolbul.2017.01.082

APHA, AWWA, & WEF. (2017). Standard Methods for the Examination of Water and Wastewater. In R. B. Baird, A. D. Eaton, & E. W. Rice (Eds.), *American Public Health Association* (23rd ed.).

Artham, T., Sudhakar, M., Venkatesan, R., Madhavan Nair, C., Murty, K. V. G. K., & Doble, M. (2009). Biofouling and stability of synthetic polymers in sea water. *International Biodeterioration and Biodegradation*, *63*(7), 884–890.

https://doi.org/10.1016/j.ibiod.2009.03.003

Bahçeci, H. A. (2019). *Investigation of methane production potential of industrial sludges mixed with domestic sludge during anaerobic digestion*. MS Thesis. Middle East Technical University.

Batstone, D. J., Tait, S., & Starrenburg, D. (2009). Estimation of hydrolysis parameters in full-scale anerobic digesters. *Biotechnology and Bioengineering*, *102*(5), 1513–1520. https://doi.org/10.1002/bit.22163

Bhargava, D. S., & Datar, M. T. (1989). An analysis of nitrification during the aerobic digestion of secondary sludges. *Environmental Pollution*, *58*(1), 57–72. https://doi.org/10.1016/0269-7491(89)90237-6

Bonhomme, S., Cuer, A., Delort, A. M., Lemaire, J., Sancelme, M., & Scott, G. (2003). Environmental biodegradation of polyethylene. *Polymer Degradation and Stability*, *81*(3), 441–452. https://doi.org/10.1016/S0141-3910(03)00129-0

Campanaro, A. L., Simcik, M. F., Maurer-Jones, M. A., & Penn, R. L. (2023). Sewage sludge induces changes in the surface chemistry and crystallinity of polylactic acid and polyethylene films. *Science of the Total Environment*, *890*, 164313. https://doi.org/10.1016/j.scitotenv.2023.164313

Chae, Y., & An, Y. J. (2017). Effects of micro- and nanoplastics on aquatic ecosystems: Current research trends and perspectives. *Marine Pollution Bulletin*, *124*(2), 624–632. https://doi.org/10.1016/j.marpolbul.2017.01.070

Chen, H., Tang, M., Yang, X., Tsang, Y. F., Wu, Y., Wang, D., & Zhou, Y. (2021a). Polyamide 6 microplastics facilitate methane production during anaerobic digestion of waste activated sludge. *Chemical Engineering Journal*, *408*, 127251. https://doi.org/10.1016/j.cej.2020.127251

Chen, X., Gu, X., Bao, L., Ma, S., & Mu, Y. (2021b). Comparison of adsorption and desorption of triclosan between microplastics and soil particles. *Chemosphere*, *263*, 127947. https://doi.org/10.1016/j.chemosphere.2020.127947

Chen, X., Liang, J., Bao, L., Gu, X., Zha, S., & Chen, X. (2022). Competitive and

cooperative sorption between triclosan and methyl triclosan on microplastics and soil. *Environmental Research*, *212*, 1–29. https://doi.org/10.1016/j.envres.2022.113548

Chen, X., Ning, X. an, Lai, X., Wang, Y., Zhang, Y., & He, Y. (2021c). Chlorophenols in textile dyeing sludge: Pollution characteristics and environmental risk control. *Journal of Hazardous Materials*, *416*, 125721. https://doi.org/10.1016/j.jhazmat.2021.125721

Çiftçi, G. (2024). *Investigation of the Interaction of Organics with Pristine and Aged Polyethylene: The Case for Trichlorophenol and Tetrachloroethane*. MS Thesis. Middle East Technical University.

Çiftçi, G., Türkeli, Ü. D., Özen, E. Y., Özdemir, M., Sanin, F. D., & Imamoğlu, I. (2023). Microplastics and organics – A comparative study of sorption of triclosan and malachite green onto polyethylene. *Water Science and Technology*, *87*(5), 1072–1081. https://doi.org/10.2166/wst.2023.040

Costigan, E., Collins, A., Hatinoglu, M. D., Bhagat, K., MacRae, J., Perreault, F., & Apul, O. (2022). Adsorption of organic pollutants by microplastics: Overview of a dissonant literature. *Journal of Hazardous Materials Advances*, *6*, 100091. https://doi.org/10.1016/j.hazadv.2022.100091

Cui, W., Hale, R. C., Huang, Y., Zhou, F., Wu, Y., Liang, X., Liu, Y., Tan, H., & Chen, D. (2023). Sorption of representative organic contaminants on microplastics: Effects of chemical physicochemical properties, particle size, and biofilm presence. *Ecotoxicology and Environmental Safety*, *251*, 114533. https://doi.org/10.1016/j.ecoenv.2023.114533

Do, A. T. N., Ha, Y., , Hyun-Joong Kang, J. M. K., & Kwon, J.-H. (2022). Equilibrium leaching of selected ultraviolet stabilizers from plastic products. *Journal of Hazardous Materials*. https://doi.org/10.1016/j.jhazmat.2021.128144

El-Azazy, M., El-Shafie, A. S., & Morsy, H. (2021). Biochar of spent coffee grounds as per se and impregnated with tio2: Promising waste-derived adsorbents for

balofloxacin. *Molecules*, *26*(8). https://doi.org/10.3390/molecules26082295

EPA. (2002). *Nitrification*.

Frost, H., Bond, T., Sizmur, T., & Felipe-Sotelo, M. (2022). A review of microplastic fibres: generation, transport, and vectors for metal(loid)s in terrestrial environments. *Environmental Science: Processes and Impacts*, *24*(4), 504–524. https://doi.org/10.1039/d1em00541c

Fu, L., Li, J., Wang, G., Luan, Y., & Dai, W. (2021). Adsorption behavior of organic pollutants on microplastics. *Ecotoxicology and Environmental Safety*, *217*, 112207. https://doi.org/10.1016/j.ecoenv.2021.112207

Gangadharan Puthiya Veetil, P., Vijaya Nadaraja, A., Bhasi, A., Khan, S., & Bhaskaran, K. (2012). Degradation of triclosan under aerobic, anoxic, and anaerobic conditions. *Applied Biochemistry and Biotechnology*, *167*(6), 1603–1612. https://doi.org/10.1007/s12010-012-9573-3

Gao, P., Ju, C., Tang, Z., & Qin, Y. (2022). Enhanced adsorption of tetracycline on polypropylene and polyethylene microplastics after anaerobically microbial-mediated aging process. *Journal of Hazardous Materials Advances*, *6*, 100075. https://doi.org/10.1016/j.hazadv.2022.100075

Gaston, F., Dupuy, N., Marque, S. R. A., Barbaroux, M., & Dorey, S. (2016). One year monitoring by FTIR of γ-irradiated multilayer film PE/EVOH/PE. *Radiation Physics and Chemistry*, *125*, 115–121. https://doi.org/10.1016/j.radphyschem.2016.03.010

Grause, G., Chien, M. F., & Inoue, C. (2020). Changes during the weathering of polyolefins. *Polymer Degradation and Stability*, *181*, 109364. https://doi.org/10.1016/j.polymdegradstab.2020.109364

Hameed, B. H., & El-Khaiary, M. I. (2008). Batch removal of malachite green from aqueous solutions by adsorption on oil palm trunk fibre: Equilibrium isotherms and kinetic studies. *Journal of Hazardous Materials*, *154*(1–3), 237–244. https://doi.org/10.1016/j.jhazmat.2007.10.017

Hatinoglu, D., Adan, A., Perreault, F., Imamoglu, I., & Apul, O. G. (2023). Linear solvation energy relationships for adsorption of aromatic organic compounds by microplastics. *Chemical Engineering Science*, *282*(August), 119233. https://doi.org/10.1016/j.ces.2023.119233

Hatinoğlu, M. D., & Sanin, F. D. (2022). Fate and effects of polyethylene terephthalate (PET) microplastics during anaerobic digestion of alkaline-thermal pretreated sludge. *Waste Management*, *153*, 376–385. https://doi.org/10.1016/j.wasman.2022.09.016

He, S., Tong, J., Xiong, W., Xiang, Y., Peng, H., Wang, W., Yang, Y., Ye, Y., Hu, M., Yang, Z., & Zeng, G. (2023). Microplastics influence the fate of antibiotics in freshwater environments: Biofilm formation and its effect on adsorption behavior. *Journal of Hazardous Materials*, *442*, 130078. https://doi.org/10.1016/j.jhazmat.2022.130078

Higgins, C. P., Paesani, Z. J., Abbott Chalew, T. E., Halden, R. U., & Hundal, L. S. (2011). Persistence of triclocarban and triclosan in soils after land application of biosolids and bioaccumulation in Eisenia foetida. *Environmental Toxicology and Chemistry*, *30*(3), 556–563. https://doi.org/10.1002/etc.416

Ho, W. K., Law, J. C. F., Zhang, T., & Leung, K. S. Y. (2020). Effects of Weathering on the Sorption Behavior and Toxicity of Polystyrene Microplastics in Multi-solute Systems. *Water Research*, *187*, 116419. https://doi.org/10.1016/j.watres.2020.116419

Holliger, C., Alves, M., Andrade, D., Angelidaki, I., Astals, S., Baier, U., Bougrier, C., Buffière, P., Carballa, M., De Wilde, V., Ebertseder, F., Fernández, B., Ficara, E., Fotidis, I., Frigon, J. C., De Laclos, H. F., Ghasimi, D. S. M., Hack, G., Hartel, M., … Wierinck, I. (2016). Towards a standardization of biomethane potential tests. *Water Science and Technology*, *74*(11), 2515–2522. https://doi.org/10.2166/wst.2016.336

Holliger, C., de Laclos, H. F., & Hack, G. (2017). Methane production of full-scale anaerobic digestion plants calculated from substrate's biomethane potentials

compares well with the one measured on-site. *Frontiers in Energy Research*, *5*, 1–9. https://doi.org/10.3389/fenrg.2017.00012

Hüffer, T., & Hofmann, T. (2016). Sorption of non-polar organic compounds by micro-sized plastic particles in aqueous solution. *Environmental Pollution*, *214*, 194–201. https://doi.org/10.1016/j.envpol.2016.04.018

Hummel, D., Fath, A., Hofmann, T., & Hüffer, T. (2021). Additives and polymer composition influence the interaction of microplastics with xenobiotics. *Environmental Chemistry*, *18*(3), 101–110. https://doi.org/10.1071/EN21030

Istomina, A., Chelomin, V., Mazur, A., Zhukovskaya, A., Karpenko, A., & Mazur, M. (2024). Biodegradation of polyethylene in digestive gland homogenates of marine invertebrates. *PeerJ*, *12*. https://doi.org/10.7717/peerj.17041

Jemec Kokalj, A., Kuehnel, D., Puntar, B., Žgajnar Gotvajn, A., & Kalčikova, G. (2019). An exploratory ecotoxicity study of primary microplastics versus aged in natural waters and wastewaters. *Environmental Pollution*, *254*. https://doi.org/10.1016/j.envpol.2019.112980

Jiang, N., Shang, R., Heijman, S. G. J., & Rietveld, L. C. (2020). Adsorption of triclosan, trichlorophenol and phenol by high-silica zeolites: Adsorption efficiencies and mechanisms. *Separation and Purification Technology*, *235*, 1–9. https://doi.org/10.1016/j.seppur.2019.116152

Jih-Gaw, L., Ying-Shih, M., Chao, A. C., & Huang, C. L. (1999). BMP test on chemically pretreated sludge. *Bioresource Technology*, *68*(2), 187–192. https://doi.org/10.1016/S0960-8524(98)00126-6

Jirka, A. M., & Carter, M. J. (1975). Micro Semi-Automated Analysis of Surface and Waste Waters for Chemical Oxygen Demand. *Analytical Chemistry*, *47*(8), 1397–1402. https://doi.org/10.1021/ac60358a004

Karapanagioti, H. K., & Werner, D. (2019). Sorption of Hydrophobic Organic Compounds to Plastics in the Marine Environment: Sorption and Desorption Kinetics. *Handbook of Environmental Chemistry*, *78*, 205–219.

https://doi.org/10.1007/698_2018_256

Kumar Sen, S., & Raut, S. (2015). Microbial degradation of low density polyethylene (LDPE): A review. *Journal of Environmental Chemical Engineering*, *3*(1), 462–473. https://doi.org/10.1016/j.jece.2015.01.003

L. Metcalf, H.P. Eddy, G. T. (2004). *Wastewater engineering : treatment, disposal, and reuse* (4th ed.). McGraw-Hill.

Lee, Y. C., Kim, J. Y., & Shin, H. J. (2013). Removal of Malachite Green (MG) From Aqueous Solutions by Adsorption, Precipitation, and Alkaline Fading Using Talc. *Separation Science and Technology (Philadelphia)*, *48*(7), 1093–1101. https://doi.org/10.1080/01496395.2012.723100

Lessa Belone, M. C., Brosens, D., Kokko, M., & Sarlin, E. (2024). Effects of mesophilic and thermophilic anaerobic digestion of sewage sludge on different polymers: Perspectives on the potential of the treatment to degrade microplastics. *Science of the Total Environment*, *907*, 168014. https://doi.org/10.1016/j.scitotenv.2023.168014

Li, L., Geng, S., Li, Z., & Song, K. (2020). Effect of microplastic on anaerobic digestion of wasted activated sludge. *Chemosphere*, *247*. https://doi.org/10.1016/j.chemosphere.2020.125874

Li, X., Mei, Q., Chen, L., Zhang, H., Dong, B., Dai, X., He, C., & Zhou, J. (2019a). Enhancement in adsorption potential of microplastics in sewage sludge for metal pollutants after the wastewater treatment process. *Water Research*, *157*, 228–237. https://doi.org/10.1016/j.watres.2019.03.069

Li, Y., Li, M., Li, Z., Yang, L., & Liu, X. (2019b). Effects of particle size and solution chemistry on Triclosan sorption on polystyrene microplastic. *Chemosphere*, *231*, 308–314. https://doi.org/10.1016/j.chemosphere.2019.05.116

Li, Y., Li, X., Wang, P., Su, Y., & Xie, B. (2022). *Size-dependent effects of polystyrene microplastics on anaerobic digestion performance of food waste :*

Focusing on oxidative stress , microbial community , key metabolic functions. *438*, 0–3. https://doi.org/10.1016/j.jhazmat.2022.129493

Lim, J. W., Ting, D. W. Q., Loh, K. C., Ge, T., & Tong, Y. W. (2018). Effects of disposable plastics and wooden chopsticks on the anaerobic digestion of food waste. *Waste Management*, *79*, 607–614. https://doi.org/10.1016/j.wasman.2018.08.033

Lin, L., Tang, S., Wang, X., Sun, X., & Yu, A. (2021). Hexabromocyclododecane alters malachite green and lead(II) adsorption behaviors onto polystyrene microplastics: Interaction mechanism and competitive effect. *Chemosphere*, *265*, 129079. https://doi.org/10.1016/j.chemosphere.2020.129079

Ling, Y. Y., & Mohd Suah, F. B. (2017). Extraction of malachite green from wastewater by using polymer inclusion membrane. *Journal of Environmental Chemical Engineering*, *5*(1), 785–794. https://doi.org/10.1016/j.jece.2017.01.001

Liu, L., Xu, M., Ye, Y., & Zhang, B. (2022a). On the degradation of (micro)plastics: Degradation methods, influencing factors, environmental impacts. *Science of the Total Environment*, *806*, 151312. https://doi.org/10.1016/j.scitotenv.2021.151312

Liu, X., Deng, Q., Zheng, Y., Wang, D., & Ni, B. J. (2022b). Microplastics aging in wastewater treatment plants: Focusing on physicochemical characteristics changes and corresponding environmental risks. *Water Research*, *221*, 118780. https://doi.org/10.1016/j.watres.2022.118780

Lončarsk, M., Tubic, A., Isakovski, M. K., Jovic, B., Apostolovic, T., Nikic, J., & Agbaba, J. (2020). Modelling of the adsorption of chlorinated phenols on polyethylene and polyethylene terephthalate microplastic. *Journal of the Serbian Chemical Society*, *85*(5), 697–709. https://doi.org/10.2298/JSC190712124L

Lu, Q., Zhou, Y., Sui, Q., & Zhou, Y. (2023). Mechanism and characterization of microplastic aging process: A review. *Frontiers of Environmental Science and*

Engineering, *17*(8), 1–19. https://doi.org/10.1007/s11783-023-1700-6

Ma, J., Zhao, J., Zhu, Z., Li, L., & Yu, F. (2019). Effect of microplastic size on the adsorption behavior and mechanism of triclosan on polyvinyl chloride. *Environmental Pollution*, *254*, 113104. https://doi.org/10.1016/j.envpol.2019.113104

Ma, Y., Wu, S., Xu, Y., Zhou, X., & Ruan, A. (2023). Degradation characteristics of polyethylene film by microorganisms from lake sediments. *Environmental Pollution*, *333*, 122115. https://doi.org/10.1016/j.envpol.2023.122115

Martín, J., Santos, J. L., Aparicio, I., & Alonso, E. (2022). Microplastics and associated emerging contaminants in the environment: analysis, sorption mechanisms and effects of co-exposure. *Trends in Environmental Analytical Chemistry*, *35*, e00170. https://doi.org/10.1016/j.teac.2022.e00170

Martínez-Romo, A., González-Mota, R., Soto-Bernal, J. J., & Rosales-Candelas, I. (2015). Investigating the Degradability of HDPE, LDPE, PE-BIO, and PE-OXO Films under UV-B Radiation. *Journal of Spectroscopy*, *2015*. https://doi.org/10.1155/2015/586514

Mo, Q., Yang, X., Wang, J., Xu, H., Li, W., Fan, Q., Gao, S., Yang, W., Gao, C., Liao, D., Li, Y., & Zhang, Y. (2021). Adsorption mechanism of two pesticides on polyethylene and polypropylene microplastics: DFT calculations and particle size effects. *Environmental Pollution*, *291*, 118120. https://doi.org/10.1016/j.envpol.2021.118120

Moore, H. R. (1970). *The effects of pH on aerobic sludge digestion. Master thesis*.

National Center for Biotechnology Information. (2024a). *PubChem Compound Summary for CID 13618, 2,3,6-Trichlorophenol*. https://pubchem.ncbi.nlm.nih.gov/compound/13618

National Center for Biotechnology Information. (2024b). *PubChem Compound Summary for CID 2724411, Malachite Green Oxalate*.

National Center for Biotechnology Information. (2024c). *PubChem Compound*

Summary for CID 5564, Triclosan. https://pubchem.ncbi.nlm.nih.gov/compound/Triclosan

Owen, W. F., Stuckev, D. C., Healv, J. B., Young, L. Y., & Mccagrv, P. L. (1979). *Bioassay for monitoring biochemical methane potential and anaerobic toxicity*. *13*(5).

Oxalate, M. G. (2012). Malachite Green Oxalate 2437-29-8. *Sax's Dangerous Properties of Industrial Materials*, 1–2. https://doi.org/10.1002/0471701343.sdp41620

Patel, R. M. (2016). Polyethylene. *Multilayer Flexible Packaging: Second Edition*, 17–34. https://doi.org/10.1016/B978-0-323-37100-1.00002-8

Phan, S., Padilla-Gamiño, J. L., & Luscombe, C. K. (2022). The effect of weathering environments on microplastic chemical identification with Raman and IR spectroscopy: Part I. polyethylene and polypropylene. *Polymer Testing*, *116*. https://doi.org/10.1016/j.polymertesting.2022.107752

Pinto, M., Zhao, Z., Klun, K., Libowitzky, E., & Herndl, G. J. (2022). Microbial Consortiums of Putative Degraders of Low-Density Polyethylene-Associated Compounds in the Ocean. *MSystems*, *7*(2). https://doi.org/10.1128/msystems.01415-21

Priyanka, M., & Saravanakumar, M. P. (2022). New insights on aging mechanism of microplastics using PARAFAC analysis: Impact on 4-nitrophenol removal via Statistical Physics Interpretation. *Science of the Total Environment*, *807*, 150819. https://doi.org/10.1016/j.scitotenv.2021.150819

Puckowski, A., Cwięk, W., Mioduszewska, K., Stepnowski, P., & Białk-Bielińska, A. (2021). Sorption of pharmaceuticals on the surface of microplastics. *Chemosphere*, *263*. https://doi.org/10.1016/j.chemosphere.2020.127976

Raposo, F., De La Rubia, M. A., Fernández-Cegrí, V., & Borja, R. (2012). Anaerobic digestion of solid organic substrates in batch mode: An overview relating to methane yields and experimental procedures. *Renewable and Sustainable*

Energy Reviews, *16*(1), 861–877. https://doi.org/10.1016/j.rser.2011.09.008

Rashed, M., Mamun, A., Mamun, A. L., & Torii, S. (2015). Possibility of Anaerobic Co-digestion of Cafeteria, Vegetable and Fruit Wastes for Biogas Production without Inoculum. *International Journal of Renewable Energy and Environmental Engineering*, *03*(04), 219–225. https://www.researchgate.net/publication/313440505

Road, S., & Lincolnshire, N. (2014). *SeaQuantum X200 - 2 (UK) SECTION 1 : Identification of the substance / mixture and of the company / SECTION 2 : Hazards identification SECTION 2 : Hazards identification*. *2006*(1907), 1–15.

Rochman, C. M., Hoh, E., Hentschel, B. T., & Kaye, S. (2013). Long-term field measurement of sorption of organic contaminants to five types of plastic pellets: Implications for plastic marine debris. *Environmental Science and Technology*, *47*(3), 1646–1654. https://doi.org/10.1021/es303700s

Ronca, S. (2017). Polyethylene. In *Brydson's Plastics Materials: Eighth Edition* (Issue 1930). Elsevier Ltd. https://doi.org/10.1016/B978-0-323-35824-8.00010-4

Roš, M., & Zupančič, G. D. (2002). Thermophilic aerobic digestion of waste activated sludge. *Acta Chimica Slovenica*, *49*(4), 931–943.

Sam, S. T., Nuradibah, M. A., Ismail, H., Noriman, N. Z., & Ragunathan, S. (2014). Recent Advances in Polyolefins/Natural Polymer Blends Used for Packaging Application. *Polymer - Plastics Technology and Engineering*, *53*(6), 631–644. https://doi.org/10.1080/03602559.2013.866247

Sertchook, H., Elimelech, H., Makarov, C., Khalfin, R., Cohen, Y., Shuster, M., Babonneau, F., & Avnir, D. (2007). Composite particles of polyethylene @ silica. *Journal of the American Chemical Society*, *129*(1), 98–108. https://doi.org/10.1021/ja0653167

Sheng, C., Zhang, S., & Zhang, Y. (2021). The influence of different polymer types of microplastics on adsorption, accumulation, and toxicity of triclosan in

zebrafish. *Journal of Hazardous Materials*, *402*, 123733. https://doi.org/10.1016/j.jhazmat.2020.123733

Shi, J., Dang, Q., Zhang, C., & Zhao, X. (2022a). Insight into effects of polyethylene microplastics in anaerobic digestion systems of waste activated sludge: Interactions of digestion performance, microbial communities and antibiotic resistance genes. *Environmental Pollution*, *310*, 119859. https://doi.org/10.1016/j.envpol.2022.119859

Shi, K., Zhang, H., Xu, H. M., Liu, Z., Kan, G., Yu, K., & Jiang, J. (2022b). Adsorption behaviors of triclosan by non-biodegradable and biodegradable microplastics: Kinetics and mechanism. *Science of the Total Environment*, *842*, 156832. https://doi.org/10.1016/j.scitotenv.2022.156832

Siddiqa, A. J., Chaudhury, K., & Adhikari, B. (2014). Letrozole dispersed on poly (vinyl alcohol) anchored maleic anhydride grafted low density polyethylene: A controlled drug delivery system for treatment of breast cancer. *Colloids and Surfaces B: Biointerfaces*, *116*, 169–175. https://doi.org/10.1016/j.colsurfb.2013.12.040

Şimşek, İ. (2023). *Fate and effect of polyamide microplastics during anaerobic digestion process of sludge*. MS Thesis. Middle East Technical University.

Singh, A., & Kaur, I. (2023). Remediation of triclosan contaminated water - A comprehensive reprint. *Journal of Water Process Engineering*, *55*, 104149. https://doi.org/10.1016/j.jwpe.2023.104149

Speece, R. E. (1996). *Anaerobic Biotechnology For Industrial Wastewaters* (J. M. Speece (ed.)). Archae Press.

Sudhakar, M., Doble, M., Murthy, P. S., & Venkatesan, R. (2008). Marine microbe-mediated biodegradation of low- and high-density polyethylenes. *International Biodeterioration and Biodegradation*, *61*(3), 203–213. https://doi.org/10.1016/j.ibiod.2007.07.011

Sun, Y., Wang, L., & Liu, H. (2012). Myoglobin functioning as cytochrome P450

for biosensing of 2,4-dichlorophenol. *Analytical Methods*, *4*(10), 3358–3363. https://doi.org/10.1039/c2ay25574j

Takada, H. (2019). Hazardous Chemicals Associated with Plastics in the Marine Environment. In *The Handbook of Environmental Chemistry (Springer Nature)* (Vol. 78).

Tang, M., Zhou, S., Huang, J., Sun, L., & Lu, H. (2022). Stress responses of sulfate-reducing bacteria sludge upon exposure to polyethylene microplastics. *Water Research*, *220*, 118646. https://doi.org/10.1016/j.watres.2022.118646

Tong, H., Hu, X., Zhong, X., & Jiang, Q. (2021). Adsorption and Desorption of Triclosan on Biodegradable Polyhydroxybutyrate Microplastics. *Environmental Toxicology and Chemistry*, *40*(1), 72–78. https://doi.org/10.1002/etc.4902

Trzcinski, A. P., & Stuckey, D. C. (2012). Determination of the hydrolysis constant in the biochemical methane potential test of municipal solid waste. *Environmental Engineering Science*, *29*(9), 848–854. https://doi.org/10.1089/ees.2011.0105

Tsai, C. Y., Lin, P. Y., Hsieh, S. L., Kirankumar, R., Patel, A. K., Singhania, R. R., Dong, C. Di, Chen, C. W., & Hsieh, S. (2022). Engineered mesoporous biochar derived from rice husk for efficient removal of malachite green from wastewaters. *Bioresource Technology*, *347*, 126749. https://doi.org/10.1016/j.biortech.2022.126749

Tu, C., Chen, T., Zhou, Q., Liu, Y., Wei, J., Waniek, J. J., & Luo, Y. (2020). Biofilm formation and its influences on the properties of microplastics as affected by exposure time and depth in the seawater. *Science of the Total Environment*, *734*. https://doi.org/10.1016/j.scitotenv.2020.139237

Tubić, A., Lončarski, M., Maletić, S., Jazić, J. M., Watson, M., Tričković, J., & Agbaba, J. (2019). Significance of chlorinated phenols adsorption on plastics and bioplastics during water treatment. *Water (Switzerland)*, *11*(11). https://doi.org/10.3390/w11112358

Tyagi, V. K., Lo, S. L., Campoy, R. A., Álvarez-Gallego, C. J., Romero García, L. I., Sun, L. P., & Qiu, C. S. (2014). Sono-biostimulation of aerobic digestion: A novel approach for sludge minimization. *Journal of Chemical Technology and Biotechnology*, *89*(7), 1060–1066. https://doi.org/10.1002/jctb.4202

USEPA. (2016). *Definition and Procedure for the Determination of the Method Detection Limit*.

Verdú, I., Amariei, G., Rueda-Varela, C., González-Pleiter, M., Leganés, F., Rosal, R., & Fernández-Piñas, F. (2023). Biofilm formation strongly influences the vector transport of triclosan-loaded polyethylene microplastics. *Science of the Total Environment*, *859*. https://doi.org/10.1016/j.scitotenv.2022.160231

Verdú, I., González-Pleiter, M., Leganés, F., Rosal, R., & Fernández-Piñas, F. (2021). Microplastics can act as vector of the biocide triclosan exerting damage to freshwater microalgae. *Chemosphere*, *266*. https://doi.org/10.1016/j.chemosphere.2020.129193

Wang, D., He, D., Liu, X., Xu, Q., Yang, Q., Li, X., Liu, Y., Wang, Q., Ni, B. J., & Li, H. (2019). The underlying mechanism of calcium peroxide pretreatment enhancing methane production from anaerobic digestion of waste activated sludge. *Water Research*, *164*, 114934. https://doi.org/10.1016/j.watres.2019.114934

Wang, S., Wang, X., Fessler, M., Jin, B., Su, Y., & Zhang, Y. (2022a). Insights into the impact of polyethylene microplastics on methane recovery from wastewater via bioelectrochemical anaerobic digestion. *Water Research, 221,* 118844. https://doi.org/10.1016/j.watres.2022.118844

Wang, X., Andrade, N., Shekarchi, J., Fischer, S. J., Torrents, A., & Ramirez, M. (2018). Full scale study of Class A biosolids produced by thermal hydrolysis pretreatment and anaerobic digestion. *Waste Management, 78,* 43–50. https://doi.org/10.1016/j.wasman.2018.05.026

Wang, X., Zhang, Y., Zhao, Y., Zhang, L., & Zhang, X. (2023). Inhibition of aged microplastics and leachates on methane production from anaerobic digestion of

sludge and identification of key components. *Journal of Hazardous Materials*, *446*, 130717. https://doi.org/10.1016/j.jhazmat.2022.130717

Wang, Y., Ding, K., Ren, L., Peng, A., & Zhou, S. (2022b). Biodegradable Microplastics: A Review on the Interaction with Pollutants and Influence to Organisms. *Bulletin of Environmental Contamination and Toxicology*, *108*(6), 1006–1012. https://doi.org/10.1007/s00128-022-03486-7

Wang, Y., Wang, X., Li, Y., Li, J., Wang, F., Xia, S., & Zhao, J. (2020). Biofilm alters tetracycline and copper adsorption behaviors onto polyethylene microplastics. *Chemical Engineering Journal*, *392*, 123808. https://doi.org/10.1016/j.cej.2019.123808

Wei, W., Chen, X., Peng, L., Liu, Y., Bao, T., & Ni, B. J. (2021). The entering of polyethylene terephthalate microplastics into biological wastewater treatment system affects aerobic sludge digestion differently from their direct entering into sludge treatment system. *Water Research*, *190*, 116731. https://doi.org/10.1016/j.watres.2020.116731

Wei, W., Huang, Q. S., Sun, J., Dai, X., & Ni, B. J. (2019). Revealing the Mechanisms of Polyethylene Microplastics Affecting Anaerobic Digestion of Waste Activated Sludge. *Environmental Science and Technology*, *53*(16), 9604–9613. https://doi.org/10.1021/acs.est.9b02971

Wu, X., Liu, P., Huang, H., & Gao, S. (2020). Adsorption of triclosan onto different aged polypropylene microplastics: Critical effect of cations. *Science of the Total Environment*, *717*, 137033. https://doi.org/10.1016/j.scitotenv.2020.137033

Xu, B., & Ghossein, R. A. (2018). The contribution of molecular pathology to the classification of thyroid tumors. *Diagnostic Histopathology*, *24*(3), 87–94. https://doi.org/10.1016/j.mpdhp.2018.02.001

Zafar, R., Bang, T. H., Lee, Y. K., Begum, M. S., Rabani, I., Hong, S., & Hur, J. (2022). Change in adsorption behavior of aquatic humic substances on microplastic through biotic and abiotic aging processes. *Science of The Total Environment*, *843*, 157010. https://doi.org/10.1016/j.scitotenv.2022.157010

Zaman, N. Q. (2010). the Applicability of Batch Tests To Assess Biomethanation Potential of Organic Waste and Assess Scale Up To Continuous Reactor Systems. *PhD Thesis*, 293.

Zhang, Q., Fan, D., Pang, X., Zhu, W., Zhao, J., & Xu, J. (2021a). Effects of polyethylene microplastics on the fate of antibiotic resistance genes and microbial communities in anaerobic digestion of dairy wastes. *Journal of Cleaner Production*, *292*, 125909. https://doi.org/10.1016/j.jclepro.2021.125909

Zhang, Z., Liu, H., Wen, H., Gao, L., Gong, Y., Guo, W., Wang, Z., Li, X., & Wang, Q. (2021b). Microplastics deteriorate the removal efficiency of antibiotic resistance genes during aerobic sludge digestion. *Science of the Total Environment*, *798*, 149344. https://doi.org/10.1016/j.scitotenv.2021.149344

Zhong, Y., Wang, K., Guo, C., Kou, Y., Hassan, A., Lu, Y., Wang, J., & Wang, W. (2022). Competition adsorption of malachite green and rhodamine B on polyethylene and polyvinyl chloride microplastics in aqueous environment. *Water Science and Technology*, *86*(5), 894–908. https://doi.org/10.2166/wst.2022.252

Zhou, Q., Tu, C., Liu, Y., Li, Y., Zhang, H., Vogts, A., Plewe, S., Pan, X., Luo, Y., & Waniek, J. J. (2022). Biofilm enhances the copper (II) adsorption on microplastic surfaces in coastal seawater: Simultaneous evidence from visualization and quantification. *Science of the Total Environment*, *853*, 158217. https://doi.org/10.1016/j.scitotenv.2022.158217

APPENDICES

A. Bio-aging of Polyethylene During Anaerobic and Aerobic Digestion

A.1 Summary Description of Reactors and MPs

Table A.1 Summary description of reactors and MPs of this study.

Reactor Notation	Type of PE	Type of Bio-Aging	Description
HB	HDPE	Anaerobic Digestion	Biotic BMP test reactor containing HDPE
HB0	None	Anaerobic Digestion	Biotic BMP control reactor (HDPE Set-up)
HA	HDPE	Anaerobic Digestion (Sterilized seed)	Abiotic BMP test reactor containing HDPE
HA0	None	Anaerobic Digestion (Sterilized seed)	Abiotic BMP control reactor
HS0	None	Seed Control (HDPE Set-up)	Biotic BMP seed control reactor (HDPE Set-up)
HO	HDPE	Aerobic Digestion	Aerobic test reactor containing HDPE
HP	HDPE	None	Pristine HDPE
HPW	HDPE	None	Pristine HDPE-H_2O_2 Washed
HBW	HDPE	Anaerobic Digestion	Bio-aged HDPE- H_2O_2 Washed
HAW	HDPE	Anaerobic Digestion	Bio-aged HDPE- H_2O_2 Washed
HOW	HDPE	Aerobic Digestion	Bio-aged HDPE- H_2O_2 Washed
LB	LDPE	Anaerobic Digestion	Biotic BMP test reactor containing LDPE
LB0	None	Anaerobic Digestion	Biotic BMP control reactor (LDPE Set-up)
LS0	None	Anaerobic Digestion	Biotic BMP seed control reactor (LDPE Set-up)
LO	LDPE	Aerobic Digestion	Aerobic test reactor containing LDPE
LP	LDPE	None	Pristine LDPE
LPW	LDPE	None	Pristine LDPE-H_2O_2 Washed
LBW	LDPE	Anaerobic Digestion	Bio-aged LDPE- H_2O_2 Washed
LOW	LDPE	Aerobic Digestion	Bio-aged LDPE- H_2O_2 Washed

A.2 Equations Used in Kinetics Computations of BMP Reactors

Hydrolysis rate (k) and biochemical CH_4 potential (B_0) were calculated using a first-order kinetic and a sum of squared errors. Equation A.1 was utilized to compute the degree of WAS degradation (Y_0). To determine k and B_0, a one-substrate model is used in conjunction with the first-order kinetic model (Equation A.2). The objective function utilized for parameter estimation involved minimizing the residual sum of squared (SSR) errors (Batstone et al., 2009).

$$Y_0 = \frac{B_0}{380} \times RSS$$ Equation A.1

Y_0: Apparent VS destruction

B_0: Biochemical CH_4 potential (L CH_4/kg VS added)

The maximum theoretical methane potential of sludge at standard temperature and pressure (STP, 25 °C, 1 atm) is represented by 380 (L CH_4/kg tCOD)

RSS: VS/tCOD ratio of the WAS

$$B_t = B_0(1 - e^{-kt})$$ Equation A.2

B_t: Cumulative CH_4 yield (L CH_4/kg VS added) at time t

t: Time (day)

A.3 Equations Used to Calculate Carbonyl Index and Crystallinity

CI was calculated using the specific area under band method (SAUB) method (Equation A.3) (Almond et al., 2020), as well as keto CI, ester CI, vinyl bond index, and internal double bond index (Equation A.4 - Equation A.8) (Artham et al., 2009; Sudhakar et al., 2008).

$$Carbonyl\ index\ (CI) = \frac{Area\ under\ band\ 1850 - 1650\ cm^{-1}}{Area\ under\ band\ 1500 - 1420\ cm^{-1}}$$ Equation A.3

$$Keto\ CI = \frac{I_{1715}}{I_{1465}}$$ Equation A.4

Ester $CI = \frac{I_{1740}}{I_{1465}}$ Equation A.5

$$Vinyl\ bond\ index = \frac{I_{1640}}{I_{1465}}$$ Equation A.6

$$Internal\ double\ bond\ index = \frac{I_{908}}{I_{1465}}$$ Equation A.7

$$Xc = \left(\frac{\Delta H_f}{\Delta H_f^c}\right) \times 100$$ Equation A.8

ΔH_f: Heat of fusion of the PE samples as determined by DSC analysis,

ΔH_f^c: Heat of fusion of the extrapolated 100% crystalline PE (ΔH_f^c = 293 J/g) (Sertchook et al., 2007).

A.4 Average Cumulative Methane Production in BMPs

Notably in Figure A.1, biogas and CH_4 production commenced from day one without any lag or transition period, with consistent trends and rates observed across all reactor sets over the designated time intervals. In the HDPE set-up, after 27 days, the daily proportion of biogas and CH_4 for all sets decreased to approximately 2%. Consequently, biogas and CH_4 measurements were conducted every other day thereafter. Biotic control reactors exhibited a gradual decrease in biogas content, reaching approximately 1.6% by day 41. However, biotic reactors with HDPE presence maintained biogas content above 2% until termination (day 50). For LDPE set-up 1 and set-up 2, the overall daily proportion of biogas and CH_4 for all sets decreased to about 2% after 15 and 20 days, respectively. Despite dropping to 1% of the total gas after 41 and 39 days for set-up 1 and set-up 2, respectively, reactors were not terminated as suggested by Holliger et al. (2017), instead kept in reactors allowing a longer time for bio-aging.

In the initial days of monitoring, the predominant gas detected in the reactors was N_2. This occurrence can be attributed to the utilization of N_2 gas during the setup phase to purge the reactors. However, as CH_4 production commenced on the first day, there was a notable decrease in N_2 content, accompanied by a rise in CH_4 and

carbon dioxide (CO_2) levels, ultimately dominating the headspace of biotic reactors. Across all biotic reactors, CH_4 content exhibited an increase from the first day to approximately 60% during the initial measurements, subsequently stabilizing at 50-55% for the duration of the observation period until termination day.

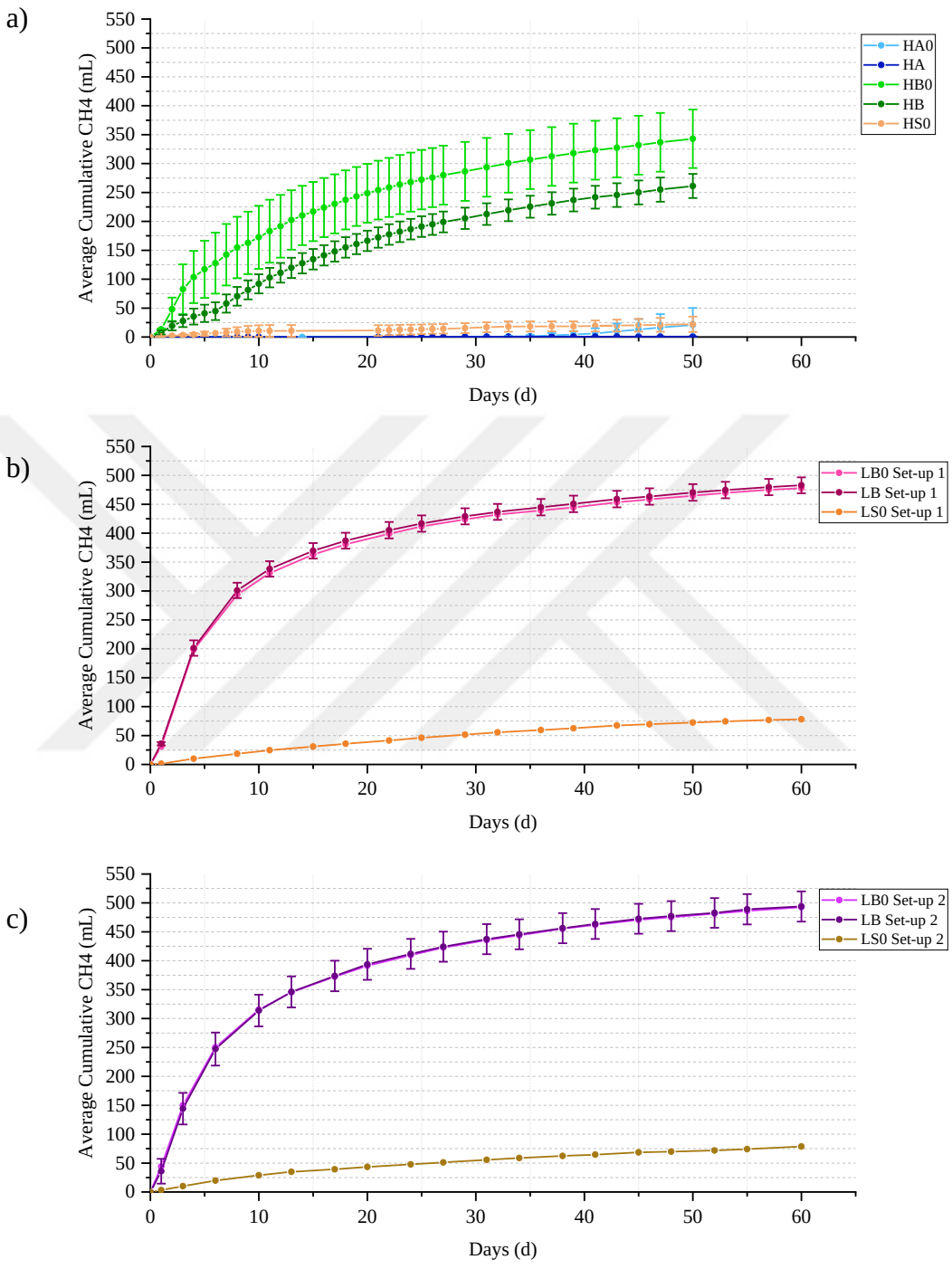

Figure A.1 Average cumulative methane of a) HDPE set-up, b) LDPE set-up 1, and c) LDPE set-up 2.

A.5 Kinetics Results of BMPs

Table A.2 Kinetic results of BMP reactors for each set-up.

	Reactor Set	B_0 (mL CH_4/g VS added)	k (day^{-1})	R^2	Y_0
HDPE Set-up	HB0	268.2	0.072	0.996	0.359
	HB	246.9	0.036	0.996	0.330
LDPE Set-up 1	LB0-1	286.2	0.143	0.993	0.427
	LB-1	289.9	0.147	0.994	0.432
LDPE Set-up 2	LB0-2	316.7	0.122	0.993	0.473
	LB-2	318.9	0.118	0.994	0.477

Table A.3 Carbonyl index (CI) values* and additional peaks observed of HDPE and LDPE MPs before and after bio-aging as obtained from FTIR analysis.

Set-up	Sample Condition	Label	CI (SAUB)	Keto CI (I_{1715}/I_{1465})	Ester CI (I_{1740}/I_{1465})	Vinyl bond index (I_{1640}/I_{1465})	Internal double bond index (I_{908}/I_{1465})
HDPE	Pristine	HP	0.022±0.022	0.052±0.045	0	0	0.025±0.043
	Pristine Washed	HPW	0	0	0	0	0.159±0.041
HDPE Bio-aged	Abiotic Washed	HAW	0.007±0.013	0.010±0.017	0.004±0.006	0	0
	BMP Washed	HBW	0	0.005±0.008	0	0.016±0.012	0
	Aerobic Washed	HOW	0	0	0	0.029±0.010	0.010±0.018
LDPE	Pristine	LP	0.012±0.014	0.023±0.039	0	0	0.058±0.025
	Pristine Washed	LPW	0.042±0.012	0.050±0.009	0	0.042±0.008	0.033±0.001
LDPE Bio-aged Set-up 1	BMP Washed	LBW-1	0.100±0.007	0.099±0.024	0	0.075±0.024	0.061±0.029
	Aerobic Washed	LOW-1	0.078±0.006	0.073±0.003	0	0.055±0.006	0.036±0.005
Bio-aged Set-up 2	BMP Washed	LBW-2	0.019±0.018	0.064±0.038	0	0.078±0.034	0.079±0.045
	Aerobic Washed	LOW-2	0.118±0.029	0.089±0.014	0	0.062±0.009	0.029±0.004

*Calculation of carbonyl as well as other indices are provided in text S3

A.7 DSC Results of PE Before and After Bio-aging

Results from the 1st heating cycle reflect the material's state post-weathering, consequently, it was used for crystallinity calculations. The subsequent heating illustrates the polymer's pure material state after the elimination of its prior history unaffected by processing, therefore it was not used for MPs characterization in this study (Grause et al., 2020).

Table A.4 DSC results for pristine and bio-aged MPs obtained in this study.

	MP Type	ΔHf, (J/g)	Crystallinity (%)	Tm (°C)
HDPE	HP	151.22	51.61	126.78
	HPW	159.97	54.60	122.35
	HBW	155.91	53.21	123.08
	HOW	160.84	54.89	125.50
LDPE	LP #1	103.98	35.49	102.62
	LP #2	110.43	37.69	106.24
	LPW #1	100.67	34.36	106.15
	LPW #2	110.60	37.75	106.36
LDPE Set-up 1	LBW-1 # 1	109.32	37.31	103.91
	LBW-1 #2	115.87	39.55	105.78
	LOW-1 #1	109.72	37.45	103.52
	LOW-1 #2	112.11	38.26	106.32
LDPE Set-up 2	LBW-2 #1	110.70	37.78	106.11
	LBW-2 #2	115.16	39.30	105.73
	LOW-2 #1	113.84	38.85	105.97
	LOW-2 #2	111.60	38.09	105.43

Tm: Melting Temperature, ΔHf: Heat of fusion, Tc: Crystallization Temperature
H: HDPE MPs Type, L: LDPE MPs Type
P: Pristine, PW: Pristine - H_2O_2 washed
BW: Anaerobic bio-aged - H_2O_2washed, OW: Aerobic bio-aged - H_2O_2washed

B. The Effect of Bio-Aged Polyethylene on The Sorption Potential of Trichlorophenol and Triclosan

B.1 Characteristics of PE

Table B.1 Characteristics of pristine and bio-aged HDPE and LDPE used in sorption studies.

	MPs Type	Label	Melting Temperature (T_m, °C)	Crystallinity (%)	Carbonyl Index (CI)*
Pristine	HDPE	HP	126.78	51.6	0.022±0.022
	LDPE	LP	102.62	35.5	0.012±0.014
H2O2 Washed Pristine	HDPE	HPW	122.35	54.6	0.000
	LDPE	LPW	106.15	36.4	0.042±0.012
Anaerobic bio-aged	HDPE	HBW	123.08	53.2	0.000
	LDPE	LBW	103.91-106.11	38.5±1.1	0.019±0.018-0.100±0.007
Aerobic bio-aged	HDPE	HOW	125.50	54.9	0.000
	LDPE	LOW	103.52-106.32	38.2±0.6	0.078±0.006-0.118±0.029

*CI was calculated using SAUB method (Almond et al., 2020)

B.2 Physiochemical Properties of OCs

Table B.2 Physical and Chemical Properties of OCs used in this study.

Common Name	2,3,6-Trichlorophenol (TCP)	Triclosan (TCS)
IUPAC Name	2,3,6-trichlorophenol	5-Chloro-2-(2,4-Dichlorophenoxy)Phenol
Molecular Structure	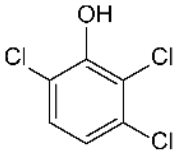	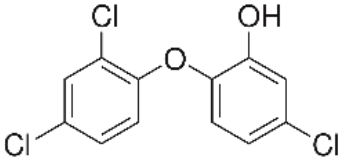
Molecular Formula	$C_6H_3Cl_3O$	$C_{12}H_7Cl_3O_2$
Molecular Weight (g/mol)	197.4	289.54
Solubility in water (g/L)	< 1 (at 20 °C)	0.010 (at 20 °C)
pKa	5.8	7.9
Octanol-water Partitioning Coefficient (Log K_{ow})	3.77	4.76
Physical Description	Colorless solid needles	White to off-white crystalline solid powder
Colors at different pH in aqueous solution	Colorless	Colorless
CAS	933-75-5	3380-34-5
Purity	99.5%	>99%
References	(National Center for Biotechnology Information, 2024a)	(National Center for Biotechnology Information, 2024c), (Singh & Kaur, 2023)

B.3 Sorption Isotherm Models

Table B.3 Isotherm models used in this study*.

Model**	Equation	Parameters (Unit)
Henry (L)	$q_e = K_d C_e$	K_d (L/g)
Freundlich (NL)	$q_e = K_F C_e^{\frac{1}{n}}$	n, K_F (L/g)
Temkin (NL)	$q_e = \frac{RT}{b_T} \ln (K_T C_e)$	b_T (J/mol), K_T (L/g)
Dubinin-Radushkevich (D-R) (NL)	$q_e = q_m \exp (-K(RTln\left(1 + \frac{1}{C_e}\right))^2)$	q_m (µg adsorbate/ g adsorbent), K (mol^2/KJ)
Langmuir (NL)	$q_e = \frac{q_m K_L C_e}{1 + K_L C_e}$	q_m (µg adsorbate/ g adsorbent), K_L (µg/g)

*Reference: El-Azazy et al., 2021

**L: Linear model, NL: Non-linear model

Table B.4 Isotherm models summary for TCS and TCP.

		LPW				LBW				LOW			
OC	Model	R^2	Adj. R^2	RMSE	Parameters	R^2	Adj. R^2	RMSE	Parameters	R^2	Adj. R^2	RMSE	Parameters
TCS	Henry (L)	0.971	0.967	86.412	K_{pew}=0.399	0.94	0.934	94.2	K_{pew}=0.158	0.99	0.989	51.7	K_{pew}=0.465
	Freundlich (NL)	0.897	0.877	87.929	n=0.791 Kf=0.059	0.78	0.738	103	n=0.999 Kf=0.157	0.97	0.964	48.1	n=0.851 Kf=0.134
	Temkin (NL)	0.836	0.804	110.96	RT/bT=339.4 Kt=0.004	0.79	0.743	102	RT/bT=258.1 Kt=0.002	0.941	0.929	67.4	RT/bT=394.3 Kt=0.004
	D-R (NL)	0.82	0.784	116.26	K=0.116 qm=830.0	0.75	0.697	111	K=0.267 qm=555.6	0.894	0.873	90.4	K=0.085 qm=856.0
	Langmuir (NL)	0.671	0.605	157.3	Kl=0.0001 qm=5530.4	0.63	0.557	134	Kl=0.0001 qm=2416.3	0.772	0.726	133	Kl=0.0001 qm=6288.0
TCP	Henry (L)	0.995	0.994	17.575	K_{pew}=0.011	0.39	0.282	96.7	K_{pew}=0.003	0.959	0.952	79.5	K_{pew}=0.018
	Freundlich (NL)	0.995	0.994	13.92	n=1.147 Kf=0.042	N/A	N/A	N/A	N/A	0.95	0.94	70.5	n=1.247 Kf=0.173
	Temkin (NL)	0.755	0.706	94.021	RT/bT=75.9 Kt=0.002	0.21	0.047	116	RT/bT=33.5 Kt=0.0003	0.814	0.777	136	RT/bT=158.2 Kt=0.001
	D-R (NL)	0.909	0.891	57.31	K=43.1 qm=500.5	N/A	N/A	N/A	N/A	0.984	0.981	39.5	K=17.36 qm=716.4
	Langmuir (NL)	0.643	0.571	113.49	Kl=0.0001 qm=580.9	0.14	-0.027	121	Kl=0.0001 qm=96.2	0.824	0.789	132	Kl=0.0001 qm=784.4

B.5 Change of pH during isotherms of TCS and TCP

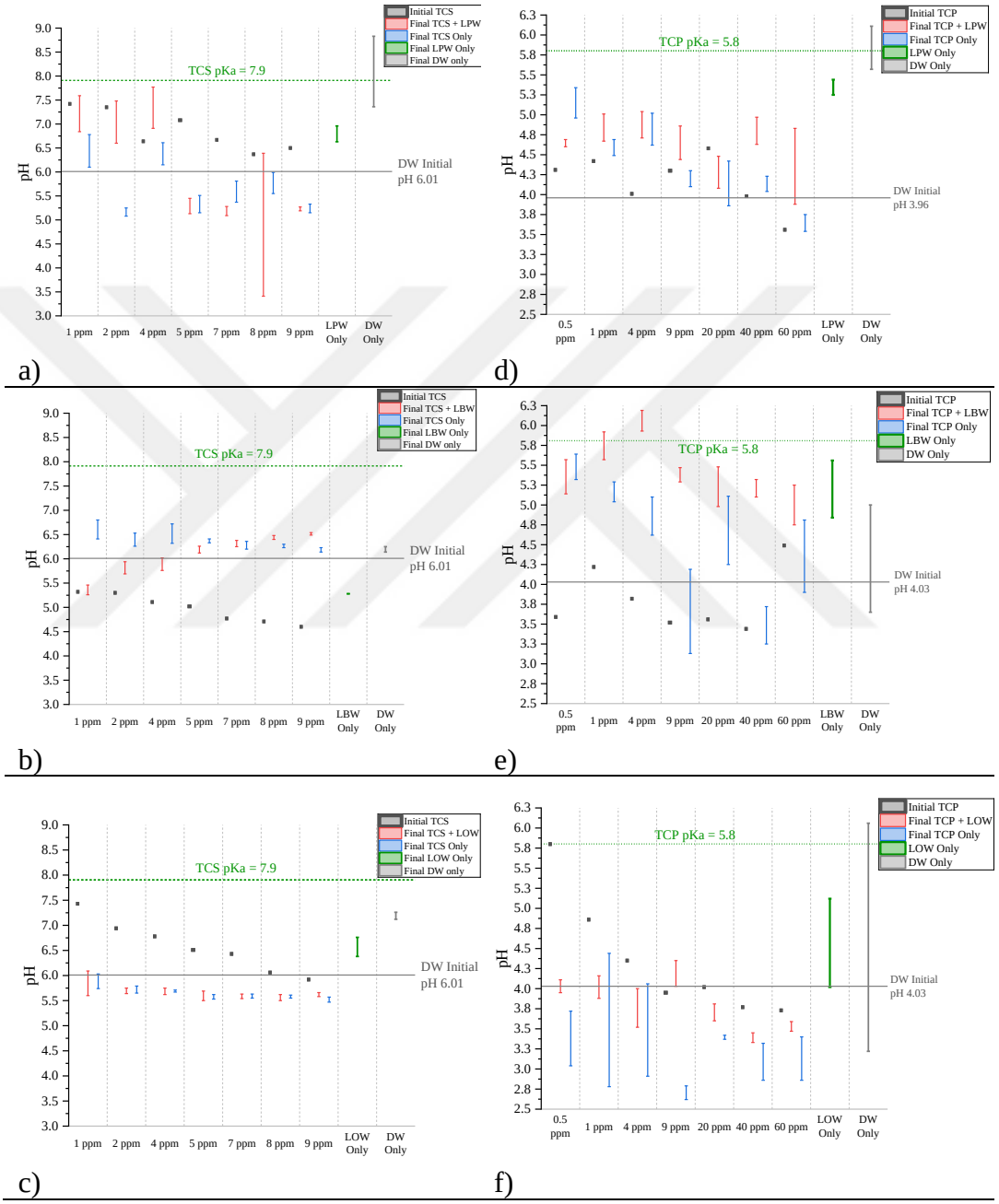

Figure B.1 pH measurements at equilibrium of TCS (a-c) and TCP (d-f) for pristine washed LDPE (LPW), anaerobically aged LDPE (LBW), and aerobically aged LDPE (LOW), respectively.

B.6 TCS Absorbance scans

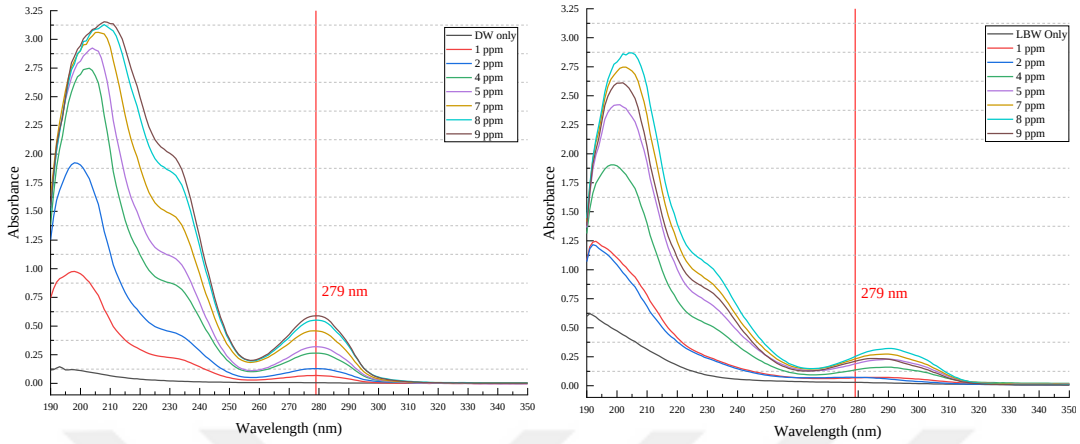

Figure B.2 Absorbance scans of TCS at equilibrium concentrations for a) TCS-only control reactors and b) test reactors containing TCS and anaerobically aged LDPE (LBW).

C. Thesis Extra Information

Extra information on the fate and impact of HDPE and LDPE type MPs during the operation of aerobic and anaerobic reactors is summarized in this appendix. Information on the outcomes of aerobic and anaerobic aging of PE is summarized in the first two sections. The third section looks into the characterization of MPs used in the reactor before and after termination and how aerobic and anaerobic digestion affected HDPE and LDPE differently. The fourth section adds information on the sorption of TCP and TCS into bio-aged PE extracted from the bio-aging reactors. The last section summarizes the results of MG sorption and isotherms conducted on pristine and bio-aged LDPE.

C.1 Performance of Anaerobic Reactors

Table C.1 and Table C.2 present the initial and final sludge characterization of BMP reactors. Initial sludge parameters exhibited close alignment across all setups, indicating a uniform distribution of sludge into each reactor. The targeted TS value for all BMP setups was 2%, with measured TS values of 1.8±0.7%, 1.7±0.0%, and 1.9±0.0% for HDPE setup, LDPE setup 1, and LDPE setup 2, respectively, conforming to the 2% TS target. However, in the HDPE setup, the addition of $HgCl_2$ for microbial inactivation caused the TS value for abiotic sets to rise from 1.8 to 2.0±0.0%. All seed-only reactors had a lower TS value than 2% (around 1%). Initial VS values ranged between 10-12 g/L for all biotic setups, with abiotic reactors exhibiting higher VS values of 13 g/L, while seed controls had approximately half the VS values of biotic reactors. Biotic control reactors showed VS removals of 27.8%, 37.6%, and 25% for HDPE setup, LDPE setup 1, and LDPE setup 2, respectively, indicating healthy reactor operation as VS reduction stands for the removal of organic material. pH values of the biotic sets consistently fell within the optimal range (7-8.5) for AD during both the setup and termination stages (Holliger et al., 2016). Across all reactors, pH remained stable, with minor fluctuations

observed in abiotic reactors, likely attributable to the presence of $HgCl_2$ and the inactivity of the reactors. The pH values of seed controls were slightly elevated compared to samples, likely due to digestion processes.

The presence of MPs in reactors led to varied tCOD removals due to interference with measurements. The lack of reported impact of MPs on VS or tCOD measurements in the literature may be attributed to the relatively low doses of MPs present in the reactors. In our study, doses of 200 g HDPE MPs/ gTS and 300 g LDPE MPs/ gTS were utilized, which surpasses previously reported doses in the literature. In contrast, the tCOD values in abiotic reactors exhibited a wider range and higher values compared to other setups due to the presence of $HgCl_2$, which was added to suppress microbial activity. Conversely, seed controls displayed the lowest tCOD content because they are stable and do not contain WAS, resulting in nearly half the total organic content of other reactors.

During the setup phase, TSS and VSS values for all biotic sets were notably similar. Specifically, the average TSS values for HDPE, LDPE set-up 1, and LDPE set-up 2 were 19.1 g/L, 15.5±1.7 g/L, and 18.4±0.9 g/L, respectively. Subsequent to termination, there was a considerable reduction in the average TSS values by 27.9%, 25.2%, and 27.2% for HDPE set-up, LDPE set-up 1, and LDPE set-up 2 biotic control reactors, respectively, which were closely aligned. The close percentage removal values observed among the three different setups suggest stability across the reactors. However, results from reactors containing MPs were deemed unreliable due to the interference of MPs with the measurements. In the initial stage, the average VSS value ranged between 11-13 g/L for all sets. Post-termination, variations in VSS values were noted among the setups. Biotic-only reactors in the HDPE set-up exhibited the highest VSS removal (44.7%), followed by LDPE set-up 2 (39.2%) and LDPE set-up 1 (20.4%). BOD_5 tests conducted solely on LDPE set-ups yielded varied results, with a 96.3% BOD_5 removal achieved from LDPE set-up 1. However, a removal value could not be obtained from LDPE set-up 2 due to ineffective dilution ratios. Theoretical calculations based on suggested dilution ratios indicate an expected removal value of <83%.

Table C.1 Initial and final characterization of anerobic reactor set-ups (Part 1).

	Reactor Set	TS_i (g/L)	TS_f (g/L)	% TS Removal	VS_i (g/L)	VS_f (g/L)	% VS Removal	$tCOD_i$ (g/L)	$tCOD_f$ (g/L)	% tCOD Removal	pH_i	pH_f
HDPE Set-up	HA0	20.0±0.2	18.0±1.8	8.7±9.2	13.0±0.2	11.0±1.6	14.4±12.7	19.5±2.4	19.2±1.9	1.9±9.9	6.0	6.3±0.6
	HA	20.0±0.2	21.0±0.1	-3.6±0.4	13.0±0.04	14.0±0.05	-7.5±3.6	23.2±5.9	17.3±1.4	25.3±6.1	6.0	5.8±0.1
	HB0	18.0±0.5	16.0±0.1	11.4±0.7	12.0±0.7	8.3±0.1	27.8±1.0	16.9±0.5	12.7±0.5	25±5.4	8.0	7.0±0.03
	HB	19.0±0.8	20.0±0.3	-2.6±1.8	12.0±0.4	12.0±0.3	-2.5±2.7	19.8±3.6	11.7±0.5	40.7±26.4	8.0	7.0±0.02
	HS0	11.0±0.7	10.0±0.1	8.4±1.2	5.6±0.3	4.8±0.1	15.8±1.0	7.6±1.7	6.5±0.4	15.3±5.2	8.0	7.2±0.03
LDPE Set-up 1	LB0-1	17.2±0.2	12.2±0.05	29.1±0.3	10.1±0.8	6.3±0.7	37.6±6.6	23.2±1.7	17.1±1.3	26.3±5.4	7.3±0.1	7.3±0.1
	LB-1	17.2±0.2	16.7±0.9	2.9±5.2	10.1±0.8	11.2±0.6	-10.9±5.6	23.2±1.7	18.9±2.2	18.5±4.4	7.3±0.1	7.3±0.02
	LS0-1	9.6±0.2	6.8	28.9	5.2±0.2	3.5	33.5	10.0±2.4	10.8±1.4	-8.0±17.6	8.1±0.04	7.3±0.01
LDPE Set-up 2	LB0-2	19.0±0.5	15.2±0.2	20.0±4.5	10.8±0.8	8.1±0.1	25.0±4.1	24.3±1.6	16.6±0.7	31.7±2.9	7.1±0.2	7.3±0.2
	LB-2	19.0±0.5	20.1±0.8	-5.8±1.0	10.8±0.8	12.9±0.4	-19.4±1.0	24.3±1.6	17.0±1.2	30.0±4.8	7.1±0.2	7.0±0.1
	LS0-2	10.7±0.02	9.3±0.1	13.1±0.7	5.6±0.1	4.6±0.1	17.9±2.2	9.2±0.6	13.6±1.2	1.2±9.0	7.4±0.2	7.1±0.2

Table C.2 Initial and final characterization of anerobic reactor set-ups (Part 2).

	Reactor Set	TSS_i (g/L)	TSS_f (g/L)	% TSS Removal	VSS_i (g/L)	VSS_f (g/L)	% VSS Removal	BOD_i (g/L)	BOD_f (g/L)	% BOD Removal
HDPE Set-up	HA0	17.8	12.1±0.3	31.9±14.9	12.8	7.8±1.7	39.0±13.0	N/A	N/A	N/A
	HA	17.8	16.9±1.8	5.2±10.1	12.8	12.0±1.1	5.9±8.3	N/A	N/A	N/A
	HB0	19.1	13.8±1.7	27.9±9.1	14	7.8±1.2	44.7±8.8	N/A	N/A	N/A
	HB	19.1	15.4±0.8	19.5±4.6	14	10.1±0.3	27.6±2.3	N/A	N/A	N/A
LDPE Set-up 1	HS0	10.6	9.4±0.3	10.4±2.7	7.2	5.2±0.8	28.3±11.7	N/A	N/A	N/A
	LB0-1	15.5±1.7	11.6±0.8	25.2±5.3	10.8±1.2	8.6±0.1	20.4±0.7	N/A	N/A	N/A
	LB-1	15.5±1.7	16.4±1.3	-5.8±8.6	10.8±1.2	13.2±1.5	-22.2±14.0	7.2	0.3	96.3
	LS0-1	8.9±1.0	6.8±0.2	23.6±2.4	5.3±0.5	5.4±0.1	-1.9±2.0	N/A	N/A	N/A
LDPE Set-up 2	LB0-2	18.4±0.9	13.4±0.7	27.2±3.6	12.5±0.9	7.6±0.4	39.2±3.0	N/A	N/A	N/A
	LB-2	18.4±0.9	17.9±1.0	2.7±5.7	12.5±0.9	12.1±1.0	3.2±8.0	14.8	N/A	N/A
	LS0-2	9.9±0.6	8.4±0.4	15.2±4.0	6.3±0.3	4.5±0.2	28.6±3.7	N/A	N/A	N/A

Table C.3 displays the ratios of sludge parameters across all performed setups. The initial VS/TS ratio consistently appears higher for both biotic and abiotic reactors compared to seed control, indicating greater stability in the seed. Initial TSS/TS and VSS/VS ratios consistently hover close to 1, suggesting that the majority of solids in the sludge are in suspended form. Values exceeding 1 denote experimental error resulting from low sampling volumes and suggest loss of soluble components due to the thickening process. Utilizing larger sampling volumes may mitigate the errors.

Table C.3 Sludge characterization ratios of anaerobic reactors.

	Reactor Set	TSS/ TS_i	TSS/ TS_f	VSS /VS_i	VSS/ VS_f	VS/ TS_i	VS/ TS_f	VSS/ TSS_i	VSS/ TSS_f	BOD/ COD_i	BOD/ COD_f
HDPE Set-up	HA0	0.90	0.67	1.00	0.71	0.64	0.60	0.72	0.64	N/A	N/A
	HA	0.89	0.81	1.00	0.87	0.64	0.66	0.72	0.71	N/A	N/A
	HB0	1.06	0.86	1.22	0.93	0.64	0.52	0.74	0.56	N/A	N/A
	HB	1.00	0.79	1.20	0.85	0.61	0.61	0.74	0.66	N/A	N/A
	HS0	0.96	0.93	1.28	1.09	0.51	0.47	0.69	0.55	N/A	N/A
LDPE Set-up 1	LB0-1	0.90	0.95	0.98	1.36	0.64	0.51	0.70	0.74	N/A	N/A
	LB-1	0.90	0.98	0.98	1.17	0.64	0.67	0.70	0.80	0.31	0.01
	LS0-1	0.93	1.27	1.02	1.92	0.55	0.52	0.60	0.79	N/A	N/A
LDPE Set-up 2	LB0-2	0.97	0.88	1.16	0.94	0.57	0.53	0.68	0.57	N/A	N/A
	LB-2	0.97	0.89	1.16	0.94	0.57	0.64	0.68	0.68	0.61	N/A
	LS0-2	0.93	0.91	1.13	0.98	0.52	0.50	0.64	0.54	N/A	N/A

The total biogas production from the reactors for HDPE and LDPE set-ups is illustrated in Figure C.1. Notably, biogas production commenced from day one without any lag or transition period, with consistent trends and rates observed across all reactor sets over the designated time intervals.

In the HDPE set-up, after 27 days, the daily proportion of biogas for all sets decreased to approximately 2%. Consequently, biogas and CH_4 measurements were

conducted every other day thereafter. Biotic control reactors exhibited a gradual decrease in biogas content, reaching approximately 1.6% by day 41. However, biotic reactors with HDPE present maintained biogas content above 2% until termination (day 50). Figure C.2a indicated a high standard deviation in biogas data during the initial days due to probable leakage, which was subsequently addressed. Despite that, the difference between BMPs containing HDPE MPs and those without did not overlap, suggesting microbial inhibition as the likely cause. Conversely, biogas production from abiotic reactors remained minimal throughout the observation period; for nearly 23 days, no biogas was produced, with slight production observed in some replicates thereafter. Given the minimal biogas production, no additional $HgCl_2$ addition was necessary until termination day.

For LDPE set-up 1 and set-up 2, the overall daily proportion of biogas for all sets decreased to about 2% after 15 and 20 days, respectively. Despite dropping to 1% of the total gas after 41 and 39 days for set-up 1 and 2, respectively, biogas measurements continued as scheduled, rather than terminating the reactors. In contrast to the HDPE set-up, biotic BMP reactors with and without LDPE MPs exhibited similar biogas production in both set-ups. Figure C.2 (b and c) depicts the data with error bars, indicating low standard deviation and reactor homogeneity.

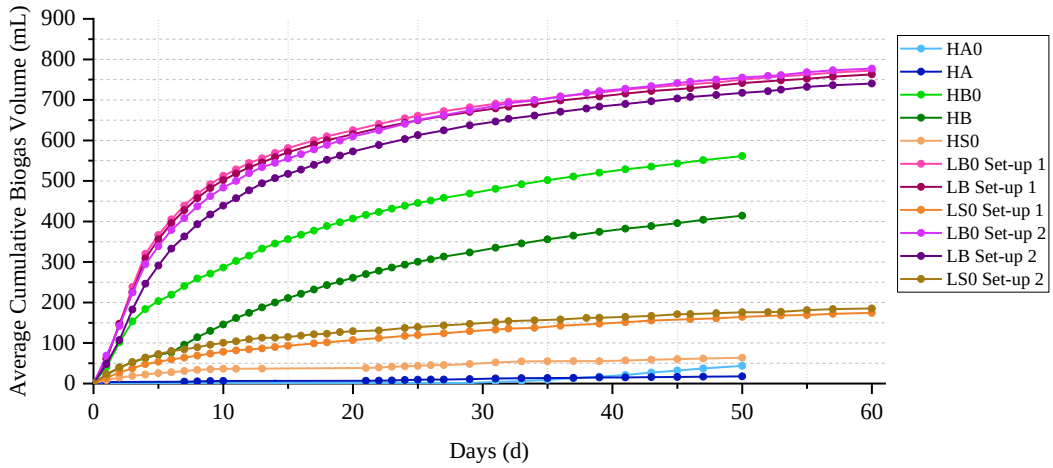

Figure C.1 Average cumulative biogas production of HDPE set-up, LDPE set-up 1, and LDPE set-up 2.

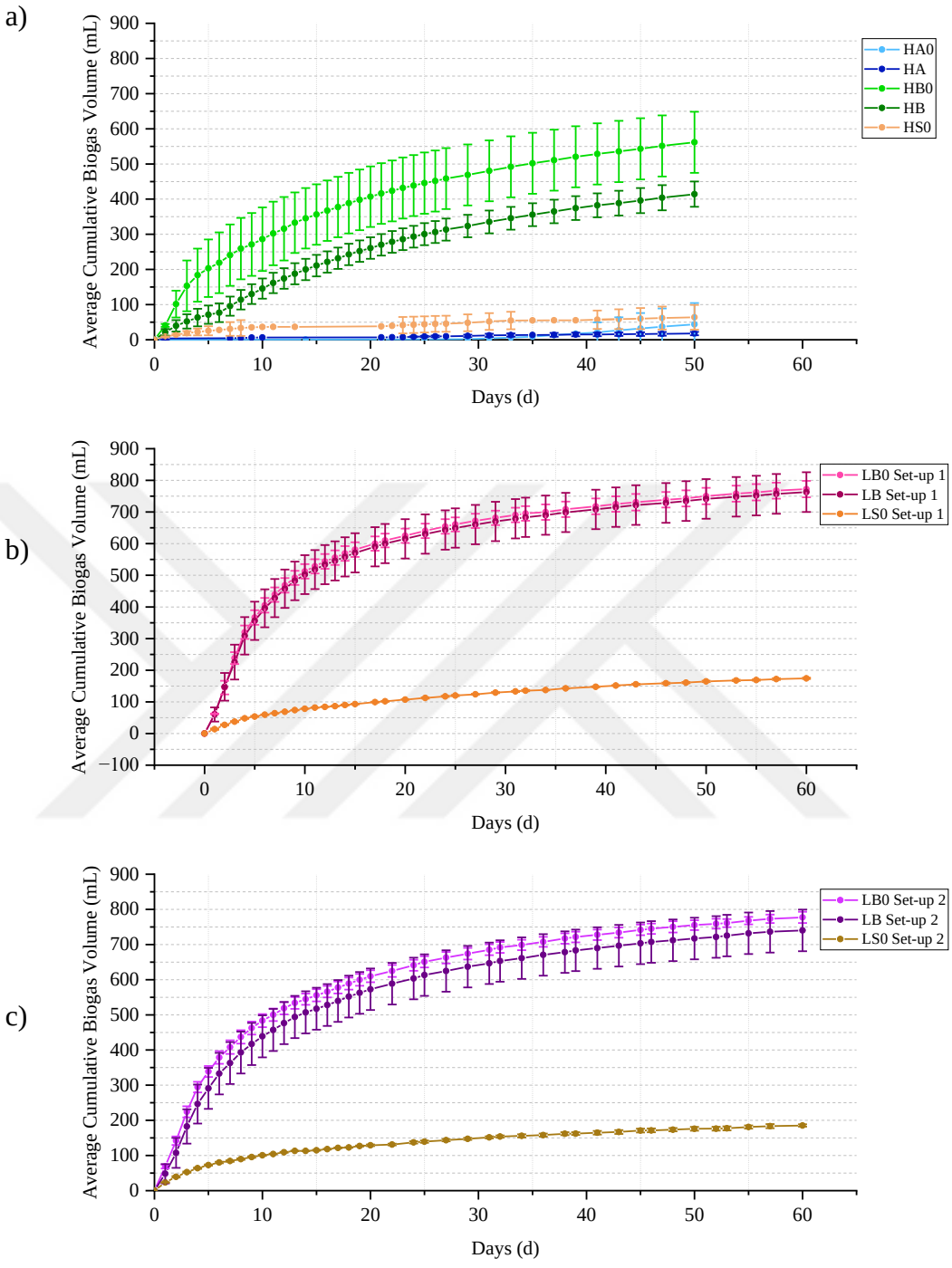

Figure C.2 Average cumulative biogas volume of a) HDPE set-up, b) LDPE set-up 1, and c) LDPE set-up 2.

Initially, the predominant gas detected in the reactors was N_2, attributed to the utilization of N_2 to purge the reactors. However, as CH_4 production commenced, there was a notable decrease in N_2, accompanied by a rise in CH_4 and CO_2 levels. Across all biotic reactors, CH_4 content exhibited an increase to almost 60%, subsequently stabilizing at 50-55% until termination day.

The CH_4 production profile (Figure C.3) exhibited a pronounced trend closely aligning the biogas. Daily CH_4 production to cumulative CH_4 ratio decreased to 2%. Consequently, the transition to measurements every other day is supported by the CH_4 graph. CH_4 inhibition was also evident in the HDPE reactors, akin to biogas production, however, the percentage of CH_4 in the biogas was not necessarily reduced. This suggests that methanogens in the reactors remained present but might have decreased in population due to MP inhibition.

Seed controls yielded minimal amounts of CH_4 during the reactor processes. It may be advisable to pre-incubate the inoculum if the seed accounts for more than 20% of the total CH_4 production (Holliger et al., 2016). However, the CH_4 production of seed controls was approximately 6.4%, 16.3%, and 16.0% for HDPE set-up, LDPE set-up 1, and set-up 2, respectively, indicating that pre-incubation was unnecessary. Additionally, extracting the CH_4 generated in seed reactors from the test reactors can be utilized to estimate the detectable CH_4 production of the seed for yield analysis.

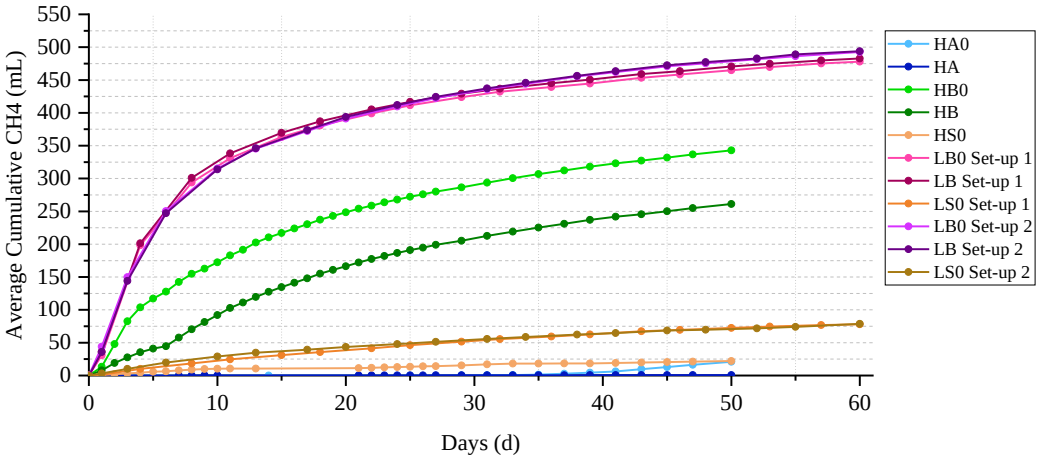

Figure C.3 Average cumulative methane production of HDPE set-up, LDPE set-up 1, and LDPE set-up 2.

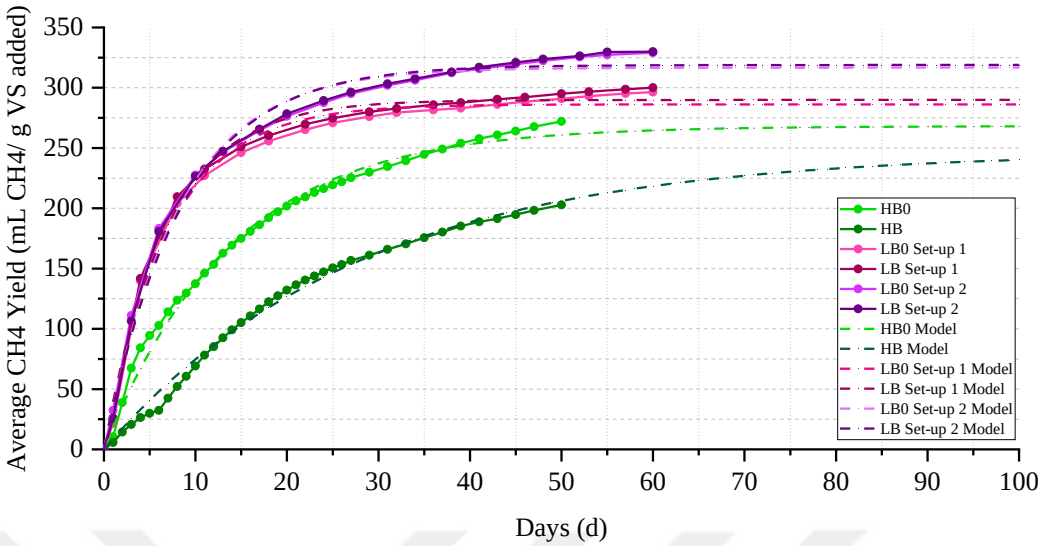

Figure C.4 Data extrapolation of setups using the one-substrate model.

Table C.4 BMPs cumulative biogas, CH_4, CH_4 yield, and CH_4 content.

	Reactor Set	Cumulative Biogas Production (mL)	Cumulative CH_4 Production (mL)	CH_4 Yield (mL CH_4/ g VS added)	CH_4 Content (%)
HDPE Set-up	HA0	43.8±60.6	20.8±29.5	N/A	47.6
	HA	17.7±4.8	0.8±0.3	N/A	4.3
	HB0	561.6±86.8	342.9±50.6	272.2	61.1
	HB	414.2±35.9	261.2±21.0	202.9	63.1
	HS0	63.8±35.2	22±13.2	N/A	34.5
LDPE Set-up 1	LB0-1	772.4±26.0	477.9±0.0	296.4	61.9
	LB-1	762.8±62.9	482.8±13.8	300.0	63.3
	LS0-1	174.3±2.1	78.1±0.0	N/A	44.8
LDPE Set-up 2	LB0-2	777.2±15.9	492.7±0.0	329.0	63.4
	LB-2	740.2±59.1	493.9±26.2	329.9	66.7
	LS0-2	185.4±3.4	78.6±0.0	N/A	42.4

C.2 Performance of Aerobic Reactors

Table C.5 summarizes the initial and final sludge characterizations of aerobic reactors along with their removals. The targeted TS value for all aerobic setups was 2%. Actual TS measurements for the reactors closely approximated this target, with values of 2.0±0.4%, 1.8±1.0%, and 1.8±0.2% for the HDPE set-up, LDPE set-up 1, and LDPE set-up 2, respectively. Initial VS values fell within the range of 13.3-14.9 g/L across all aerobic set-ups, with VS reduction serving as a key indicator of reactor performance indicating the removal of organic matter.

Measurement of TSS and VSS during setup and termination phases revealed consistency among the aerobic sets initially, with average TSS values of 19.2 g/L for HDPE, 17.2±1.7 g/L for LDPE set-up 1, and 18.9±0.9 g/L for LDPE set-up 2. Following termination, LDPE set-up 1 and LDPE set-up 2 exhibited TSS reductions of 35.4% and 37%, respectively, indicating stability between reactors. Conversely, VSS removal varied post-termination, with LDPE set-up 2 showing notably higher removal (44.7%) compared to LDPE set-up 1 (30.1%).

Table C.5 Initial and final characterization of aerobic reactor set-ups.

Parameter	HO		LO-1		LO-2	
	Initial	Final	Initial	Final	Initial	Final
TS (g/L)	19.9±0.4	N/A	18.3±1.0	12.8±0.5	18.5±0.2	14.4±0.7
TS Removal %	N/A		29.7		22.2	
VS (g/L)	14.9±0.2	N/A	13.3±0.7	8.2±1.0	14.1±0.2	8.6±0.9
VS Removal %	N/A		38.5		39.0	
TSS (g/L)	19.2±0.2	N/A	17.2±3.4	11.1±2.7	18.9±0.4	11.9±0.8
TSS Removal %	N/A		35.4		37.0	
VSS (g/L)	16.3±0.4	N/A	13.5±2.9	9.4±2.4	15.2±0.4	8.4±0.7
VSS Removal %	N/A		30.1		44.7	
tCOD (g/L)	22.3±0.1	N/A	28.4±0.02	13.7±2.1	25.4±1.1	5.6±2.3
tCOD Removal %	N/A		52.0		78.1	
BOD_5 (g/L)	17.3	0.6	10.6	0.1	13.9	0.2
BOD_5 Removal %	96.4		98.8		98.3	
pH	N/A	N/A	6.6±0.1	6.0±0.1	6.6±0.05	5.9±0.03

BOD_5 analyses were conducted at various intervals throughout the operational period of the aerobic reactors. The corresponding BOD_5 percentage reduction at different time points for the three experimental setups is presented in Table C.6.

Table C.6 BOD_5 reduction for aerobic HDPE set-up, LDPE set-up 1, and LDPE set-up 2.

Days	HO		LOW-1		LOW-2	
	BOD_5 (g/L)	Reduction (%)	BOD_5 (g/L)	Reduction (%)	BOD_5 (g/L)	Reduction (%)
0	17.3		10.6		13881.2	
6	6.6	61.8				
13	5.9	66.0				
15	2.3	86.9				
20	1.0	94.0				
23	0.7	95.7				
27	0.6	96.4				
31			0.4	96.2		
33					0.6	95.5
60			0.1	98.8	0.2	98.3

Table C.7 illustrates the ratios of sludge parameters for the three aerobic setups. Initial TSS/TS and VSS/VS ratios consistently hovered close to 1, indicating that the majority of solids in the sludge were in suspended form. Ratios exceeding 1 were attributed to experimental error.

Table C.7 Sludge characterization ratios of aerobic reactors.

Parameter	HO		LO-1		LO-2	
	Initial	Final	Initial	Final	Initial	Final
TSS/TS	0.97	N/A	0.94	0.86	1.02	0.83
VSS/VS	1.09	N/A	1.01	1.15	1.08	0.98
VS/TS	0.75	N/A	0.73	0.64	0.76	0.60
VSS/TSS	0.85	N/A	0.79	0.85	0.80	0.71
BOD/COD	0.78	N/A	0.37	0.01	0.55	0.04

C.3 Characterization of Microplastics

To elucidate the physical and chemical alterations undergone by HDPE and LDPE before and after bio-aging, MPs samples were subjected to characterization using FTIR, DSC, light microscopy, and SEM imaging. However, HDPE MPs derived from abiotic reactors underwent only FTIR and light microscopy analysis due to the absence of microbial activity in the BMPs, suggesting no anticipated bio-aging modifications. FTIR, DSC, and SEM analysis were performed on H_2O_2-washed bio-aged samples to omit interference of biofilm with the results.

ANOVA was performed by comparing the CI of pristine samples (HP & LP) to the bio-aged samples obtained from this study.

Table C.8 ANOVA comparison results of pristine samples CI vs bio-aged samples CI.

Source of Variation	SS	df	MS	F	p-value	F crit
Between HDPE Groups	0.00113	4	0.000282	2.186887	0.143917	3.47805
Within Groups	0.001291	10	0.000129			
Total	0.002421	14				
Between LDPE Groups	0.028671	5	0.005734	21.8476	1.21E-05 (<0.01)*	3.105875
Within Groups	0.00315	12	0.000262			
Total	0.031821	17				

Figure C.5 shows the significance of results when pristine and bio-aged LDPE were compared according to TUKEY. The test indicates between which groups the differences in CI were more dominant ($p<0.01$).

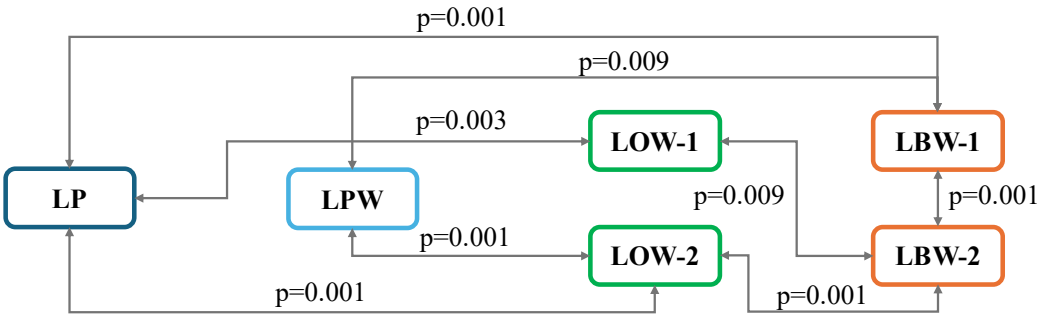

Figure C.5 Pairwise comparison of CI between LDPE groups.

Table C.9 ANOVA comparison results of pristine samples vs bio-aged samples crystallinities.

Source of Variation	SS	df	MS	F	P-value	F crit
Between LDPE Groups	11.596	5	2.319	1.117	0.440	4.387
Within Groups	12.454	6	2.076			
Total	24.050	11				

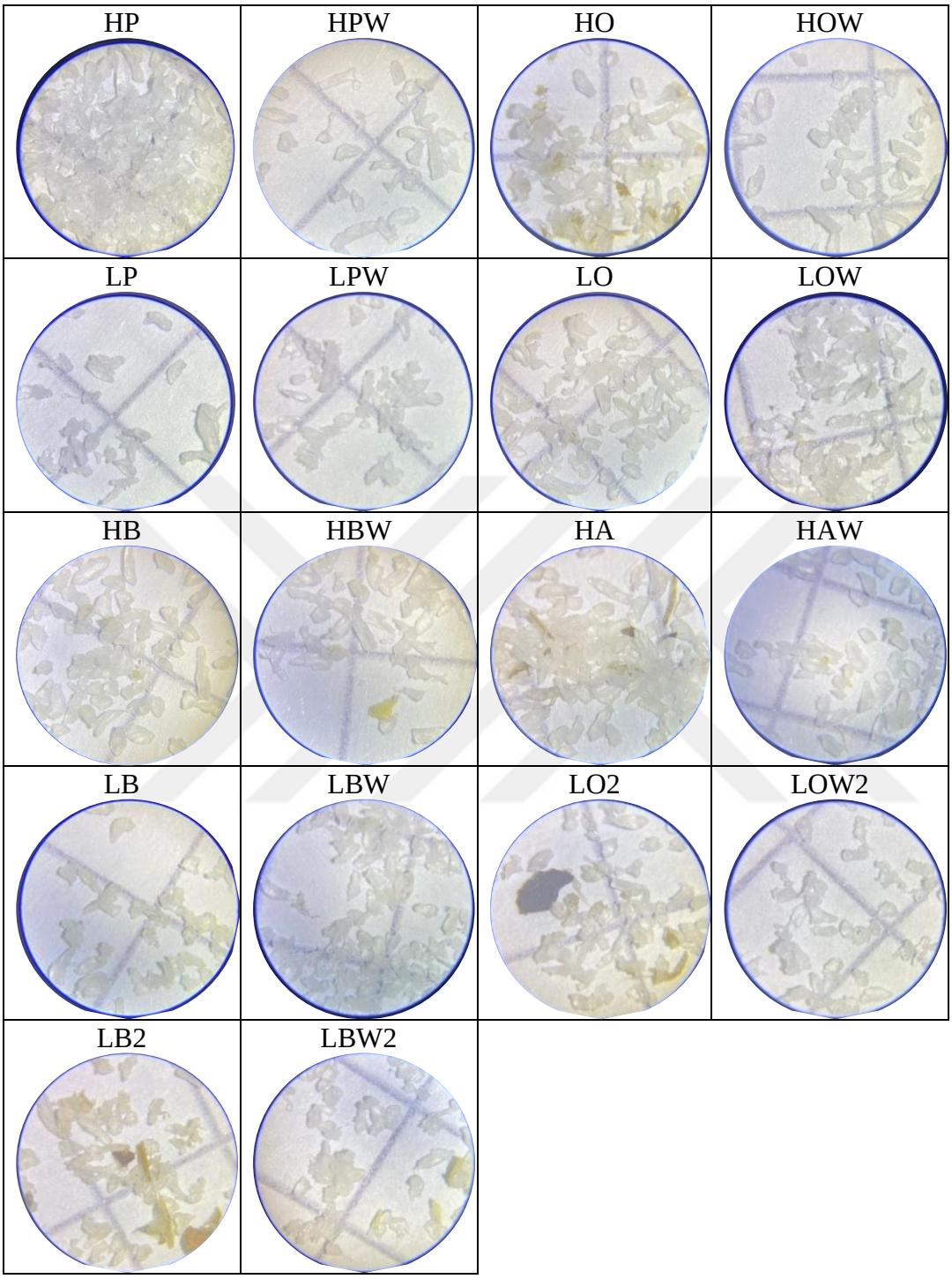

Figure C.6 Light microscope images of HDPE and LDPE before and after washing and bio-aging.

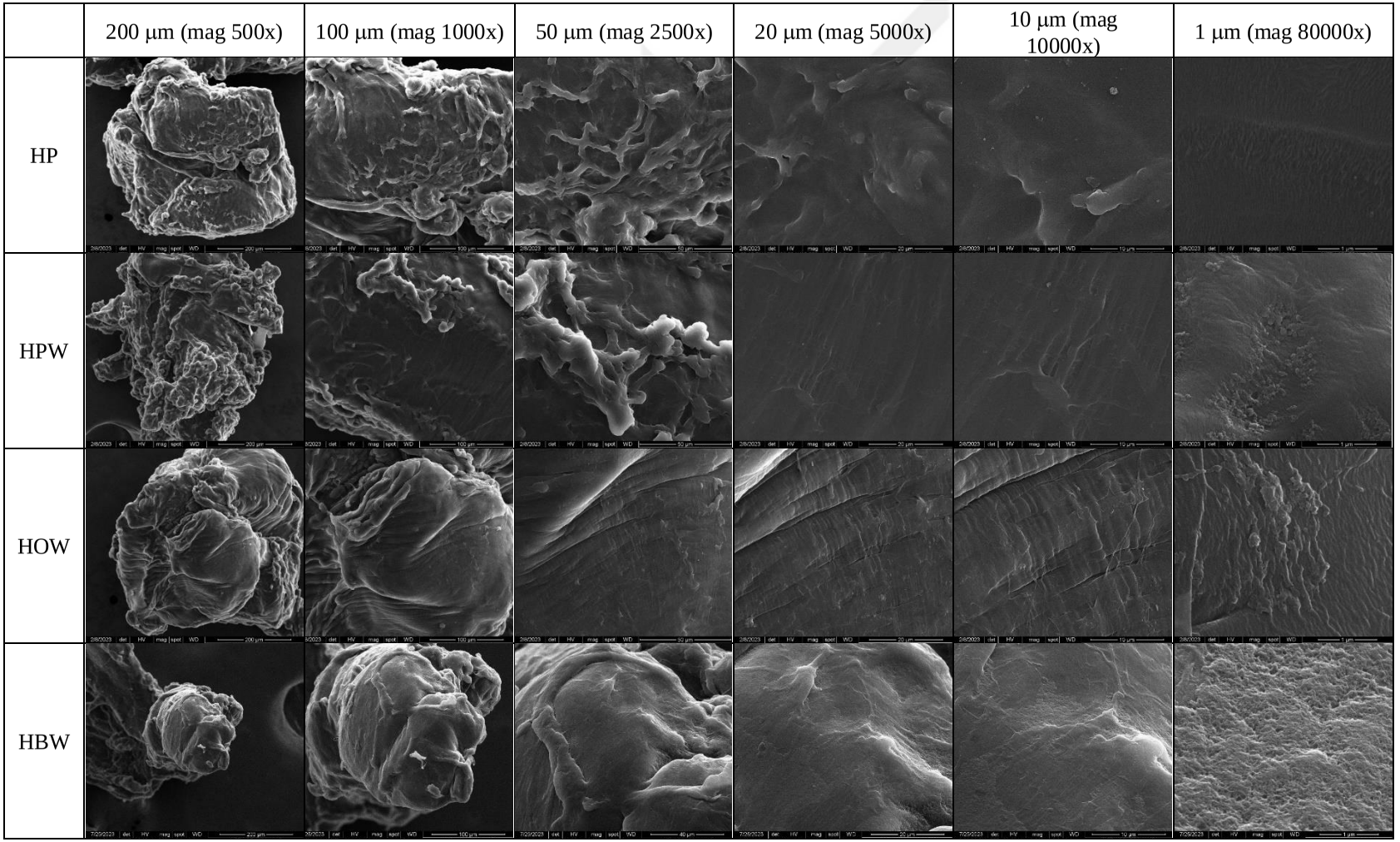

Figure C.7 SEM Images of HDPE before and after bio-aging.

	200 μm (mag 500x)	100 μm (mag 1000x)	50 μm (mag 2500x)	20 μm (mag 5000x)	10 μm (mag 10000x)	1 μm (mag 80000x)
LP	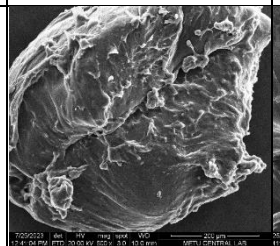	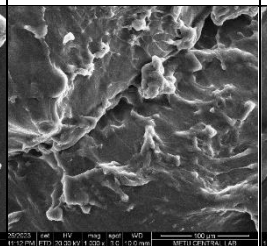	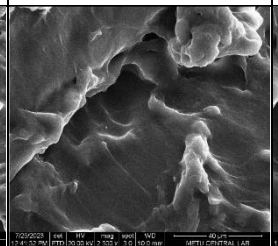	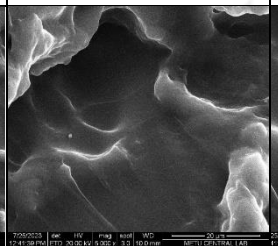	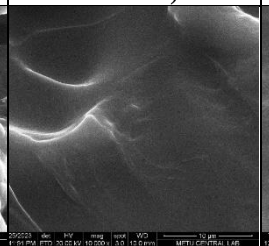	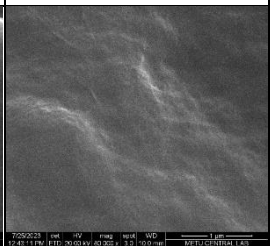
LPW	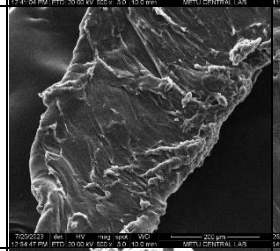	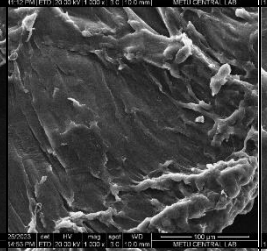	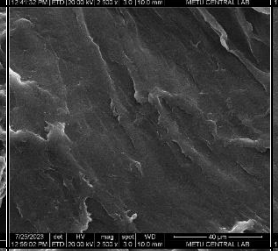	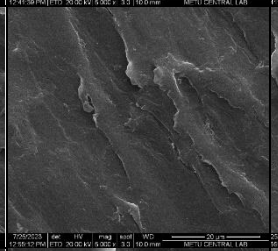	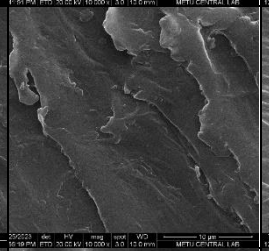	
LOW		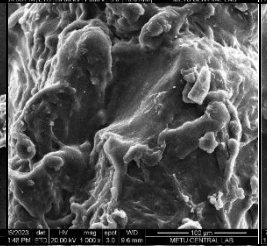	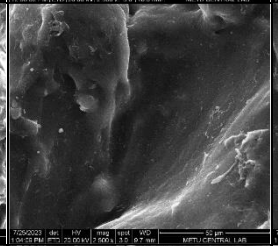	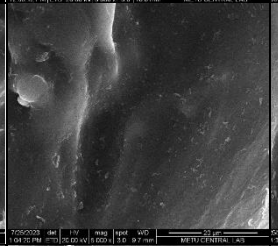	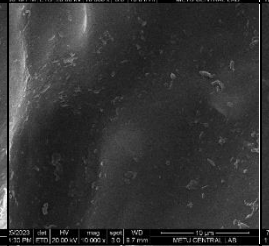	
LBW	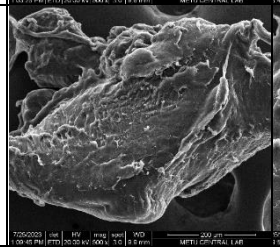	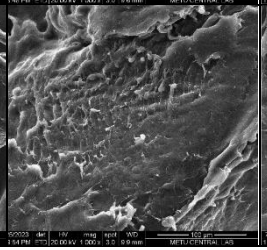	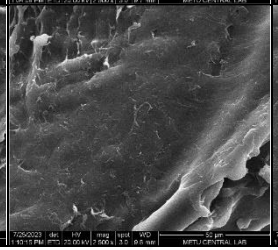	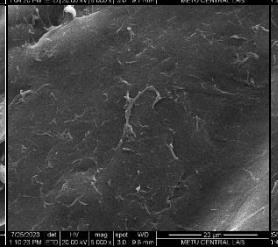	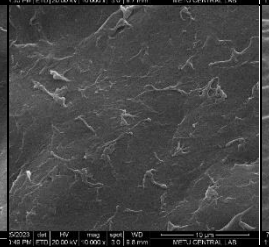	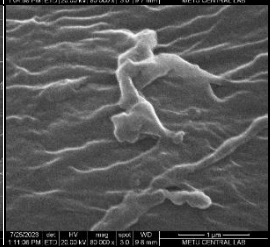

Figure C.8 SEM Images of LDPE before and after bio-aging.

C.4 Sorption of Triclosan and Trichlorophenol on PE

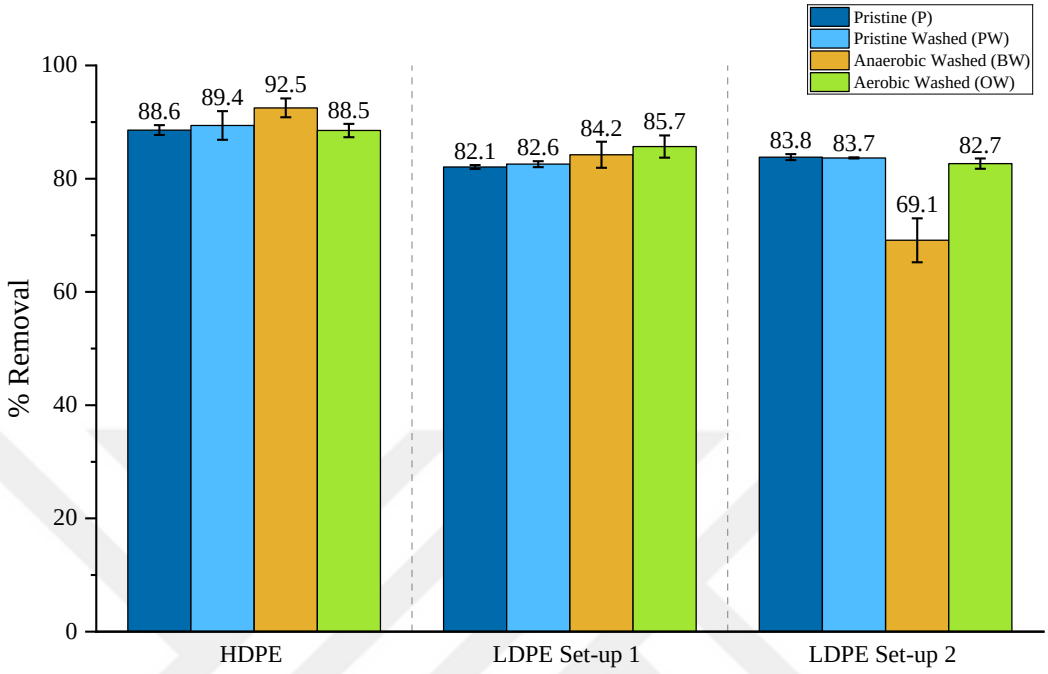

Figure C.9 Results of preliminary sorption of 9 ppm TCS on HDPE and LDPE before and after bio-aging.

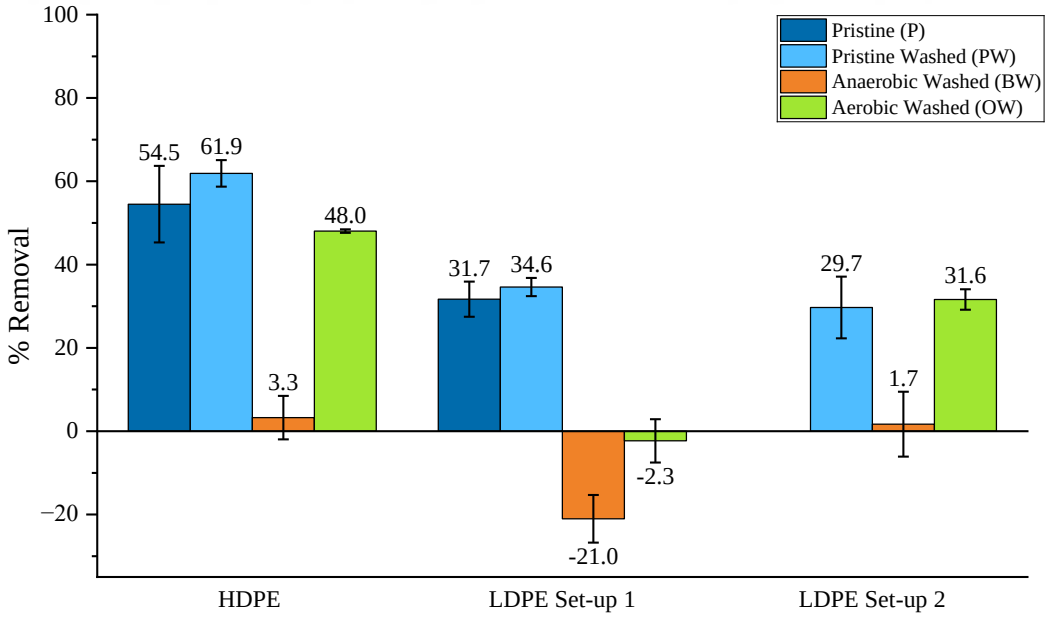

Figure C.10 Preliminary sorption removals of TCP at 8 ppm (HDPE) and 9 ppm (LDPE).

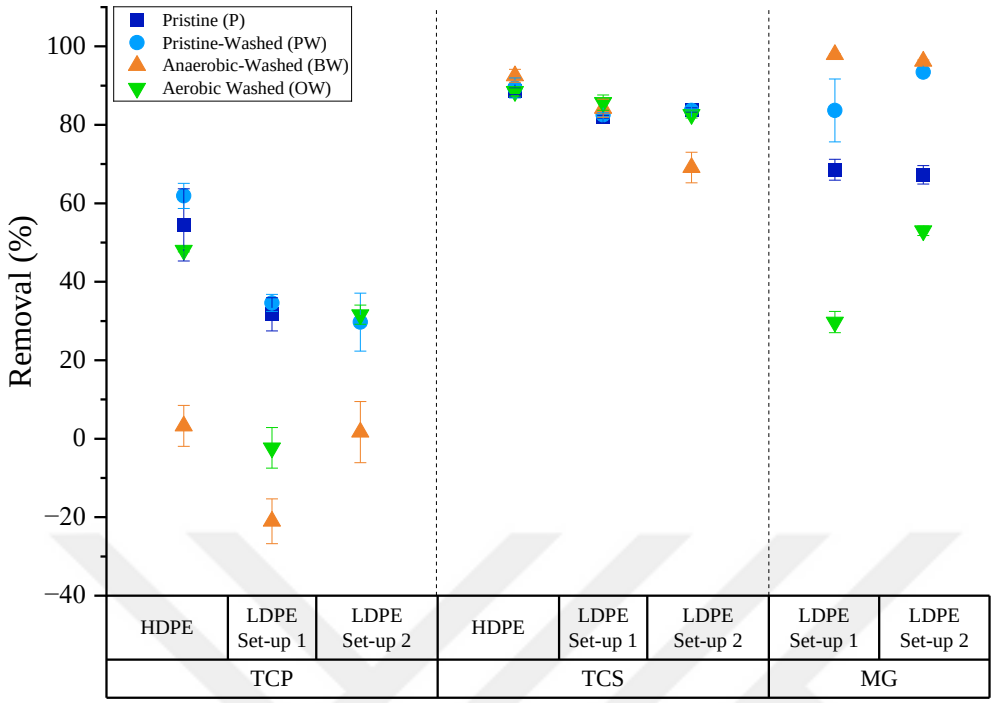

Figure C.11 Removals of TCP (8 ppm (HDPE) and 9 ppm (LDPE)), TCS (9 ppm), and MG (9 ppm (LDPE set-up 1) and 15 ppm (LDPE set-up 2)) before and after bio-aging of PE.

Figure C.12 the removal efficiencies of TCS at various isotherm concentrations for LPW, LBW, and LOW. As depicted in the figure, considering the standard deviations within the setups, which could be attributed to the heterogeneity of the MPs within the reactors, it can be concluded that there is no significant change in sorption affinity at different concentrations between LPW and LOW. However, at 1 ppm, both show a slight decrease in removals. In contrast, LBW removals exhibited variability across different concentrations, with the highest removal (69.1%) observed at 9 ppm. Overall, LBW demonstrated a lower tendency to sorb TCS compared to LPW and LOW.

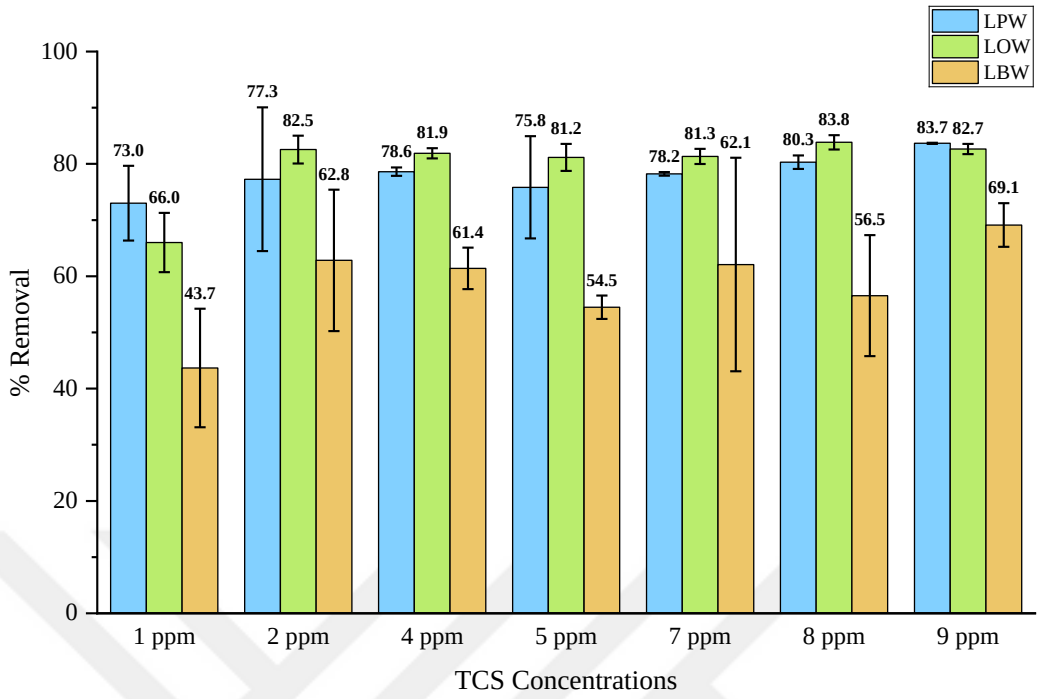

Figure C.12 Removals for TCS for pristine (LPW), Anaerobic bio-aged (LBW), and Aerobic bio-aged (LOW) LDPE at different concentrations.

Figure C.13 summarizes the removal efficiencies of TCP at various isotherm concentrations for LPW, LBW, and LOW. For LPW, there was a gradual decrease in TCP removal with increasing concentrations, with the maximum removal achieved at 1 ppm (57.3%) and the lowest at 60 ppm (21.5%). For LOW, results showed fluctuation, with no removal observed at 0.5 ppm but higher removals compared to LPW at other concentrations. LBW exhibited no sorption affinity, with no removals observed at any concentration except for 60 ppm, where a slight removal of 12.2% was noted. Negative removals were possibly due to the leaching of other chemicals, especially from bio-aged MPs at lower concentrations, which might have interfered with TCP readings at the same wavelength.

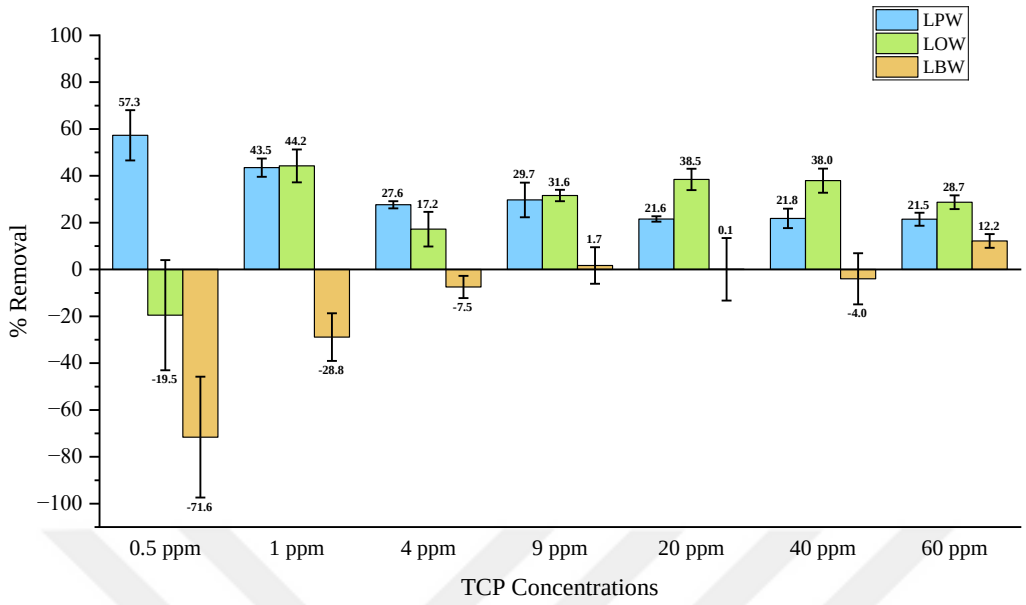

Figure C.13 Removals for TCP for pristine (LPW), Anaerobic bio-aged (LBW), and Aerobic bio-aged (LOW) LDPE at different concentrations measured with buffer.

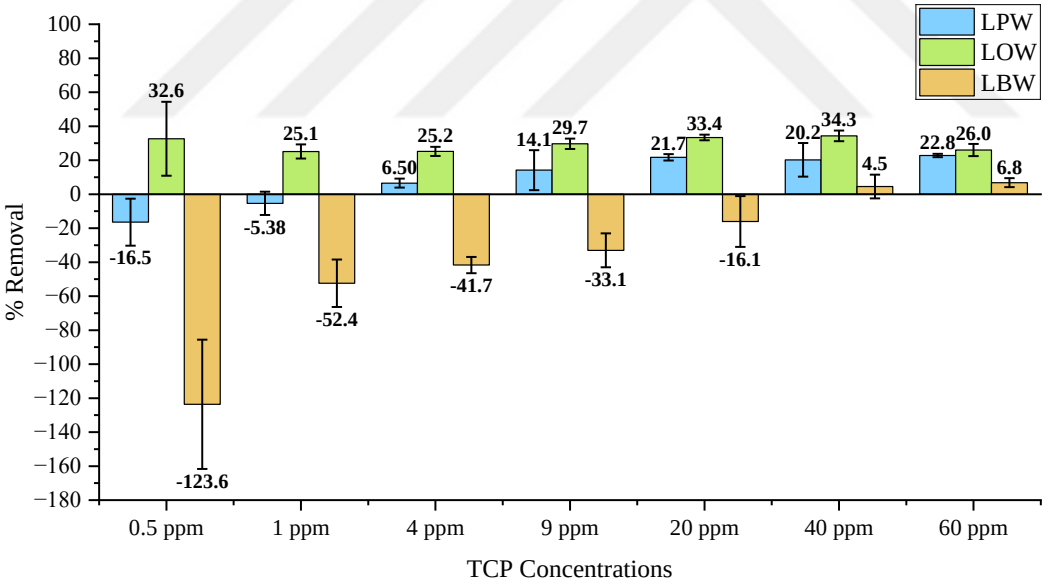

Figure C.14 Removals for TCP for pristine (LPW), Anaerobic bio-aged (LBW), and Aerobic bio-aged (LOW) LDPE at different concentrations measured without buffer.

Table C.10 Linear Isotherms Models Fits.

		LPW			LBW			LOW		
OC	Model	R^2	Slope	Intercept	R^2	Slope	Intercept	R^2	Slope	Intercept
TCS	Henry	0.971	0.4	0.0	0.943	0.158	0.0	0.990	0.5	0.0
	Freundlich	0.970	1.2	-2.4	0.897	1.241	-3.7	0.911	1.3	-3.1
	Temkin	0.836	339.4	-1898.2	0.786	258.145	-1604.1	0.941	394.3	-2216.2
	D-R	0.964	0.0	7.4	0.921	-0.001	7.0	0.919	0.0	7.7
	Langmuir	0.504	0.0	3.6	0.205	-0.001	9.7	0.320	3.8	0.0
TCP	Henry	0.995	0.0	0.0	0.385	0.003	0.0	0.959	0.0	0.0
	Freundlich	0.984	0.7	-1.5		N/A	N/A	0.899	1.0	-3.6
	Temkin	0.755	75.9	-476.0	0.206	33.509	-271.3	0.814	158.3	-1107.9
	D-R	0.788	0.0	5.3		N/A	N/A	0.634	0.0	5.9
	Langmuir	0.629	440.6	-14155.9	0.000	0.007	3789.0	0.081	0.0	8.2

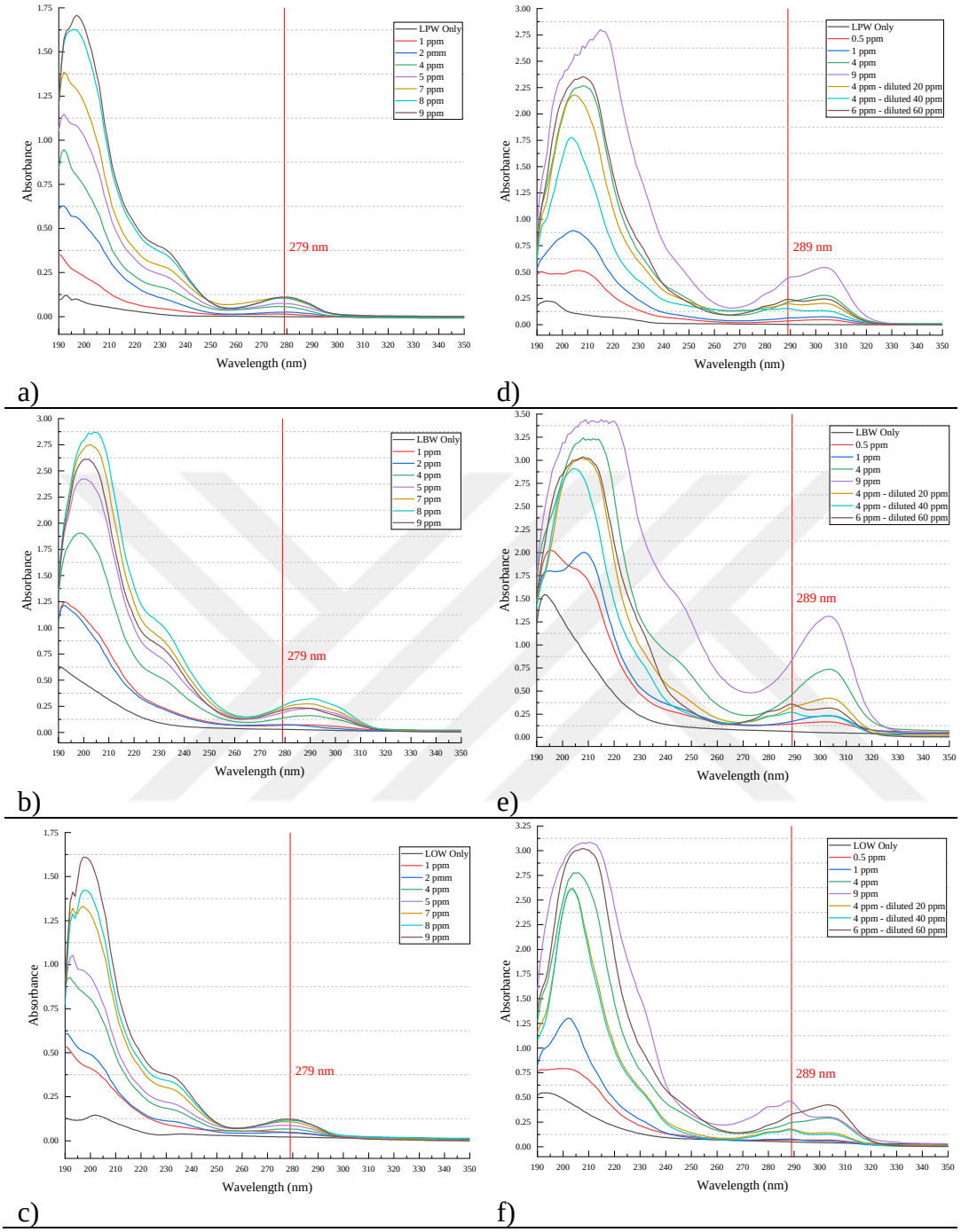

Figure C.15 Absorbance scans at equilibrium concentrations of TCS (a-c) and TCP (d-f) without buffer for LPW, LBW, and LOW respectively.

Figure C.16 illustrates the impact of using an acetate buffer to regulate pH during measurements after equilibrium concentration is reached. The test conducted on LDPE revealed no difference in measurements when an acetate buffer was

employed. The acetate buffer was utilized to ensure all reactors remained within the pKa limit at the time of measurement. Since TCP has a pKa of 5.8 and bio-aged MPs tend to raise the solution pH above 6, an acetate buffer was necessary during the measurement step to reduce the pH to around 4. Without the buffer, if the pH exceeded 5.8, a shift in the absorbance peak of TCP at 9 ppm was observed, resulting in higher absorbance readings, which correspond to higher concentration values (Figure C.16b). Therefore, the buffer was used in LDPE setups and for the LDPE isotherm experiments. The high std in LOW reactors without buffer was due to the difference in pH between the reactors influencing the removals. After the use of buffer, the standard deviation decreased.

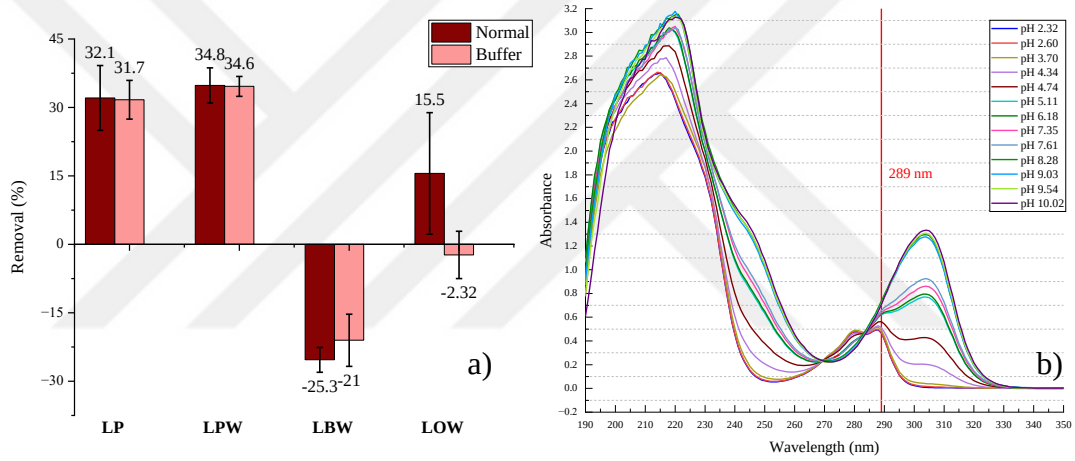

Figure C.16 a) comparison of TCP sorption with and without acetate buffer, b) Absorbance scans of 9 ppm TCP solution at different pH.

Table C.11 ANOVA and TUKEY of LP, LPW, LBW, and LOW preliminary sorption experiments with TCS.

Source of Variation	SS	df	MS	F	P-value	F crit
Between Groups	323.6396	3	107.8799	5.565405	0.004809	3.008787
Within Groups	465.2162	24	19.38401			
Total	788.8557	27				
Significant ($p<0.01$) differences occurred between LBW vs LOW Other differences ($p<0.05$) occurred between: LP vs LBW and LPW, vs LBW						

Table C.12 ANOVA and TUKEY of LPW, LBW, and LOW isotherms sorption experiments with TCS.

Source of Variation	SS	df	MS	F	P-value	F crit
Between Groups	5882.47	2	2941.235	40.94368	6.11E-12	3.150411
Within Groups	4310.167	60	71.83611			
Total	10192.64	62				
Significant ($p<0.01$) differences occurred between LPW vs LBW and LOW vs LBW						

Table C.13 ANOVA and TUKEY of LP, LPW, LBW, and LOW preliminary sorption experiments with TCP.

Source of Variation	SS	df	MS	F	P-value	F crit
Between Groups	4991.627	3	1663.876	10.46412	0.000576	3.287382
Within Groups	2385.115	15	159.0076			
Total	7376.741	18				
Significant ($p<0.01$) differences occurred between LP vs LBW and LPW vs LBW Other differences ($p<0.05$) occurred between: LBW vs LOW						

Table C.14 ANOVA and TUKEY of LPW, LBW, and LOW isotherms sorption experiments with TCP.

Source of Variation	SS	df	MS	F	P-value	F crit
Between Groups	25936.82	2	12968.41	25.56789	9.31E-09	3.150411
Within Groups	30432.89	60	507.2148			
Total	56369.71	62				
Significant ($p<0.01$) differences occurred between LPW vs LBW and LOW vs LBW						

C.5 Sorption of Malachite Green on LDPE

Preliminary Sorption Results

Sorption tests results of MG with LDPE before and after bio-aging are summarized in Figure C.17. Tests performed with 9 ppm were measured without acetate buffer, but the solutions were adjusted to a pH of 6 (well below the pKa of MG), while at 15 ppm, an acetate buffer was used. According to LP and LPW results the use of buffer did not change the removal percent, where a similar removal was observed between 9 ppm and 15 ppm concentrations. In both cases, LPW showed a higher affinity for MG sorption than LP. Anaerobically aged PE (LBW) showed the highest affinity for MG sorption with 97.9% and 96.2% removals with 9 ppm and 15 ppm respectively. Aerobically aged PE (LOW) on the other hand showed the lowest sorption affinity to MG with higher removal at 15 ppm (53%).

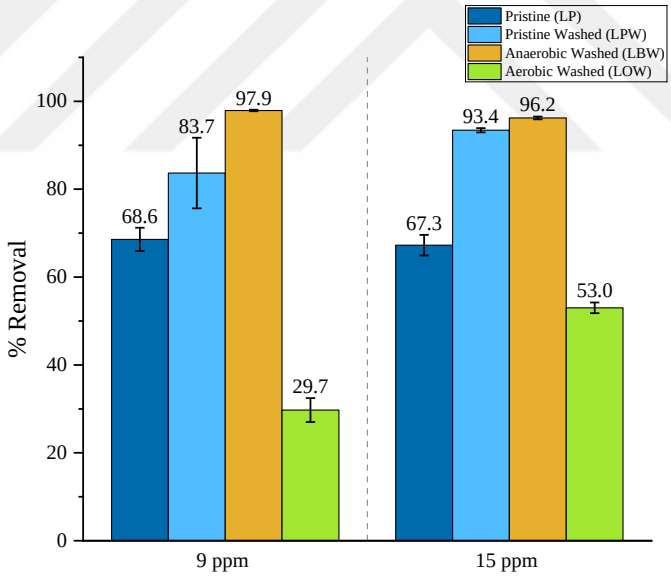

Figure C.17 Removals of MG of LDPE at 9 ppm (without buffer) and at 15 ppm (with buffer).

Isotherms Trials

Isotherms with MG using LPW, and the second batches of bio-aged PE (LBW and LOW) were conducted at seven concentrations (15, 20, 25, 30, 50, 85, and 100 ppm).

However, the sorption results were inconclusive due to a lack of understanding of MG's reaction mechanisms in water. DI water was used for the experiments. At a low concentration of 15 ppm, MG-only control reactors did not show any reduction in concentration, whereas higher concentrations resulted in significant reductions in the control reactors. To determine the actual reduction attributable to MPs' sorption of MG, the reduction observed in the control reactors was subtracted from that in the test reactors. Figure C.18 a and b illustrate the removal amounts before and after these corrections. Due to inconsistent removals across different concentrations and setups in the control reactors, the results were deemed unreliable.

In comparing bio-aged MPs, LPW and LBW demonstrated a high sorption affinity for MG, whereas LOW showed a low affinity. This suggests that different bio-aging mechanisms influence sorption affinities even at higher concentrations. However, the exact removals and the differences between LPW and LBW remain unclear due to the inconsistencies in the corrected results. To address this issue, different DI water samples from various sources were tested with a consistent MG concentration, but results remained inconsistent due to variations in the initial MG concentration over time. This indicates that MG may be sensitive to several factors including measurement conditions at higher concentrations, dilution of higher concentrations, spectrophotometric analysis, fluctuations of pH after the addition of buffer, time of mixing, and time to stabilize after the addition of buffer, or other factors.

a)

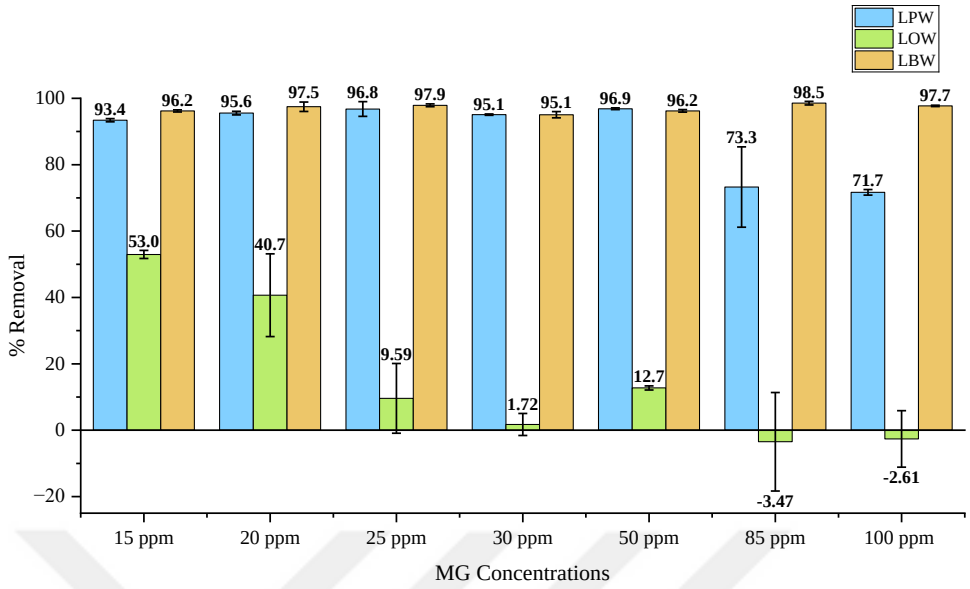

b)

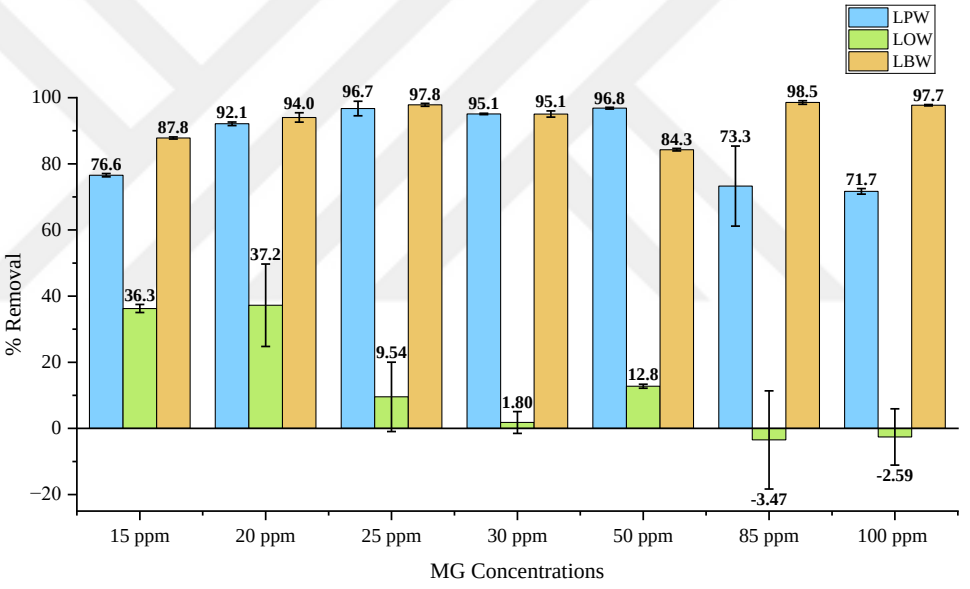

Figure C.18 Isotherm results of MG (a) before and (b) after corrections with MG-only control reactors.